PALEOSEISMICITY AND ACTIVE EARTH DEFORMATION, LAKE ROTOITI TO WEST WAIRAU VALLEY SECTION OF THE ALPINE FAULT

A thesis

submitted in partial fulfilment

of the requirements for the degree

of

Master of Science in Engineering Geology

at the

University of Canterbury

by

SAMUEL RICHARD FOUGERE

University of Canterbury

2002

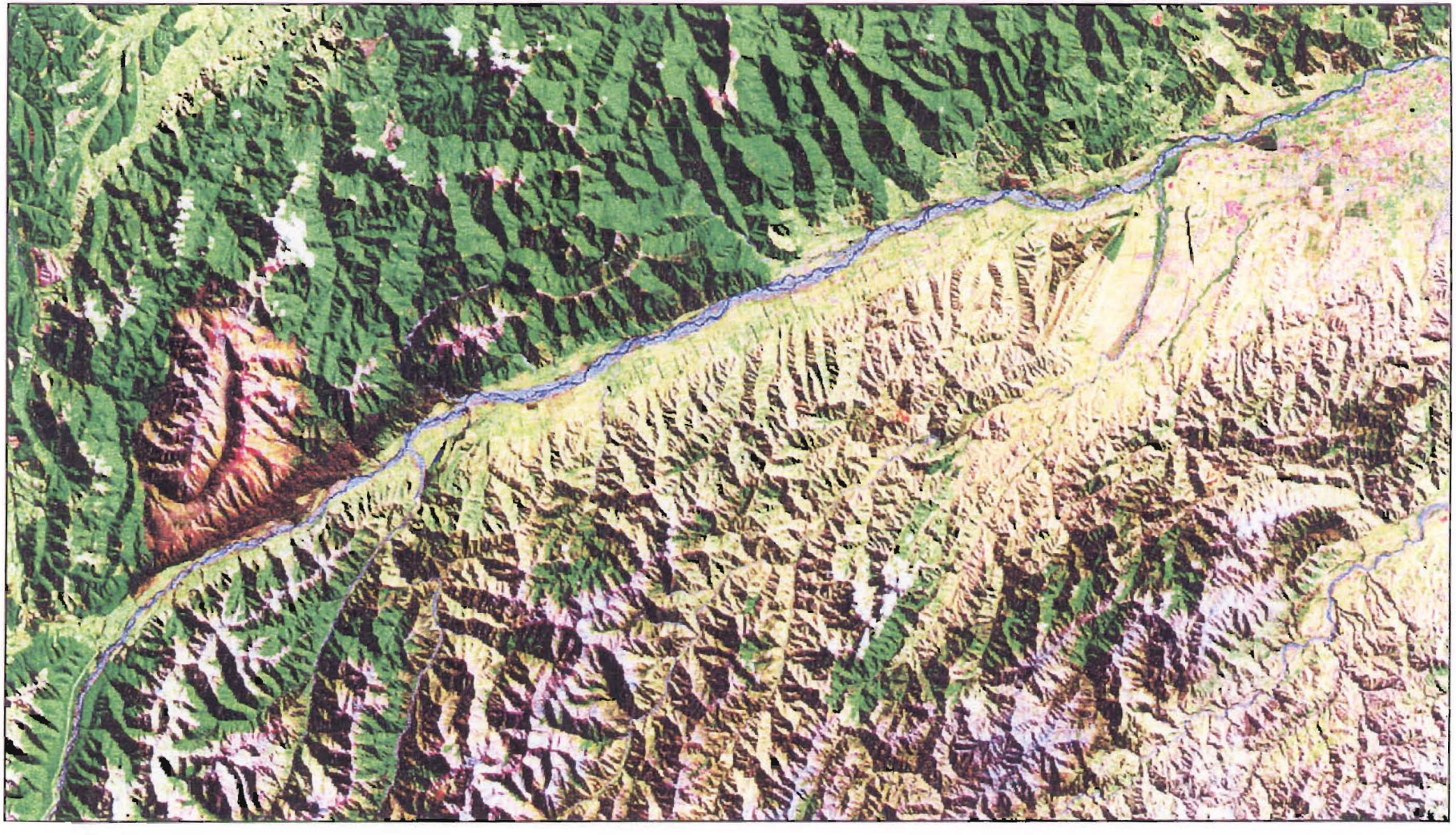

Frontispiece: Satellite Image of the Wairau Valley. Edge of field area south of the distinctive Red Hills Range.
Image courtesy of Mike Rymer, (USGS)

ABSTRACT

The Wairau Fault, the northern extension of the Alpine Fault, has not ruptured historically. Bounding the Marlborough Fault System to the north the Wairau Fault is over 100 km long and capable of generating a large earthquake rupture. From Cloudy Bay SW to Lake Rotoiti the fault is defined by a linear valley-bound trace and narrow zone of deformation. The main objective of this paleoseismic investigation of a section of this fault was to establish the pre-historic rupture history.

Trenching excavations, geomorphic mapping, differential GPS surveying and weathering rind dating techniques were used to investigate the rupture history of the Wairau Fault.

From trenching data at Tophouse, one earthquake rupture on the Wairau Fault is recorded since AD 200. No upper limit bounds this rupture date. Integration with a similar paleoseismological study of Zachariasen et al, (2001) refines the last rupture event on the Wairau Fault to between AD 200 – 1000. A branch caught in the shear zones indicates a dated event approximately 12 500 years ago but other events intervene on stratigraphic evidence. Liquefaction deposits are recognised in the trenches, in conjunction with small thrust flaps on the footwall side, suggesting seismic rupture as the dominant translation mechanism, with no significant aseismic creep based on offset linear terraces.

Dextral slip rates on the fault of 4.2 ± 1.4 mm/yr compares well with pre-existing data. A single event offset of 4.4 ± 0.5 m is consistent with others further NE along the Wairau Valley.

A temporal disparity exists between the last rupture brackets at the Tophouse and Matakitaki River trenches (Yetton, 2002), indicating that, at least for the last rupture event an earthquake segment boundary was operational between the two trench sites. Defining an earthquake rupture segment boundary by a specific structure or location is difficult as any number of faults could dissipate radiated seismic energy and several possibilities are reviewed. If a rupture segment does exist between Matakitaki River and Tophouse, it is most likely about Lake Rotoiti. An estimated earthquake magnitude for the onland section of the Wairau Fault for this rupture segment is M = 7.4 ± 0.25.

In addition to aspects of seismicity of the fault strike, both the large scale topographic setting and detailed morphology of the fault zone are discussed. In particular the complexity of interaction between fluvial processes and secondary deformation associated with the fault zone has lead to some insights into both the evolution of secondary structures and to the response of rivers behaviour to seismic cycles.

On the basis of elapsed time since the last fault rupture, and slip rates on the fault, an earthquake rupture on the Wairau Fault in the near future is a distinct possibility.

TABLE OF CONTENTS

LIST OF FIGURES

CHAPTER 3

CHAPTER 4

ATTACHED MAPS (Map Pocket)

LIST OF TABLES

LIST OF APPENDICIES

ACKNOWLEDGEMENTS

An Active Tectonics Research Grant from the University of Canterbury funded this research and I am grateful for the financial support. Radiocarbon dating expenses were shared with an Earthquake Commission study.

Mrs Jocelyn Campbell has helped this thesis immensely in the final stages, often taking a sledge hammer to some things, though in a somewhat gentler fashion. Thank you Joc. Dr Jarg Pettinga initiated this study with Dr Mark Yetton and both are thanked for help in the field and at university, thank you to Dr Jarg Pettinga for reviewing some of the work.

Professor Guilford and the Poll family from the Northridge Farm allowed access to the trench sites. As with other members of the St Arnaud community, Pat, Wendy and Cody from the Yellow House, Peter and Ann Crozier and Brian and Nola from the store made St Arnaud a very hospitable and friendly place. Mr and Mrs Armstrong from Blenheim are thanked for rented accommodation.

Flexible part time work at CRL Energy Ltd was greatly appreciated, with a special thanks to Chris Nelson and Totem for making work seem more like a holiday. My mother and Robin Young helped with fieldwork and provided some light entertainment.

A number of people are responsible for helping me finish off and through my study, most notably Emma and Andrea but also Kerry, Tanya, Greg, Jane, Kate, Andrew, Terry, Jamie and Matt. Dave Bell kept me on my toes with a fair share of banter over the last three years.

Kerry, Terry, Matt, have put up with my ramblings but also provide a sounding board and at least gave the appearance of being interested.

John Southward is thanked especially with unfaltering computer support often in the face of some rather silly questions. Cathy Knight helped immensely by accommodating field gear around everybody else's needs and still managing to find the time to use field equipment. Thank you also to Julie-Anne, Lorrie, Lee, Jane and Rob for help during the last two years.

Finally I would like to thank my family for the support and encouragement throughout, especially when I broke my leg and was laid low.

CHAPTER 1

INTRODUCTION

1.1 BACKGROUND TO THE STUDY

New Zealand straddles a dynamically deforming plate tectonic boundary (Figure 1.1). Earthquake generating processes are prominent in the mechanisms accommodating this deformation. Large earthquakes release most of the strain buildup at plate tectonic boundaries, whereas small earthquakes, though abundant, only relieve small amounts of strain. These large earthquakes are infrequent, but the energy released has the potential to cause widespread destruction. Understanding the interaction between plate tectonic motion and strain release (particularly for large earthquakes) along the Australian-Pacific plate boundary is critical when assessing seismic hazard in New Zealand.

The Alpine Fault spans the length of the South Island marking the surface boundary between the Australian and Pacific plates. By comparison with other active faults in New Zealand, the Alpine Fault is the longest, about 650 km onland length, and has the highest cumulative slip and slip rates, yet has failed to rupture in historic times. Field evidence suggests large magnitude earthquakes have occurred on the Alpine Fault in the prehistoric past (eg Berryman et al, 1992). Studies along the fault suggest strain buildup is nearing the end of the seismic cycle and a rupture is imminent (Berryman et al, 1992; Sutherland & Norris, 1995; Wright, 1998; Yetton et al, 1998). However, a detailed

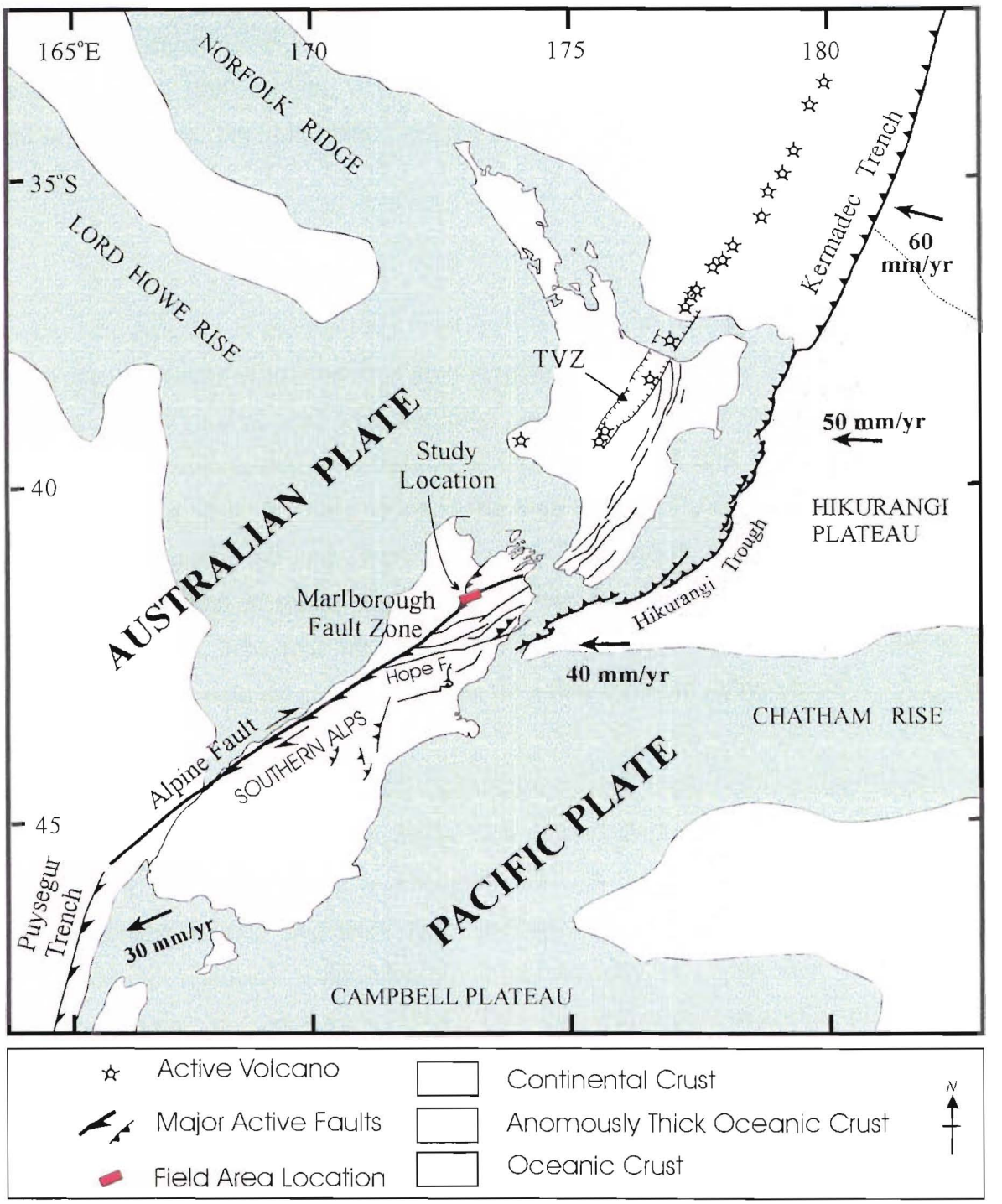

Figure 1.1: Tectonic Map of New Zealand showing the main structural features associated with the obliquely convergent Australia-Pacific plate boundary. Arrows show plate motion of Pacific plate relative to the Australian plate. Adapted from Pettinga et al (1998) & Cole (1990). Orange rectangle shows field location.

understanding of the prehistoric ruptures along the entire length of the fault is not complete. Investigations of the Alpine Fault in the Southern and Central sections (eg Cooper & Norris, 1990; Wright, 1998; Yetton et al, 1998) provide evidence of frequent prehistoric ruptures, but information on the North and Wairau sections is relatively sparse.

A systematic program of paleoseismic investigation along the Alpine Fault is attempting to alleviate the paucity of paleoseismic ground rupture data on the fault (eg Yetton, 1998; Yetton et al, 1998) and develop a rupture history of the fault. The present study is part of this continuing paleoseismic investigation of the Alpine Fault and is centered on the Nelson Lakes end of the Wairau Section of the Alpine Fault (Figure 1.1). Yetton (2002) on the North Alpine Fault and Zachariasen et al (2001) on the central section of the Wairau Fault are part of recent adjacent paleoseismic studies. As there is no historic precedent for fault behaviour on the Alpine Fault we rely solely on investigating prehistoric ruptures with the goal of preparing for a future ground rupture event.

Fault studies have shown that large faults such as New Zealand's Alpine Fault do not rupture along their entire length (Ambraseys, 1970). A fault line can often be divided into earthquake rupture segments each individually capable of generating large earthquakes by rupturing independently, or occasionally in conjunction with other segments (Schwarz & Coppersmith, 1984). Therefore, information regarding the timing of the most recent ruptures on the fault in the context of individual segment histories is critical. Constraining and identifying segment boundaries, rupture propagation and rupture stopping zones, is essential when assessing seismic hazard, as it provides vital information regarding fault rupture length, which is used for estimating earthquake magnitude. Slip rate data can also help to constrain rupture segments as fault segment boundaries often absorb a component of slip (Cowan 1990; McCalpin, 1996). Faults may be segmented into both large and small segments, however larger segments are the most important with respect to seismic hazard (Schwarz & Coppersmith, 1986).

1.2 Study Objectives and Methods

1.2.1 Thesis Objectives

Until recently there has been no detailed paleoseismic investigations of the Wairau section of the Alpine Fault, although some slip-rate data exists (eg Lensen, 1968) (Figure 1.2). Zachariasen et al, (2001) completed a paleoseismic investigation near Wairau Valley township. Paleoseismic history is essential when attempting to determine the probability of future earthquakes, especially in New Zealand as we have such a brief historic record. The main aim of this study is to provide paleoseismic information and develop a paleoseismic history of the Wairau section of the Alpine Fault.

In this study I attempt to achieve the following key objectives:

- Detailed geomorphic mapping at selected localities to define the late Quaternary evolution of the fault zone
- Define the approximate timing of the most recent earthquake ruptures on the fault
- Determine a slip rate of the Alpine Fault in this northern location
- Compare fault activity on this northern section of the fault with data already available for sections further south on the Alpine Fault

Paleoseismic history of the Wairau section of the Alpine Fault will provide valuable information in helping to assess seismic hazard of the Wairau section of the Alpine Fault and allow comparison of large earthquake occurrence with the better studied fault

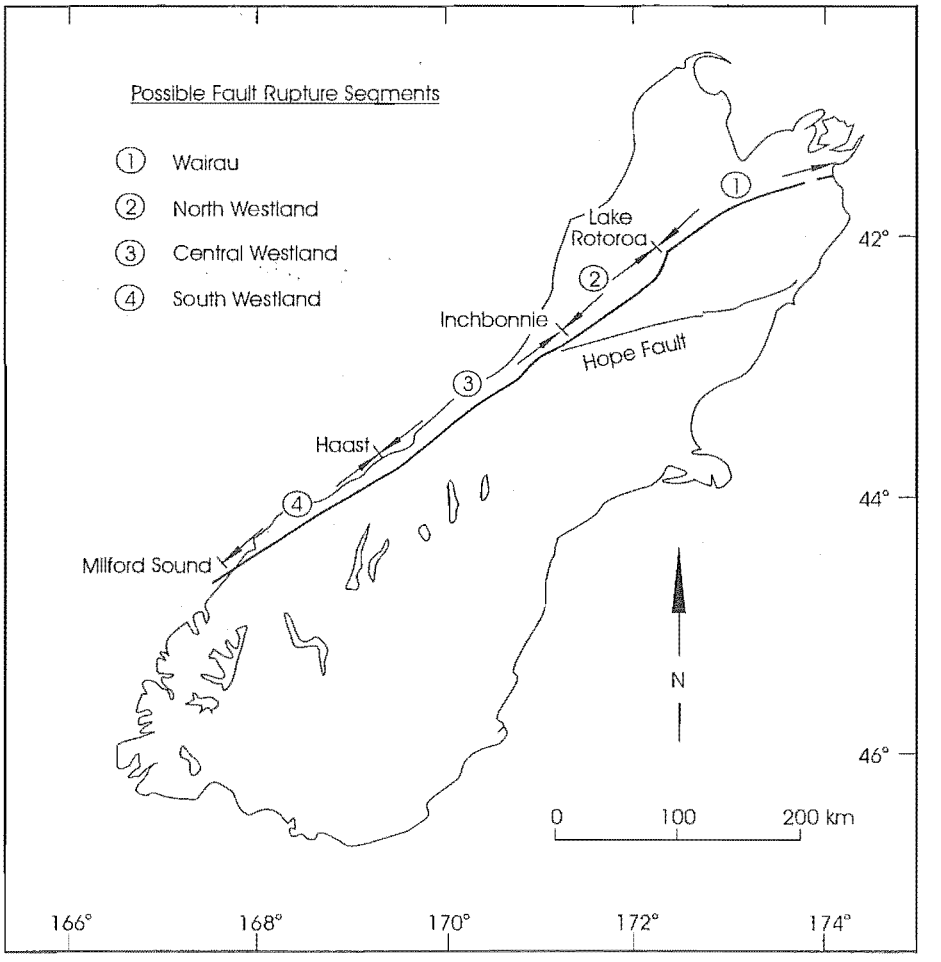

Figure 1.2: Four onland fault sections of the Alpine Fault from Berryman et al (1992). Possible fault segments are indicated from geomorphic and structural style characteristics.

sections further south.

1.2.2 Thesis Methods

During the study a number of investigation techniques and methods have been applied to achieve the objectives stated in Section 1.2.1. These include aerial photograph interpretation and analysis, geomorphic field mapping, electronic distance measuring (EDM) surveying, and differential global positioning system (GPS) surveying of offset geomorphic markers (e.g. moraines, terraces and relict, ephemeral and permanent stream channels). Tape measure and compass angle surveys were used for forested sites without adequate satellite visibility. Weathering rind-dating (WRD) techniques were used to determine geomorphic surface ages in the Wairau Valley where appropriate. Mechanised excavation of two trench sites, detailed face logging and radiocarbon dating (^{14}C) of relevant organic material has been used to constrain the timing of ruptures on the fault, attempting to establish first order recurrence intervals, fault segment indicators and seismic hazard.

1.2.3 Study Location

The extent of the study area is shown in Figures 1.1 & Section 1.6. Broadly, the study area follows the trace of the Alpine Fault from Lake Rotoiti in the SW to the upper Wairau Valley in the NE. St Arnaud, a small settlement by Lake Rotoiti, straddles the fault trace and is the only settlement in the study area. Nelson approximately 60 km NNE, Blenheim approximately 100 km ENE and Murchison approximately 40 km W are the closest regional centres.

There is good foot access to the study area from State Highway 63 (SH 63), which runs sub parallel to the fault trace. However access and visibility along the trace itself was often extremely difficult as dense brush, bracken, forest and steep local topography provided obstacles. Fortunately, the fault trace generally follows the base of the ranges or valley floor, so no major expeditions amongst the 1500m plus peaks were necessary.

Draining Lake Rotoiti to the west is the Buller River, one of three major drainage systems in the study area. The Motupiko River flows northward from the Tophouse area, and on the eastern side of the St Arnaud Range and Tophouse Saddle the Wairau River flows NE to the sea.

To place the Wairau Fault section of the Alpine Fault in its context, the background to the present state of knowledge relating to the system as a whole is reviewed in the following sections. This chapter concludes with a brief outline and description of the subsequent chapters.

1.3 Outline of Alpine Fault Geology

1.3.1 Tectonic Setting

New Zealand is situated on the boundary of two tectonic plates, the Australian plate to the west and the Pacific plate to the east (Figure 1.1). The Australian/Pacific plate boundary is a dynamic boundary, in the New Zealand region there is evidence of continental collision, subduction zones, major transform faulting, and volcanic activity. North of New Zealand the Pacific plate is subducting under the Australian plate, the Kermadec Trench in the north merging southward to the Hikurangi Trough marks the

surface subduction interface. South of New Zealand the situation is reversed with the Australian plate subducting beneath the Pacific plate expressed by the Puysegur subduction zone.

Linking the opposite dipping Hikurangi and Puysegur subduction zones is the Alpine Fault system which forms the backbone of the South Island of New Zealand. The trace, or on-land expression, of the Alpine fault is remarkably linear when viewed from space, however closer inspection at some locations reveals complex segmentation structures accommodating slip which are non-linear (Norris et al, 1990; Berryman et al, 1992).

Between the Hikurangi Margin and the Alpine Fault another link system, the Marlborough Fault System (MFS), is in operation. This accommodates deformation from the westward dipping Hikurangi subduction zone to the moderately eastward dipping Alpine Fault (Sibson et al, 1979; Anderson et al, 1993; Davey et al, 1995). The MFS comprises a number of generally right lateral strike-slip faults, aligned roughly parallel to the plate motion vector, which coalesce to form the single structure of the Alpine Fault. Relative slip on the major faults appears to be increasing on each structure progressively southward.

1.3.2 Plate Motion, Crustal Structure and Seismicity

Relative plate tectonic motion vectors decrease southward along the Australian/Pacific plate boundary, but the dextral strike-slip component relative to convergence becomes more oblique, progressively southward (Figure 1.1). This convergent obliquity manifests itself in fault parallel and fault normal components, partitioned most markedly in the North Island, but largely accommodated together on the Alpine Fault. Approximately seven million years ago, the pole of rotation of the Pacific plate began to migrate, this

gave rise to increased plate motion obliquity and continent-continent collision, the most visible expression being the formation of the Southern Alps (Walcott, 1998). Estimates on the order of shortening across the Southern Alps are approximately 100 km on the northern Alpine Fault since 6.4 Ma (Walcott, 1998).

Earthquake data of Anderson & Webb (1994) clearly defines the Hikurangi Benioff zone beneath Marlborough as having a moderate dip to about 100 km depth and descending almost vertically below this depth. In the Marlborough region shallow earthquakes tend to exhibit strike-slip motion agreeing with displacement data from surface geology, whereas subduction related surface geology is conspicuously lacking above the Wairau Section of the Alpine Fault implying some partitioning of plate motion. South east facing thrusts and uplift along the east coast of Marlborough are related to the SW end of the Hikurangi Margin (Van Dissen & Yeats, 1991). Reyners (1989) shows subcrustal earthquake focal mechanisms having almost pure strike slip motion above depths of 40 km in the Marlborough region. Results from Arabasz & Robinson (1976) agree with the shallow ENE trending strike-slip motion. Cowan (1992) demonstrated a mid crustal decoupling between upper crust strike-slip and deep dip-slip associated with the downgoing slab.

Pettinga & Wise (1994) propose a model whereby the subducting slab and a regional surface slab are semidetached with the surface slab deforming as a crustal scale flower structure accommodating the strike-slip motion. Microseismicity studies of Arabasz & Robinson (1976) over a short period in 1972 suggest seismic activity on the Wairau Section of the Alpine Fault was very low, whereas activity on the Awatere and Clarence faults was greater. Depth to the base of the seismogenic zone below the MFS is approximately 15 km, this excludes deeper subduction related earthquakes (Anderson et al, 1993).

1.3.3 The Alpine Fault

The trace of the Alpine Fault spans the length of the South Island. Fault sections have been determined by Berryman et al (1992) based on structural style and geomorphic expression along fault strike (Figure 1.2). Berryman et al (1992) point out that the divisions are geographic sections and not necessarily defined seismogenically independent geological segments, although the sections are based on geological information. Four sections, or possible fault rupture segments are identified, the Wairau, North Westland, Central Westland and the South Westland sections (see Figure 1.2). The convention of Yetton (2002) is followed for this thesis, whereby the Westland term of the named Alpine Fault sections is dropped for the Central and North sections, and the Wairau section is referred to as the Wairau section of the Alpine Fault, historically referred to as the Wairau Fault, a separate entity and treated as the northern element of the MFS. For the sake of brevity, the term Wairau Fault will continue to be used in this study to denote the section of the Alpine Fault extending from Cloudy Bay SE to Lake Rotoroa.

South of the coalescing of the MFS dextral slip on the Alpine Fault has a rate of 27 ± 5mm/yr. The fault normal component of the slip varies considerably along fault strike with highest rates of 8-12 mm/yr west of the Mt Cook region coinciding with the highest elevations along the Southern Alps (Norris & Cooper, 2001).

1.3.4 Fault Section Descriptions

Geomorphic expression of the South Westland section is remarkably linear and fault plane data indicates almost pure horizontal movement (Berryman et al, 1992). Contrasting with fault sections further north, the South Westland section's convergent component of oblique plate motion is not accommodated on the Alpine Fault itself but

over a broader region of deformation (Berryman et al, 1992; Norris & Cooper, 2001).

The strike of the Central section of the Alpine Fault from Haast to Inchbonnie is oblique relative to the current plate motion vector, oblique continental collision and slip partitioning prevail. A visible manifestation of the slip partitioning is the vertical elevation of the Southern Alps, greatest in the Central section of the fault, that has a tendency to mask the greater, though less visibly distinguishable, fault parallel displacement (Norris & Cooper, 2001). When viewed from space or at a regional scale the trace of the Alpine Fault in the Central section appears linear. Norris & Cooper (1995) note however, that in detail the oblique slip is taken up on the near surface by a series of oblique thrusts linked by steep strike slip faults for which they introduce the term 'serial partitioning' (Norris & Cooper, 1997) on a transpressional fault. A notable feature of this section of the fault is that the slip on the fault is resolved oblique to plate motion and not partitioned, although some off plane deformation is accommodated in backthrusts to uplift the Southern Alps as a double sided orogenic wedge (Koons, 1990).

Surface segmentation on the order of 1-10 km does not appear to hinder large rupture propagation (Norris & Cooper, 1995), as small displacements on individual fault segments have not been recorded. Norris & Cooper (1995) suggest that the segmentation results from perturbations of the local stress field (1-4 km depth) caused by deeply incised valleys of the hanging wall. More importantly, from a paleoseismic perspective the Central Alpine Fault appears to behave as a single rupture segment rather than a series of small segments rupturing independently.

The North Alpine Fault follows the range front. All known Holocene faults are linear, though there are some minor right steps linking lobate overthrusting similar to those found further south (Berryman et al, 1992). Lake Rotoroa marks the northern extent of the North Alpine Fault, past the major structural perturbation 'the bends' area of the fault

(Berryman et al, 1992). Also of interest, the SW end of the North Alpine section of the fault marks the onset of major faults branching to the east of the MFS including the Hope, Clarence and Awatere faults respectively. These faults reduce the amount of displacement accommodated on the northern sections of the Alpine Fault. From a paleoseismic perspective this decrease in slip accommodated by the Alpine Fault, or bleeding off slip, has implications regarding fault segmentation and rupture magnitude and frequency on the Alpine Fault further north.

The remaining section of the Alpine Fault, the Wairau section, transects Lake Rotoiti striking about 065° and passes through the Tophouse Saddle before running along the Wairau Valley and exiting seaward at Cloudy Bay, near Blenheim. This section of the fault is sub parallel to the plate motion vector and exhibits almost pure strike-slip motion though is locally complex (Lensen 1976; Berryman et al, 1992). Various authors have mapped this fault section, though most intensively by Lensen (1976) and Johnston (1990). Grapes & Wellman (1986) have described a short trace terminating within a kilometer of the sea. Continuation of the Wairau section of the Alpine Fault and other MFS faults into Cook Straight linking to the Wellington Fault System has been the source of much conjecture amongst researchers (Carter et al, 1988). Modern seismic reflection data has shown that the faults of the MFS pass and splay into the fold and thrust system of the southern Hikurangi Margin structures and while debate continues it is clear that a simple, and uninterrupted continuation across Cook Straight is unlikely.

1.3.5 The Marlborough Fault System

A series of roughly parallel predominantly dextral strike slip faults comprise the Marlborough Fault System which collectively serve as a linking structure between the Hikurangi subduction zone and the Alpine Fault (see Figure 1.1). Slip rates on the faults (Wairau, Awatere, Clarence and Hope), increase progressively southward from the northernmost Wairau Fault to the southern Hope Fault structure, the latter

accommodating most of the relative plate motion. Faults in the MFS young to the south, consistent with a southward migration of the Hikurangi subduction zone (Campbell, 1973).

With recent investigations a more detailed rupture history of the MFS faults is beginning to emerge. The average slip rate on the Hope Fault is about 25 mm/yr, however, published estimates of slip rates have varied between 14-40 mm/yr (Cowan, 1990; Cowan & McGlone, 1991; Van Dissen & Yeats, 1991; Knuepfer, 1992; McMorran, 1992). Single event horizontal displacements on the Hope Fault west of Hanmer Basin are on the order of 4-5 m with a relatively short recurrence interval of about 200 years (Cowan & McGlone, 1991).

Slip rates on the Clarence, Awatere and Wairau Faults are significantly less than the Hope Fault. A slip rate of about 4-8 mm/yr in the last 18 000 years is recorded on the Clarence Fault (Keickhefer, 1979; Van Dissen & Nicol, 1998). A slightly greater slip rate on the western Awatere Fault, 6-8 mm/yr, decreases eastward to less than 1.5 mm/yr near the coast for late Quaternary offset features (McCalpin, 1996; Little et al, 1998). The Wairau Fault has a slip rate of 3-5 mm/yr in the late Quaternary (Lensen, 1968; Campbell, 1973; Kneupfer, 1992; Zachariasen et al, 2001).

Cumulative dextral displacement on MFS faults is significantly less than the Alpine Fault, with the Awatere beginning to deform in a strike slip fashion about 7 Ma with 34 ± 10 km dextral separation since that time (Little & Jones, 1998). This suggests that MFS faults south of the Wairau Section of the Alpine Fault are much less evolved. The older Alpine Fault structure has accommodated approximately 480 km of right lateral strike slip separation, smoothing major irregularities by repeatedly rupturing since inception approximately 23 Ma (Norris et al, 1990). Wesnousky's (1988; 1990) cumulative slip theory indicates the Wairau Section of the fault should rupture as a single segment. He

argues that there are no apparent structural barriers or major faults bleeding slip as progressive displacements have essentially smoothed any major discontinuities. This assumption is debatable and will be readdressed later.

Only two large historic surface ruptures have occurred on the MFS, in AD 1848 on the Awatere, and AD 1888 on the Hope fault (Cowan, 1991; Grapes et al, 1998; Little et al, 1998). These ruptures were confined to sections of the faults, and there is no historic record of ruptures on the Wairau or Clarence Faults.

1.4 Previous Paleoseismic Work on the Alpine Fault

1.4.1 Introduction

Relative to most geological sub disciplines paleoseismology is in its infancy, consequently many faults in New Zealand have not been subject to extensive paleoseismic investigation. Until recently there had been very little paleoseismological investigations on either of the North and Wairau Alpine Fault sections. The paucity of paleoseismological data prompted this thesis project in conjunction with a northern Alpine Fault study of Yetton (2002) and complimentary to a study further NE on the Wairau Fault by Zachariasen et al, (2001). The following sections outline the present paleoseismological information on the Alpine Fault and define the historic/prehistoric boundary.

1.4.1.1 Historic/Pre-Historic Boundary

There has been no recorded rupture of any onland section of the Alpine Fault since European settlement began in about AD 1840. Local Maori did pass through the region when journeying to Canterbury and the Tasman Sea as Lakes Rotoiti and Rotoroa provided a plentiful food source. Unfortunately Te Rauparaha decimated local Maori as he began settling the South Island with the aid of muskets. Loss of oral history consequent on this massacre results in a very brief historical earthquake period commencing about AD 1840. The first record of european exploration in the area is in AD 1842 when J S Cotterell and a Maori guide passed Tophouse Saddle. Subsequent exploration and surveying of the area began in AD 1846. In the early 1850's Julius von Haast was commissioned to explore the area primarily in search of gold and this marks the first recorded geological investigations of the area (history of region from DuFrense (1989) and from http://www.nzine.co.nz/life/rotoiti.html). Eiby (1980) documented a rupture in AD 1848 at the east end of the Wairau Fault, however, recent investigations suggest this earthquake was along the Awatere Fault (Grapes et al, 1998).

To avoid confusion the date of AD 1840 will be used as the historic/prehistoric paleoseismic boundary throughout this thesis (as per other authors eg Berryman et al (1992); Yetton et al (1998)).

1.4.2 Southern, Central and Northern Alpine Fault Sections

More extensive paleoseismological investigations have been performed on the southern and central sections of the Alpine Fault as field evidence suggests numerous large prehistoric earthquakes. In addition, the Alpine Fault in this location accommodates approximately 70-75% of interplate slip (Norris & Cooper, 2000) suggesting this section of the Alpine Fault has the highest probability of being the locus of any major earthquake.

Paleoseismic investigation of the Alpine Fault began with the work of Adams (1980). Radiocarbon dates from landslides and aggradation terraces were collected throughout Westland. According to McCalpin (1996) paleoseismic evidence such as this is classed as secondary or indirect evidence of earthquake rupture. Dates obtained, and conclusions drawn by Adams (1980) are considered with caution as the relation of landslides and aggradation terraces to paleoseismic rupture events is ambiguous. A number of other triggering factors could cause the landslides, especially the high rainfall, abundance of other smaller faults and vigorous erosion processes on the West Coast of the Southern Alps. Adams (1980) proposed that over the last 2000 years there had been recurrence intervals of approximately 500 years with the most recent event 550 years ago.

Direct paleoseismic investigation of the Alpine Fault began with the study in South Westland of Cooper & Norris (1990). Trench excavated radiocarbon dates were supplemented with tree age estimates (trees that had lost their crown from seismic shaking) and provided the first direct rupture bracket on the Alpine Fault. Cooper & Norris (1990) defined the period between AD 1650 and AD 1725 as the period when the most recent large rupture event occurred on the Alpine Fault.

Lichenometry was the next paleoseismological technique used to determine rupture history of the Alpine Fault. Bull (1996) dated rockfalls, on the assumption of uniform lichen growth rates on fresh rock surfaces. Modal lichen peaks were inferred as earthquake ruptures on the Alpine Fault. Data from extensive sampling over the northern South Island allowed the distribution of coeval rock fall events to be delineated relative to epicentres on specific faults, eg the Hope Fault. Those attributed to the Alpine Fault gave the following dates for events: AD 1748 ± 10 yrs, AD 1489 ± 10yrs, and AD 1226 ± 10 yrs and a possible event around AD 967 ± 10yrs. These dates provide a remarkably consistent revised recurrence interval of 260 ± 15 yrs, almost halving the previous recurrence interval of Adams (1980).

All the dates provided by Bull (1996) were from rockfalls classed as secondary paleoseismic evidence occurring coseismically (McCalpin, 1996). Interestingly all of the rockfalls dated by Bull (1996) were at least 20 km from the trace of the Alpine Fault. When you consider the tectonic environment, the assumption that these rockfalls are related to Alpine Fault rupture, is ambiguous. Bull (1996) does however internally check the lichenometry technique on historic rockfalls with positive results. Therefore the dates are likely to be robust even though the relation to the Alpine Fault rupture may not be. Bull has recently revised his inferred rupture dates in light of recent paleoseismic evidence (discussed below) to AD 1718 ± 10 yrs, AD 1615 ± 10 yrs, AD 1578 ± 10 yrs, AD 1428 ± 10 yrs and AD 224 ± 10 yrs which agree closely to the current understanding of dates of rupture on the Alpine Fault (pers.comm. in Wright, 1998 & Norris et al, 2001).

Numerous paleoseismological techniques were used in a comprehensive study of the Central and North Alpine Fault detailed in Yetton (1998); Yetton et al, (1998); Wells et al, (1998) and Yetton (2000), the results from these authors are discussed below. Excavation of trenches and radiocarbon dating of pertinent carbonaceous material provided primary evidence for the time bracket of rupture events on the Alpine Fault itself. Secondary evidence was used to further refine the date of rupture. Modes of terrace and landslide dates, forest age modes, and tree ring chronologies were used with varying success to determine the last three major rupture events on the North and Central Alpine Fault (Yetton 1998: 2000; Yetton et al, 1998) (see Figure 1.3).

Refinement of the trench constrained rupture dates by dating of terraces and landslides provides only a moderate improvement (Figure 1.3). This suggests that the dates of Adams (1980) could be ambiguous without another dating method defining a relationship to fault rupture. Modal forest ages increased the date precision markedly and suggest three unequally spaced ruptures with ages not readily conforming

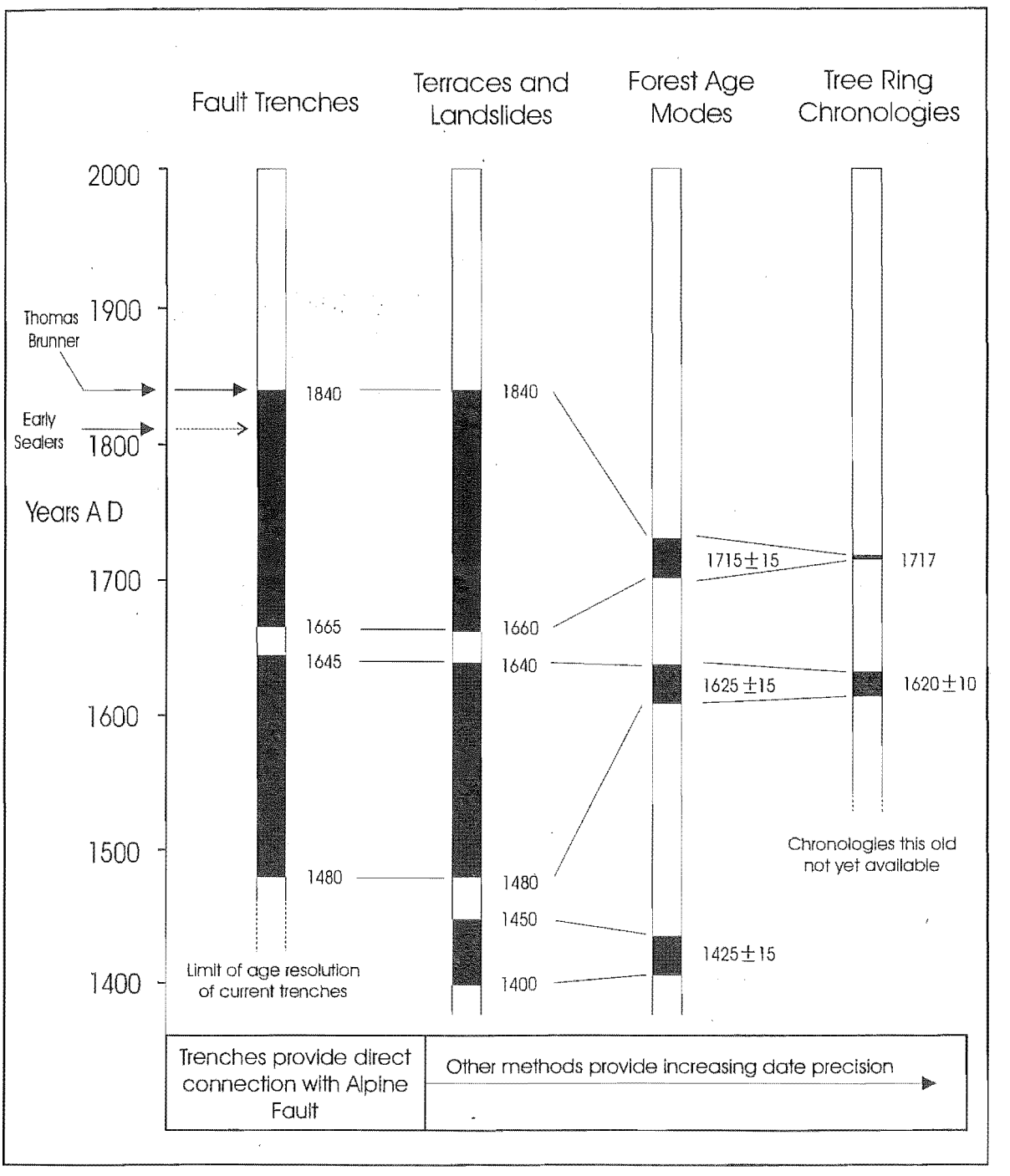

Figure 1.3: Paleoseismic information from four indepent lines of evidence constraining the timing of the the most recent ruptures on the Central and part of the North Alpine Fault (Yetton et al, 1998; Yetton, 2002)

to the characteristic fault model recurrence interval of Schwarz & Coppersmith (1984). Where applicable, analysis of tree rings provides the most precise paleoseismic indicator. For the last and penultimate events extremely well defined rupture brackets were identified. The penultimate rupture at AD 1620 ± 10 yr, and the last rupture event confined to the tree-growing season of AD 1717 (Yetton, 1998: 2000; Yetton et al, 1998).

Paleoseismological investigations at Waitaha River on the central section of the fault reveal numerous ground ruptures. Wright et al (1998) infer a minimum of four ground-rupturing episodes in the last 900 years from trench excavations and dendrochronology. A date for the most recent rupture found at Waitaha River was AD 1720 ± 5, with other ruptures AD 1620 ± 10yr, AD 1578 ± 10 yr, AD 1428 ± 15 yr, AD 1224 ± 15 yr, AD 961 ± 20 yr and AD 565 ± 60yr respectively.

Berryman et al (1998) conducted trenching investigations in the South Westland section of the fault, near Haast. Three definitive ground rupturing events were recognised in the last 900 years, with the most recent rupture probably in AD 1718 ± 5 yr, each rupture had dextral fault parallel displacement on the order of 8 m and vertical displacement on the order of 1-2 metres.

Paleoseismic investigation of the North Alpine Fault section at Blue Grey River, Maruia River, and the Matakitaki River by Yetton (2002) indicates the last earthquake occurred between AD 1450 and AD 1700. The rupture bracket is further refined, if each site is considered part of the same fault segment, to between AD 1600 and AD 1700. Encapsulated in this bracket is the 1620 ± 10 yr earthquake rupture recorded in fault sections to the SW. However, the surface offsets of the North Alpine Fault are smaller raising the possibility of an independent fault segment rupturing coseismically or independently of the fault further to the SW.

1.4.3 Wairau Section of Alpine Fault

Zachariasen et al (2001) provide the only subsurface paleoseismological data on the Wairau Section of the Alpine Fault. Three trenches were excavated in the vicinity of the Wairau Valley township, named Wadsworth, Dillon and Marfell trenches respectively. The Wairau Fault is expressed on the surface in two strands near Wairau Valley (Lensen, 1976; Zachariasen et al, 2001). The Marfell and Dillon trenches were excavated across the northern strand, and the Wadsworth trench was along strike from where the north and south strand coalesce. Zachariasen et al (2001) infer that their data help place some constraints on the last three to four rupture events on this section of the Wairau Fault. The last rupture being between AD 600 and 600 BC, and a penultimate rupture between 600 BC and 1300 BC, possibly nearer 600 BC. Other events prior to this speculatively suggested from the data available, include a rupture since BC ~2700, and possibly another since BC 3600. These ages equate to about 1400 - 2600 yr BP, ~2600 – 3300 yr BP, since ~4700 yr BP and possibly since 5600 yr BP.

At the NE end of the Wairau Fault Grapes & Wellman (1986) describe the fault cutting late Holocene beach ridges. Ridges spanning the last 800 years are reported as unfaulted. Assuming the dating technique is correct, this section of the fault has not ruptured in the last 800 years.

1.4.4 Paleoseismological Summary

Some prehistoric rupture events on the Alpine Fault are clearly recognised. The most recent event on the South and Central sections of the fault is well recorded and occurred in AD 1717 (Yetton et al, 1998). The penultimate event is also tightly constrained at AD 1620 ± 10 yr. Wright et al (1998) provide evidence of rupture in AD 1580 ± 10 yr at Waitaha River which is inferred to be a separate event to the AD 1620 ± 10 yr event. The

preceding rupture event is recorded from trench excavations at three separate localities with tree ring analyses refining the date to around AD 1425 ± 15 yr (Yetton et al, 1998). Two prior events are recognised around AD 1200 and AD 900.

The paleoseismological history of the North Alpine Fault and the Wairau section of the fault is brief and spans a large geographical distance. The last rupture event recognised by Yetton (2002) between the Blue Grey River and the Matakitaki River occurred sometime between AD 1600 and AD 1700. The AD 1620 ± 10 yr rupture event recognised further SW indicates that at least on some occasions the North Alpine Fault and sections to the SW could rupture as a whole. The AD 1717 rupture falls outside this bracket suggesting a rupture segment boundary between the Haupiri River and Crane Creek as described by Yetton (1998).

None of the events in the Southern, Central, and Northern sections of the fault are recognised in the trenches of Zachariasen et al (2001) at Wairau Valley. It is therefore likely that there is a segment boundary between the Matakitaki River and the Wairau Valley site. A distance of approximately 100 km separates these two sites, therefore tightly constraining a rupture segment boundary with this information alone is difficult. Additional information from this study attempts to improve the accuracy of the segment boundary and prehistoric rupture history of the Alpine Fault in the Wairau region.

1.5 Geology and Glacial Geomorphology of the St Arnaud Area

1.5.1 Regional Geology

Evidence of New Zealand's dynamic geological nature is clearly present in the St Arnaud area. Most striking is the Alpine Fault, which juxtaposes rocks of similar ages of

dramatically different geological origin. Rocks south of the Alpine Fault are part of the Torlesse Supergroup and of Mesozoic age (Johnston, 1990). Mapping by Johnston (1990) demonstrated that the Torlesse rocks south of the Alpine Fault comprise a series of tectonic slices dissected by the NNE trending Raglan, Silverstream and Leatham Fault Zones dividing older units (Upper Triassic-Lower Jurassic) in the west from younger units (Upper Jurassic-Lower Cretaceous) further east respectively. The three fault zones strike NNE, parallel to the NNE trending structural element visible from the myriad of smaller faults within the proposed tectonic slices (Johnston, 1990).

North of the Alpine Fault the dominant structural element trends NNE (Adamson, 1964; Johnston, 1990). Fault drag on the active Waimea Fault is evident as it trends NE sub parallel to the Alpine Fault before swinging to a more northerly trend. The poorly exposed Speargrass Fault Zone (Median Tectonic Line, MTL) separates rocks of the Western Province from those of the Eastern Province in Nelson in a manner replicated by the rocks in Otago and Southland (Johnston, 1990). Wellman (1955) first recognised the rocks of similar origin offset dextrally approximately 500 km along the Alpine Fault. East of the MTL rocks of the Brook Street, slivers of Murihuku, Dun Mountain-Maitai, and Caples terranes are exposed bounded to the south by the Alpine Fault (Adamson, 1964; Johnston, 1990). Terranes to the NW of the Speargrass Fault Zone are obscured by Moutere Gravels of the Moutere Depression.

1.5.2 Late Quaternary Glacial History and Deposits

A succession of ice advances in the St Arnaud area have deposited various glacial units which have been subsequently offset along the Alpine Fault. Glaciers emerging from the Travers Valley have advanced and in some instances split at the present head of Lake Rotoiti and exited via either the Motupiko River or the Buller River Occasionally, ice from the Wairau Valley spilled over Tophouse Saddle into the Tophouse area (Adamson, 1964). Lake Rotoiti is formed behind a terminal moraine of the last major glacial

advance and breached by the Buller River exiting through the Speargrass Valley. An extensive outwash surface, the Speargrass Formation (Suggate, 1965), begins at the head of Lake Rotoiti and is incised by the Buller River. Johnston (1990) mapped the sediments of the progressively smaller successive ice advances on the basis of height above valley floor. Glacial formations mapped by Johnston (1990) are the Manuka, Harry, Tophouse, Roundell and Speargrass formations decreasing in age respectively. Adamson (1964) assigned different names to the glacial features of Motupiko, Kikiwa, Tophouse, Birchdale, Black Valley and Rotoiti formations respectively. Age constraints on the age of respective glacial deposits are poor (Adamson, 1964; Suggate 1988). Speargrass deposits are sub-divided into two parts and the older Speargrass Two deposits from Johnston (1990) are inferred to correlate with the 18 000 yr BP last glacial maximum (Suggate, 1988). Earlier Adamson (1964) refers to these deposits as the Black Valley deposits.

1.6 THESIS OUTLINE

Chapter 2 provides a detailed investigation of features along the fault trace in the study area. Offset features across the fault are investigated with the view to determine slip rate and single event displacements of the fault in this location. Small-scale fault features are also identified and their geomorphic evolution is investigated.

Paleoseismic trenching and selection of trench sites is the major component of Chapter 3. Data from the trenching is analysed and discussed, and a summary is presented of radiocarbon dates obtained. These dates together with structure and stratigraphy of the trenches are interpreted with respect to considering prehistoric rupture chronology and local geomorphic conditions in the Holocene.

Chapter 4 attempts to integrate findings from this investigation with previous paleoseismic investigations in a regional context to propose possible fault segment boundaries along the Alpine Fault. Fault segmentation proposals make use of all the available data, especially direct radiocarbon trenching dates and slip rates. Also discussed is the effect of slip partitioning to the MFS and its effect on the future seismic hazard on the northward continuation of the Alpine Fault.

An overall summary of slip determination, fault rupture, relevance to regional paleoseismic work, possible fault segment boundaries, likely seismic hazard and recommended future work is presented in Chapter 5.

Figure 1.4 is a location map of all the smaller site maps and figures referred to throughout the thesis, the trace of the Alpine Fault is also shown on this map.

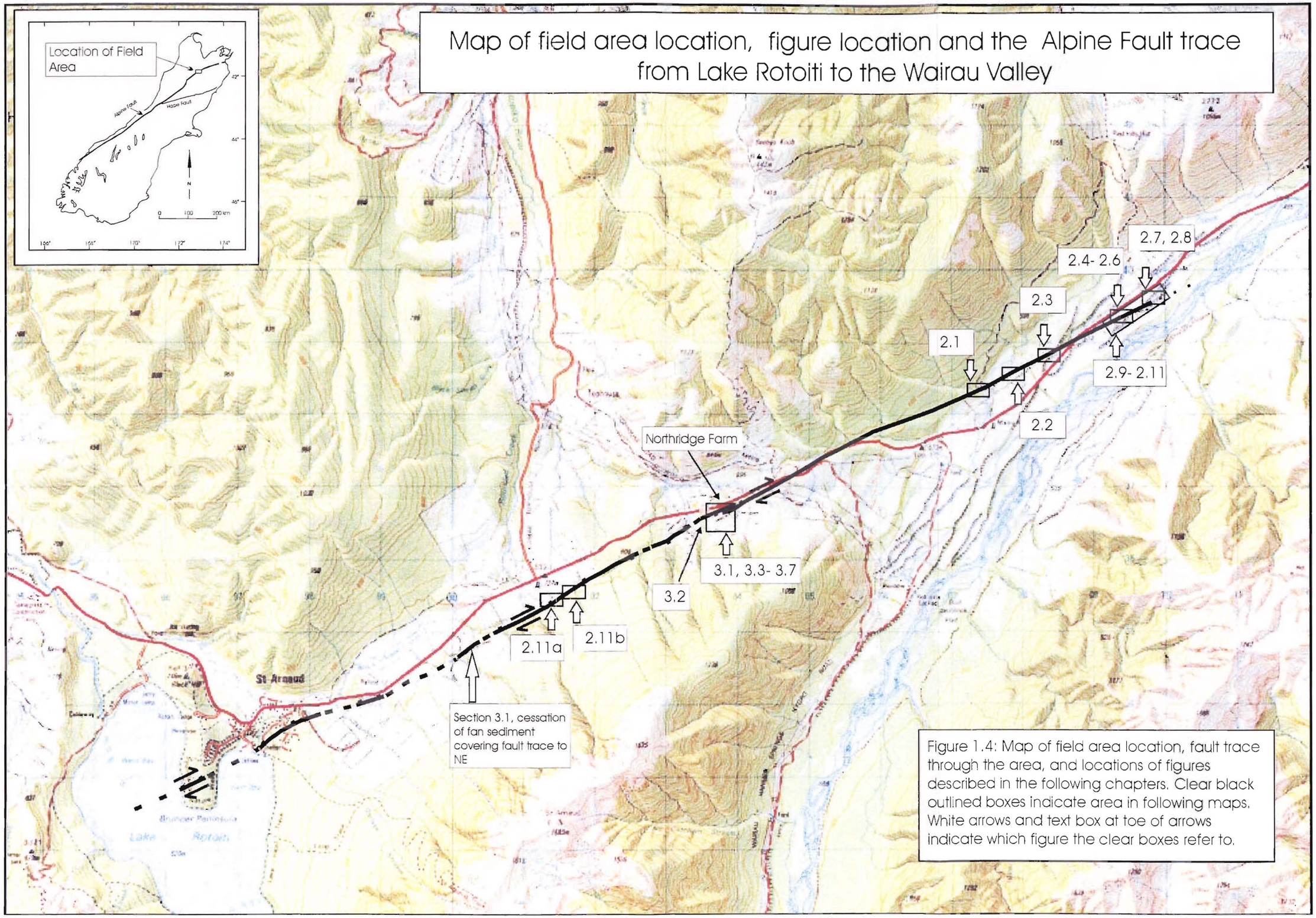

Figure 1.4: Map of field area location, fault trace through the area, and locations of figures described in the following chapters. Clear black outlined boxes indicate area in following maps. White arrows and text box at toe of arrows indicate which figure the clear boxes refer to.

CHAPTER 2

ALPINE FAULT CHARACTERISTICS AND SLIP RATE DETERMINATION

2.1 INTRODUCTION

A combination of paleoseismic and fault behaviour data is crucial when assessing paleoseismic history of a fault. Fundamental to all paleoseismic investigations is a comprehensive knowledge of fault characteristics, such as fault location, fault strike, single event displacements, and recognition, dating and documentation of offset features for long-term slip rate. This chapter provides an overview of general fault related features, followed by a detailed investigation of late Quaternary offset landform markers, fault related drainage, surface age constraints, fault related tilting, and evidence for fluvial and fault interaction, from which slip rates have been determined.

Fault investigation began at Lake Rotoiti and continued along fault strike, NE into Wairau Valley. Locations of figures in this chapter are shown in Figure 1.4 of Section 1.6 and Map 1. Most of the site names are unofficial names ascribed by the author for ease of reference, limited by lack of local geographic names but, where possible, some relation to known local points is incorporated in the site names.

Map needed

2.2 VARIATION IN STRIKE ALONG THE FAULT TRACE

Precisely locating the fault trace SW of Lake Rotoiti is complicated by relatively poor outcrop exposure and dense bush masking the fault location (Adamson, 1964; Johnston, 1990). The trace follows the range front at the base of the Mt Robert Range and begins to behave as a series of fault slivers overthrusting (Adamson, 1964) the footwall with continuing compression. A single trace clearly dissects the Brunner Peninsula, which protrudes into Lake Rotoiti. On the peninsula the fault trace offsets medial moraines dextrally and is upthrown to the SE. A summary of previously measured offsets is presented in Section 2.5 (Adamson, 1964; Campbell, 1973). Assigning a measure of separation to glacial moraines bears an associated error, as the surface profile is hummocky and irregular compared to often better-defined fluvial features (see Adamson, 1964).

Exiting Lake Rotoiti the active fault trace offsets Speargrass glacial features for the second time, allowing an offset comparison (see Section 2.5) and begins to diverge from the previous fairly constant strike of ~065°. The swing in fault strike appears as a minor releasing bend structure.

The Speargrass terminal moraine is offset (either side of the Refuse Tip, Figure 1.4) as the fault swings back to a more or less linear trace. Exact location of the trace is inhibited by numerous fan deposits derived from the slopes of the St Arnaud Range NE of the Speargrass terminal moraine. Further NE along the fault strike, near the upper reaches of the Black Water stream catchment, the fault displaces older glacial deposits, where entrenched drainage clearly delineates the fault trace position. However, fan slope deposits continue to mask the fault trace beyond this point. The fault has created linear valleys and shutter ridges (discussed in Section 2.3.6).

Towards Tophouse the fault progressively crosses older deposits forming a prominent fault scarp face, however, the most recent trace is often masked by fans and the degradation of scarps. As the fault enters the Tophouse area at the base of the St Arnaud

Range it is still remarkably linear crossing older till and moraine of the Tophouse advance, with local tilting wedges and small fault steps (see Section 3.2 & Map 1). With the progression of the fault trace into the Wairau Valley fault strike remains constant, but, the fault trace reverts to crossing Late Pleistocene and Holocene surfaces. Consequently, late Quaternary evolution of the fault can be studied in greater detail. Fault strike on the degradation terraces of the Wairau Valley is nearly linear, striking locally between 060 - 070°, and generally ~065°. However, a succession of local earth deformation features suggest even very minor swings in strike locally influence the fault expression (eg Johnston 1990 and Lensen 1976) (see Section 2.6).

2.3 FEATURES OFFSET BY THE FAULT

2.3.1 Old Tophouse Site

The Old Tophouse site is nestled at the base of the Tophouse Saddle in the Lower Wairau Valley. Prior to the turn of the century the Tophouse homestead was in the Wairau Valley, but now the homestead is situated at the head of the Motupiko River on the opposite side of the saddle. A clearly defined fault trace dissects the Old Tophouse site with different geomorphic features on either side of the fault (Figure 2.1). Vertical displacement on the fault is upthrown to the SE. Upthrow to the SE produces an uphill facing scarp forming a barrier to sediment derived from the Beebys Knob Range. Northeast of the Old Tophouse site the Wairau Valley degradation terraces commence, younging towards the active Wairau River channels. Old Tophouse marks the boundary of glacially derived lateral moraine and kame terrace material from the degradation terraces in the valley.

Geomorphic evolution of this section of the fault is complex. Assuming terraces B & B' (Figure 2.1) are related and are derived from a glacial aggradation surface, or early fluvial degradation surface, this defines the period where the fault, the stream and the terrace surface first interacted. From this time onwards successive dextral ground ruptures on the fault have disrupted drainage. A broad 4 metre deep abandoned channel

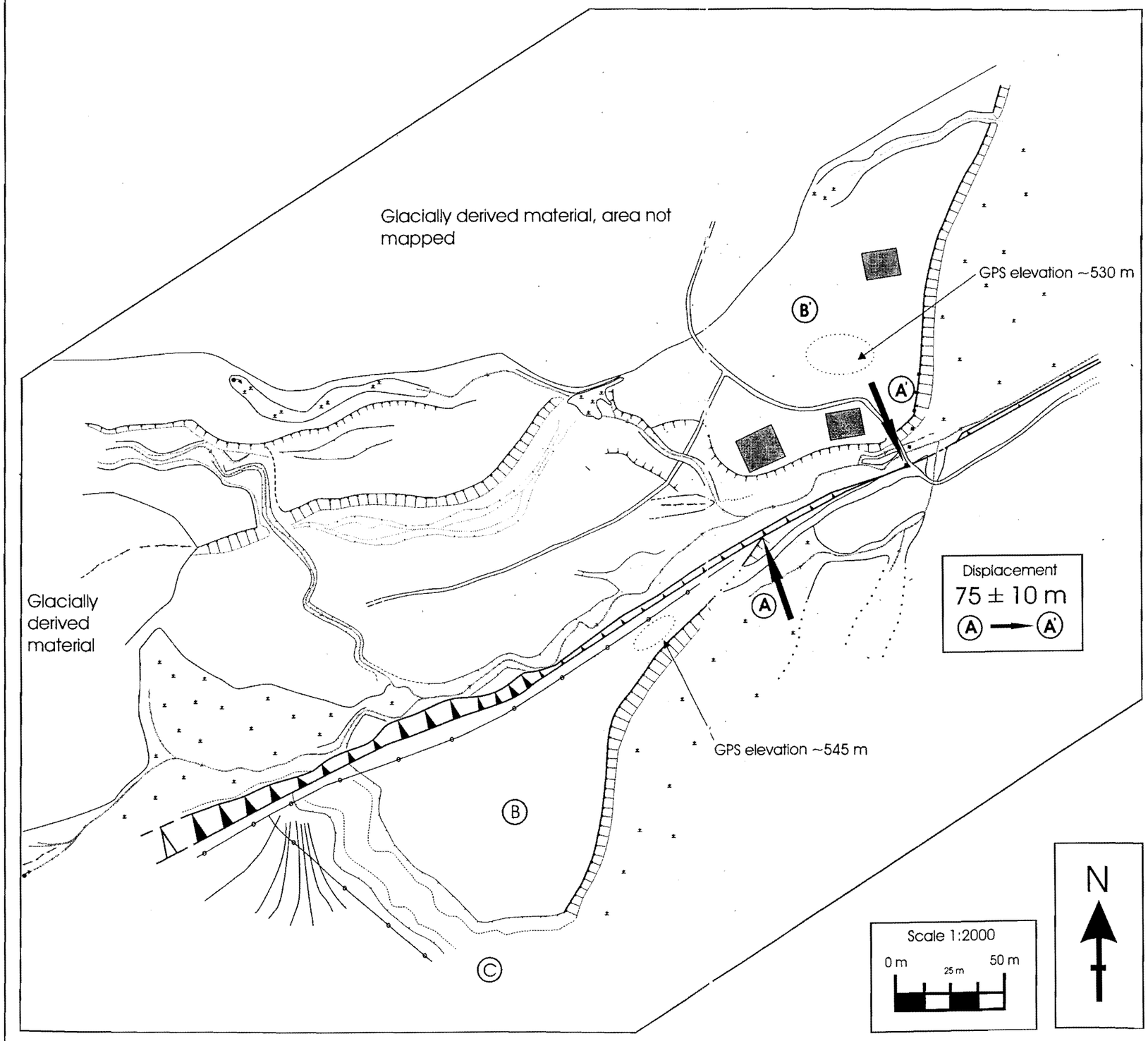

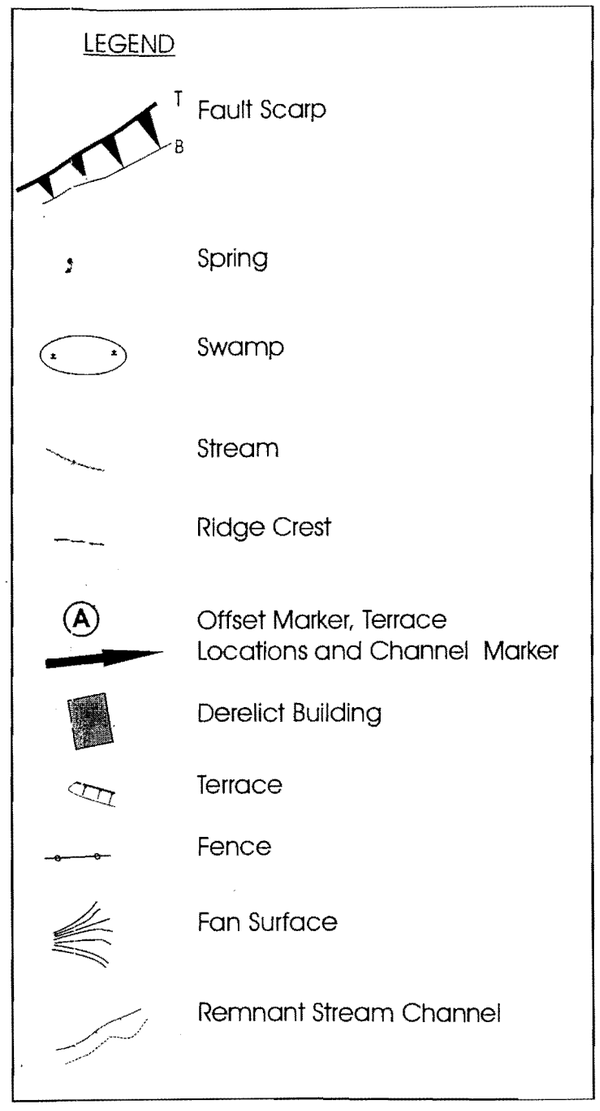

Figure 2.1: Geomorphic map of the Old Tophouse site, showing displaced terrace and abandoned stream channel. Tree and bush cover not shown for clarity.

has incised into the main terrace tread (C & B in Figure 2.1 respectively). Erosion of a channel this size requires a stream of substantial power; at present the only capable local stream is diverted along the fault trace to the NE, eventually flowing into Six Mile Creek. It appears that movement on the fault failed to deflect the stream initially. The stream continued on its original path as the SE side of the fault was uplifting the stream eroded into terrace B. The stream subsequently became entrenched in channel C. Initially, stream deposition on the NW side of the fault kept pace with fault displacement allowing the stream profile to rise; preventing deflection downslope on the NW side of the fault. Successive ground ruptures on the fault eventually forced the stream to abandon its original entrenched channel (C in Figure 2.1).

Projection of the active stream channel to the fault plane determines an offset estimate to the remnant channel of about 40 m. An approximate 40 m offset suggests the stream was entrenched across the fault for multiple events before diversion when it is compared to the 75 ± 10 m of the main offset terrace riser. Horizontal offset near Lake Rotoiti at Black Valley I terminal moraine is 85 ± 12 m (Adamson, 1964). Offset is slightly larger in comparison to the Old Tophouse displacement of 75 ± 10 m. At Branch River terraces the oldest offset surface is offset horizontally by 60 to 70 m with a vertical component of about 1 m upthrown to the SE. This surface was assigned to the Wairau Surface (Lensen, 1968) which is equivalent to the last glacial maximum outwash surface at Old Tophouse, and there is general agreement between horizontal separation of similar age deposits from the late Pleistocene at three sites along the fault. It is clear, however, that there is a disparity between the vertical component on the fault between the Branch River terrace and the Black Valley I terminal moraine. This is discussed further in Chapter Four. Vertical separation on the fault at the Old Tophouse site is outlined below.

Of particular importance at the Old Tophouse site is the nature of terrace B'. Is it either an original surface, or a modified version of terrace B. GPS measurements from the terraces B & B' in areas clear of trees provide vertical elevations of ~545 m and ~530 m, SE and NW of the fault trace respectively (Figure 2.1). Assuming that this terrace set (terrace B & B') is younger than 18 000 yrs old implies a vertical separation on the order of 15 m since the last glacial maximum (~18 000 yrs BP; Suggate, 1988). Assuming that

the vertical offset measured by Campbell (1973) of 12 ± 4.5 m and 9.7 ± 4.5 m on offset Black Valley I & II moraines respectively are of similar age to the Old Tophouse site, vertical separation can be accounted for by uplift rates alone, equating to an uplift rate of ~0.8 mm/yr over the Holocene and late Pleistocene period. Any erosion of terrace B' would increase apparent vertical separation and would augment apparent uplift rates, suggesting the uplift rate of ~0.8 mm/yr is a maximum rate.

2.3.2 Pylon Creek Site

At the Pylon Creek site the fault cuts a series of terraces and abandoned stream channels (Figure 2.2). Topography on the NW side of the fault is more subdued relative to the SE, and hence precisely locating and matching features on either side of the fault trace was complicated. Land cultivation has modified other geomorphic features along the fault trace in addition to the Pylon Creek site. Lensen (1976) classified these modified features as surface flexures. Definitive location of singular corresponding geomorphic features is slightly ambiguous, especially on the NW side of the fault at the sites of intensive modification. A series of offset geomorphic features at Pylon Creek of similar spatial intervals replicated either side of the fault increased confidence that the markers matched. Two river terraces and an abandoned stream channel are identified in Figure 2.2 either side of the fault trace at the Pylon Creek site.

The terraces and abandoned stream channel were formed by fluvial processes associated with the Wairau River flowing from the SW, obliquely across the fault, followed by subsequent downcutting and eventual abandonment of the channel. Horizontal separation at this site infers dextral fault movement with a minor component of vertical separation, upthrown to the SE. Upthrow to the SE is not ubiquitous for the length of the fault trace however, both in this study area and further NE along the fault trace (Lensen, 1976).

EDM measurements concentrating on the top and base of the offset terraces provided displacements of 53 ± 3 m and 54 ± 3 m, for Terrace One and Two respectively (Figure 2.2). Errors associated with these measurements are predominantly the result of difficulty in defining the apex flexures of the offset terraces. Although the EDM technique does

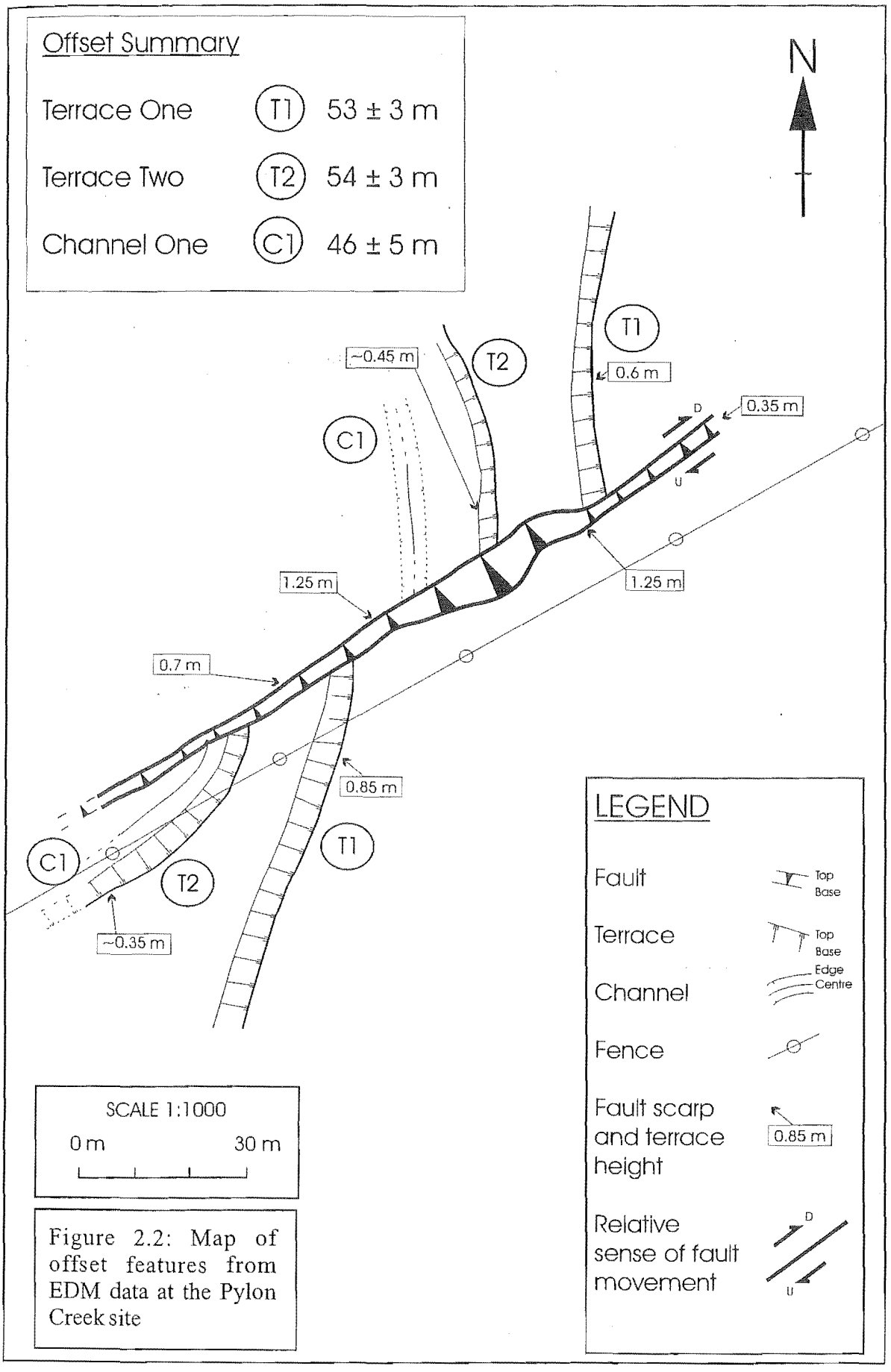

Figure 2.2: Map of offset features from EDM data at the Pylon Creek site

have an associated error it is minimal relative to that associated with correct and accurate identification of the features. The offset abandoned stream Channel One has a greater error, 46 ± 5 m as delineation of the channel centre on the NW side of the fault was complex, and extrapolation to the fault scarp compounded this error. Fortunately, the offset features strike approximately perpendicular to the fault trace, thus avoiding geometric problems associated with offset features oblique to the fault zone.

Channel One (C1) is offset less than the two terraces, and is inferred to be the youngest of the trio of offsets. The close association of terrace with a relatively ephemeral channel implies similarity of age, so the terrace offsets and the channel offset should be virtually identical. In the event that the channel was active at a time of ground rupture, it could have been deflected along the fault scarp. With subsequent ground ruptures the stream may have encountered difficulty continuing this elongate course, possibly ponded briefly, and created a new channel. The axis of C1 is further from the base of T2 suggesting that it straightened its course after a rupture event. The original channel has been concealed by sediments, followed by the terrace abandonment and subsequent upthrow on the SE side of the fault.

Lack of suitable surface rocks precluded any weathering rind dating of geomorphic surfaces at Pylon Creek. The age of the surface must be younger than the last glacial maximum (~18 000 BP; Suggate, 1988), as the river terraces are degradation terraces cut into the aggradation surface associated with the last glacial maximum.

2.3.3 Pylon Terrace Site

A prominent 15 m high terrace riser and a smaller terrace are offset by the fault at the Pylon Terrace site (Figure 2.3). The offset terrace riser links the two most extensive terrace degradation surfaces along the fault trace between the Old Tophouse site and the active Wairau River surface (see Map 1). Extensive land cultivation at the Pylon Terrace site for farming and power purposes has reduced most of the smaller geomorphic features to flexures (eg Lensen, 1976) on the ground surface. Below the main offset terraces recognition of the fault trace is difficult although it appears to be a single fault

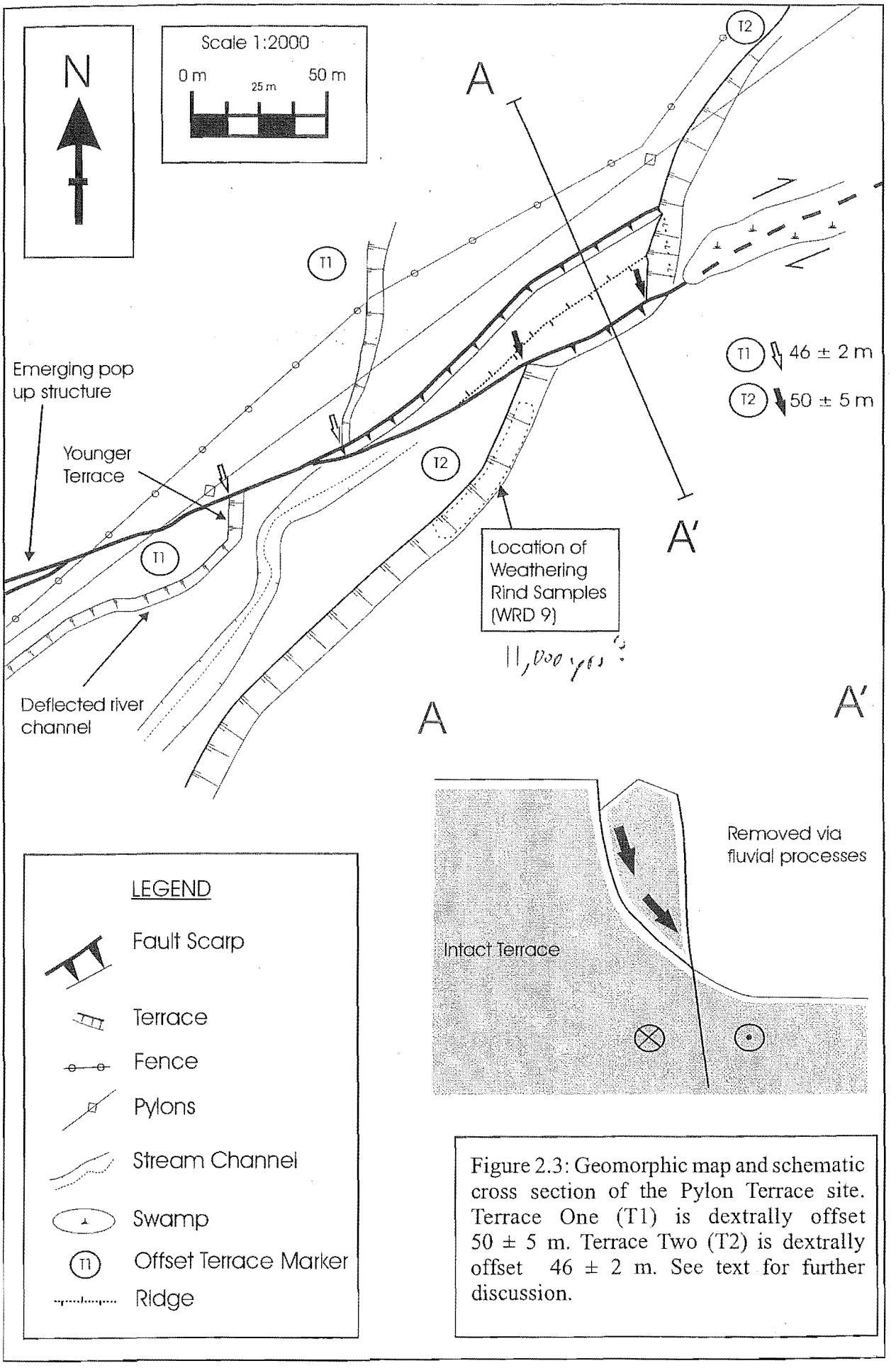

Figure 2.3: Geomorphic map and schematic cross section of the Pylon Terrace site. Terrace One (T1) is dextrally offset 50 ± 5 m. Terrace Two (T2) is dextrally offset 46 ± 2 m. See text for further discussion.

trace with minimal vertical separation, and striking approximately 065-066°. No displaced geomorphic features are visible, extensive cultivation and bulldozing of scrub material onto the predicted trace of the fault conceals any relevant information.

Geomorphic features are easily recognisable on the higher terrace. Modification by cultivation still prevents accurate location of some features and parts of the fault zone are infilled with scrub debris. Two offset features are recognised and measured, both of which display dextral horizontal separation with minimal vertical separation (Figure 2.3). Separation of 46 ± 2 m (T2) and 50 ± 5 m (T1) of the smaller and larger terraces respectively is similar to the offsets at the Pylon Creek as the offset surface is still the same general surface as at the Pylon Terrace site, presumably crossed by braided strands of the river over the same general time interval prior to the marked drop to below T2.

At the larger terrace (T2), the truncated terrace edges are naturally eroded. A complication arises in accurately defining the edges of the truncated terraces of T2. It appears that the northern fault splay is acting as a land-slump slip surface (see cross section in Figure 2.3). The presence of the small northern fault provides a slip plane for a down dropping tilting wedge, or allows a small surficial slump to slip on the fault splay surface. With each successive ground rupture displacement, more toe support is removed, or toe support effectively decreases, and further gravity-induced slip ensue. As offset T2 is similar to the better-defined T1 offset and also comparable to the offsets described previously at the Pylon Creek site, it appears that the effect on horizontal separation of the fault splay landslip is relatively minor. Figure 2.3 shows a clearly defined ridge between the fault splays that is approximately parallel to the fault trace splay indicating relatively homogeneous internal slip to the SE where the fault scarp is unsupported.

2.3.4 Matagouri Terrace

A minor terrace riser is offset dextrally at the Matagouri Terrace site (Figure 2.4). Identification of geomorphic features at the Matagouri Terrace site is relatively straight forward, with most features clearly defined or indicated by surface flexures (Figure 2.5).

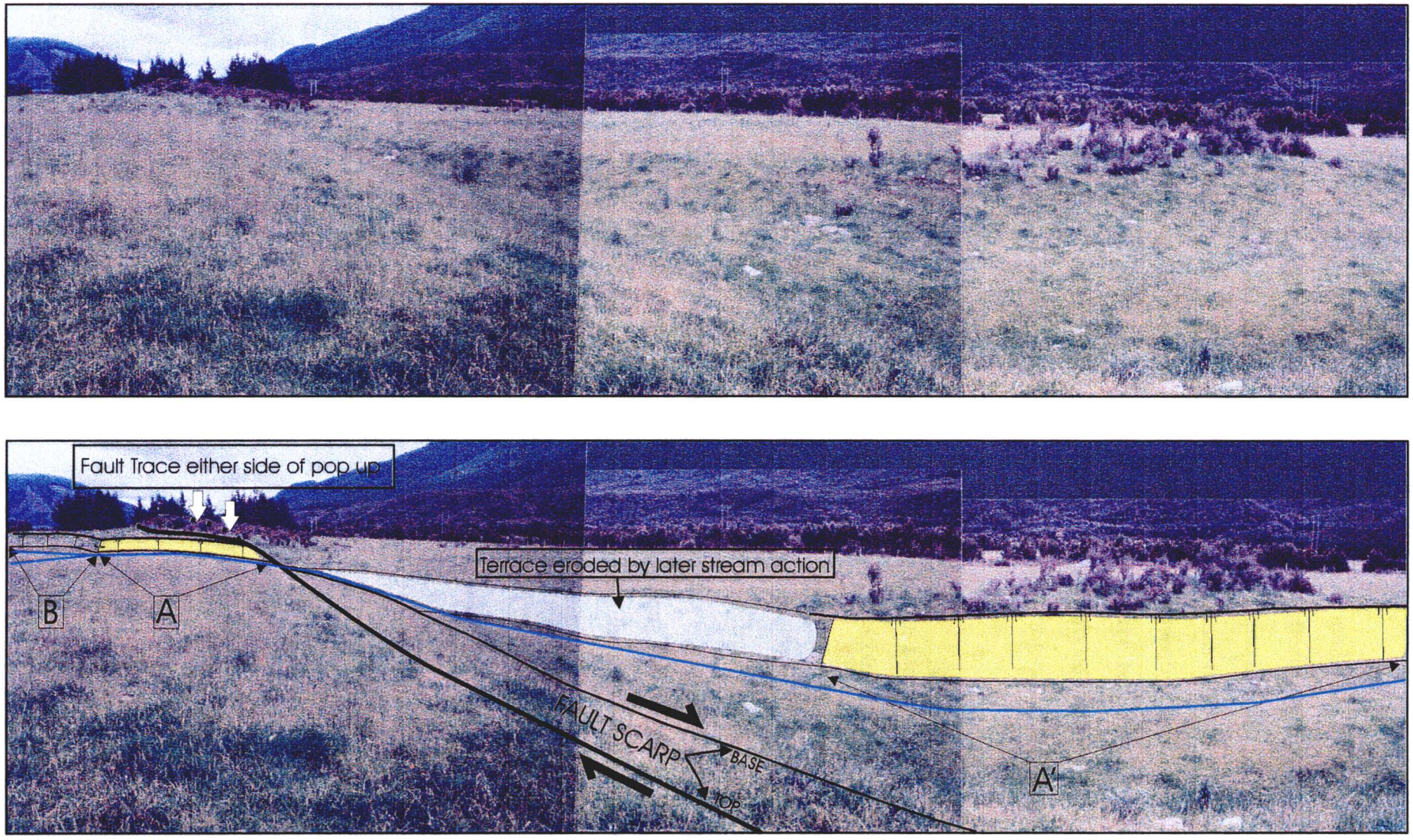

Figure 2.4: Photomosiac of the offset terrace at the Matagouri Terrace site. A to A' offset terrace (yellow), B older truncated terrace

There is one particular instance where natural erosion processes inhibit accurate offset determination. Erosion of the leading edge of the NW terrace has effectively reduced the apparent offset to zero. Other evidence suggests this cannot be the case and there must be an offset on the order of 15 metres. Closer inspection reveals a series of small remnant stream channels coalescing on the SE side of the fault, that subsequently cross the fault where they have eroded the leading edge of the truncated terrace and developed a channel at the base of the NW offset terrace. Fortunately, the area eroded is minor and an estimate of offset can be obtained by extrapolating the remnant original terrace to the fault trace (Figure 2.6a).

A horizontal separation of 19 ± 2 m and vertical separation of 1.75 ± 1 m across the fault are determined from extrapolation of the remnant offset terraces, accurately located by GPS data points (see Figure 2.6a). The extrapolation method assumes a vertical or near vertical fault plane projected up from the base of the degraded fault scarp. The top and bottom break in slope bounding the unmodified part of the terrace riser was then projected onto the fault plane parallel to the strike of the riser face (Figure 2.6a) yielding a net slip of 19 ± 2 m. Dip of the fault plane is about 70° SW along fault strike near the Northridge Farm (see Chapter 3), therefore a vertical projection of the fault plane slightly decreased the net slip. At the Matagouri Terrace site the structure contours for a 70° SW dipping fault plane do not fit the topography well, although assuming a sub vertical fault plane agrees with the topographic contours.

Vertical separation of 1.75 ± 1 m at the Matagouri Terrace site was calculated from two topographic transects parallel to the fault trace delineating the offset terrace (Figure 2.6b & Figure 2.6c for transect location). To reconcile the vertical separation the location of the unaltered offset terrace was corrected relative to horizontal separation (Figure 2.6b). Projection of the relative height of the terrace provided a vertical separation of 1.75 ± 1 m.

Geomorphic evolution of the Matagouri Terrace is discussed further in Section 2.6 with a detailed investigation of the site using GPS data.

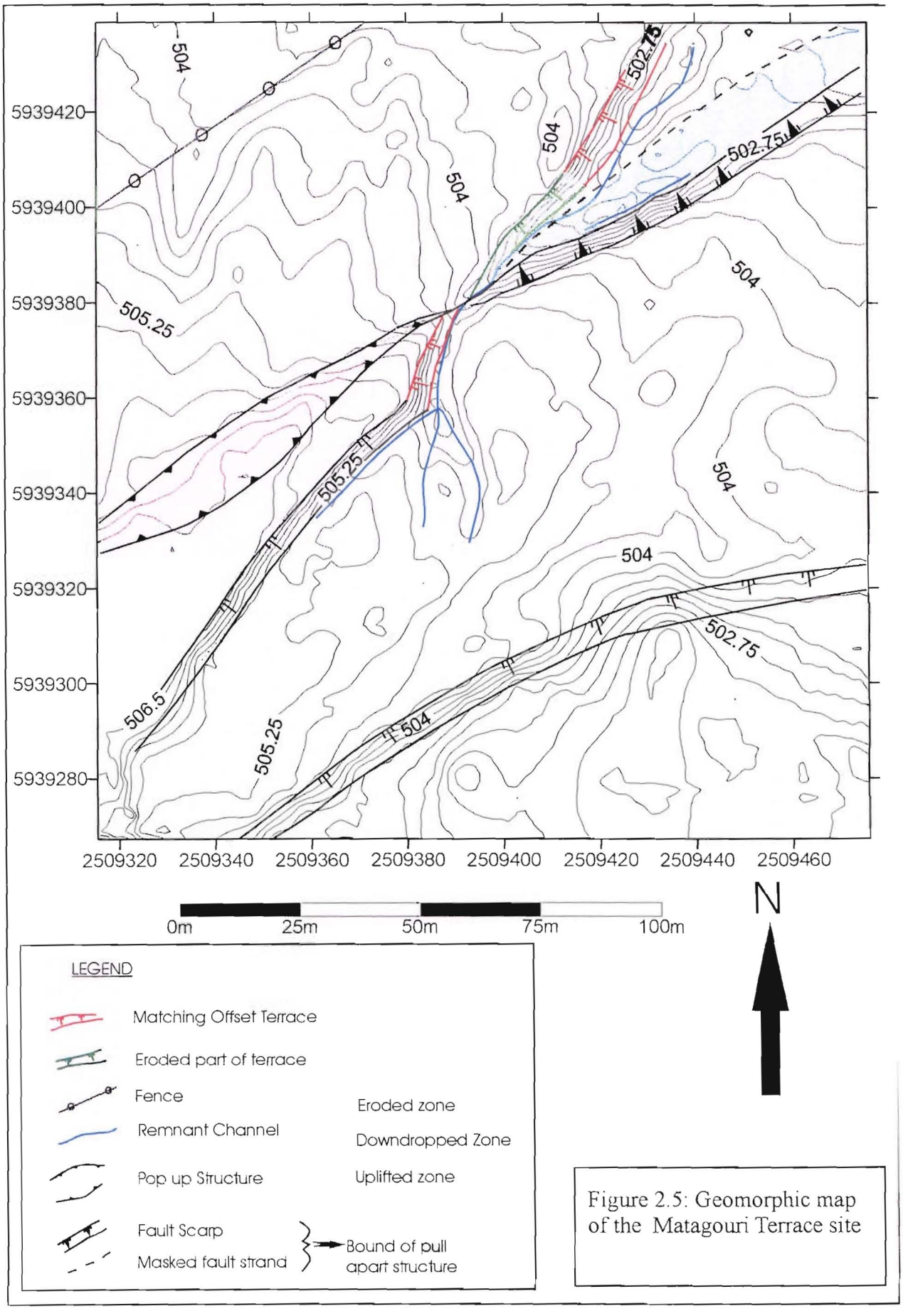

Figure 2.5: Geomorphic map of the Matagouri Terrace site

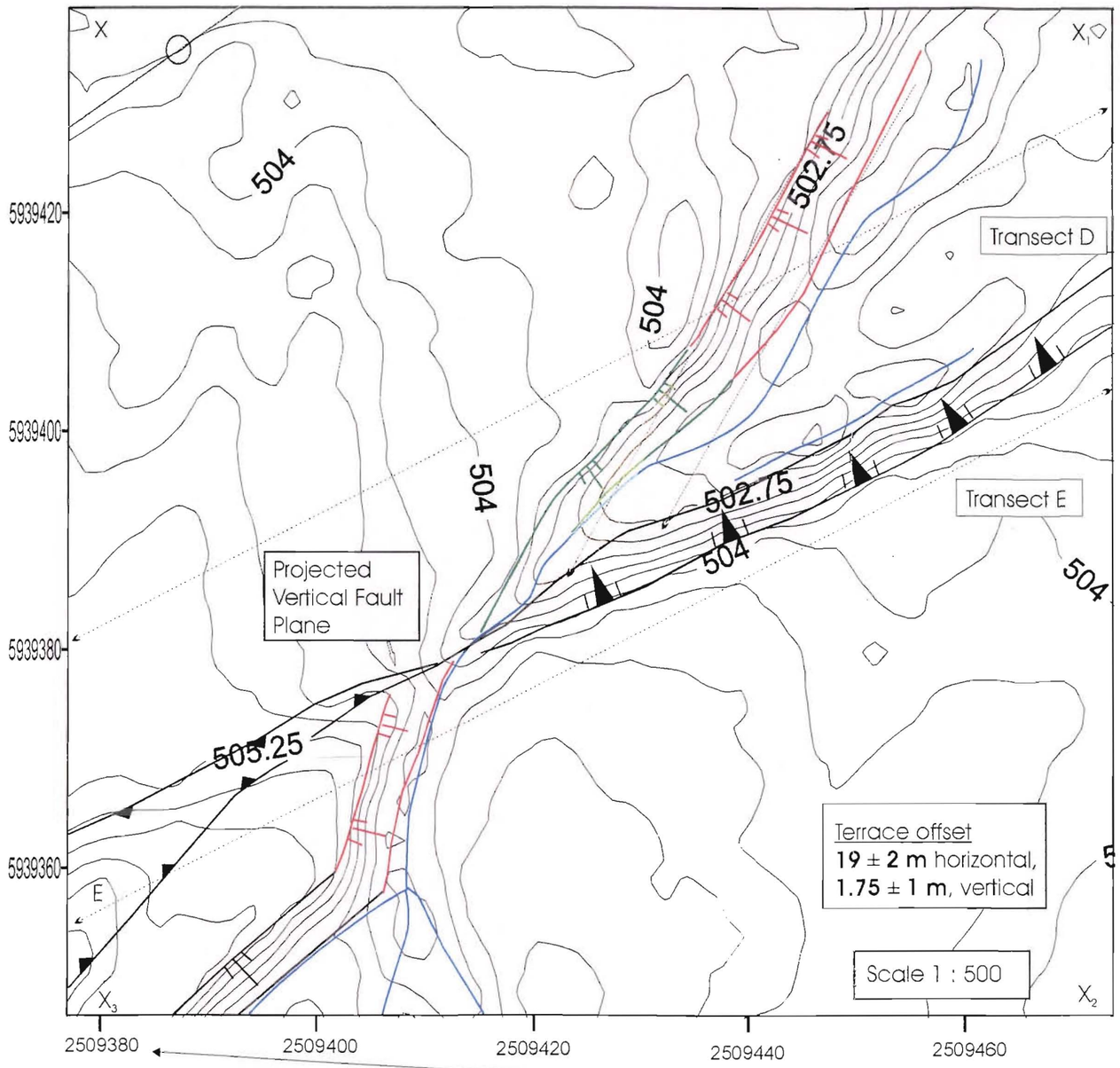

Figure 2.6a: Geomorphic map of Matagouri Terrace showing projection of the eroded northern terrace to the fault scarp, and part of transects D & E

Figure 2.6: Geomorphic map of Matagouri Terrace outlining horizontal and vertical separation across the fault trace

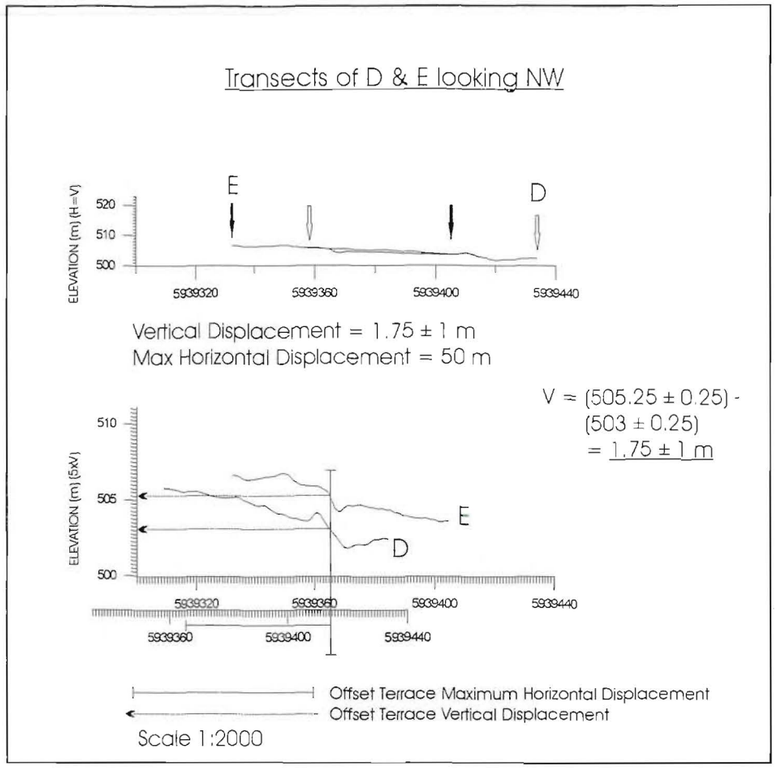

Figure 2.6b: Transect D & E determining veritcal displacement and maximum horizontal separation.

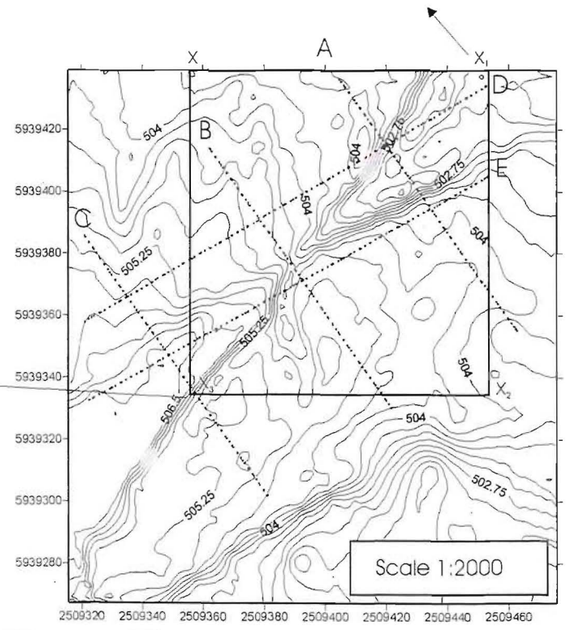

Figure 2.6c (Right): Transect locations relative to 0.25 m contour interval of Matagouri Terrace site, and location of enlarged contour box (Figure 2.6a)

2.3.5 Three Weddings Terrace

Horizontal separation between offset markers progressively decreases further NE along the fault trace as the displaced degradational terraces young in a similar direction. At the Three Weddings Terrace site, a terrace oblique to the fault trace is offset dextrally by 4.4 ± 0.5 m and upthrown to the SE (Figures 2.7 & 2.8).

Fluvial processes eroded the main terrace (T1) and occupied the lower surface for a period. Prior to ground rupture the channel abandoned this inner part of the terrace tread and a fault rupture ensued. The trace of this rupture is preserved here but vanished on the NE outer edge of the same surface, where, perhaps the river was still active. Vertical separation is now partially visible on the lower terrace tread of Figure 2.8, probably as a result of juxtaposing different topographic features. Surface bulging on the SE side of the fault is also noted (see Figures 2.7 & 2.8; discussed in Section 2.6). Offset of the main terrace at the Three Weddings site indicates a 4.4 ± 0.5 m single event displacement, and is likely to represent the most recent ground rupture.

Lensen (1968) analysed the Branch River terraces and suggested average lateral displacement along the Wairau Fault of between 17 and 22 ft (5.2-6.7m). Detailed investigation along much of the length of the fault by Lensen (1976) revealed single event displacements of about 5-7 m. Single event displacements of this order correlate well with the 4.4 ± 0.5 m displacement at the Three Weddings site. Studies elsewhere, notably Sieh (1978), have shown that single event displacements can vary markedly along the length of a fault. Sieh (1978) recorded single event offsets ranging from 3.0 – 9.5 m over a 300 km section of the San Andreas Fault, California. With only one single event displacement recognised along the studied section, commenting on any variation of single event displacement along the Wairau Section of the Alpine Fault is imprudent. A 4.4 ± 0.5 m offset is comparable to the previously recorded single event displacements of Lensen (1968). In conclusion, the present study area has an offset terrace recording a single ground rupture event of 4.4 ± 0.5 m, which is consistent with the displacement range of 5.2–6.7 m of Lensen (1968).

Figure 2.7:
Photomosiac of the offset terrace at the Three Weddings site.

Surface bulging, bulging decreasing from tail to point of arrow

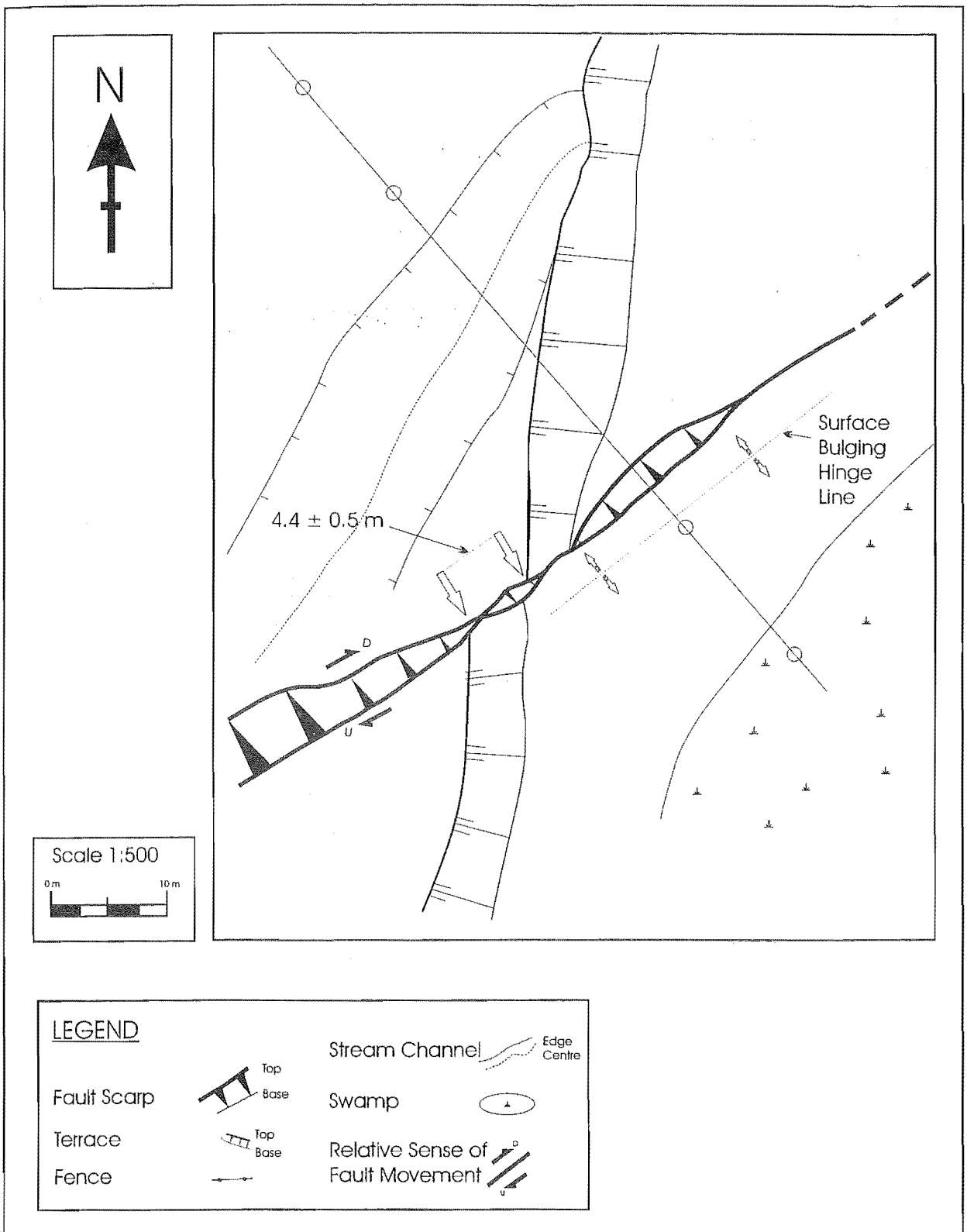

Figure 2.8: Geomorphic map of Three Weddings offset terrace. Terrace offset 4.4 ± 0.5 m. See text for further discussion.

This last surface to show evidence of a fault trace is truncated by a younger fluvial terrace, which shows no sign of offset. Beyond this point flights of low terraces and irregular channel topography conceal the fault trace NE of the Three Weddings site with the trace shown on Figure 2.8 being the last definitive location of the trace. Investigation NE along the estimated projection of the fault trace to the active Wairau River surface failed to locate any evidence of faulting, indicating that the bounding terrace formed post the last rupture event (see Figure 2.9 & 2.10).

2.3.6 Fault Related Drainage Features

Drainage features along the fault trace are characteristic of strike slip environments with many streams being deflected along the fault strike. Landforms characteristic of strike slip environments play an important role as a stream's course is directly affected by the landforms it encounters. Landforms characteristic of strike slip environments described by Keller (1986) and found in the study area include linear valleys, shutter ridges, sag ponds, scarps and linear springs. As the fault trace strikes perpendicular to the prevailing drainage direction along the base of the St Arnaud Range, larger offset drainage features are visible from topographical maps. Stream channels are more entrenched on the Lake Rotoiti side of Tophouse Saddle as the deposits are older and create a greater topographic barrier to water flow, forcing streams to maintain their original channel even though the stream length is increasing with each subsequent rupture.

2.3.6.1 Lake Rotoiti to the Wairau Valley

Numerous examples of fault related drainage anomalies are identified NE along fault strike from Lake Rotoiti. Firstly, erosion along the fault scarp has allowed streams to flow into Black Valley Stream towards Lake Rotoiti via the fault breached Late Otiran Speargrass glacial loop moraine (GR 992342). In addition, a linear series of fault springs NE of the fault breach (GR 992342) flow along the eroded fault scarp. Further NE along the fault trace (GR 997346) three streams coalesce, cross the fault, and flow into the Black Valley Stream.

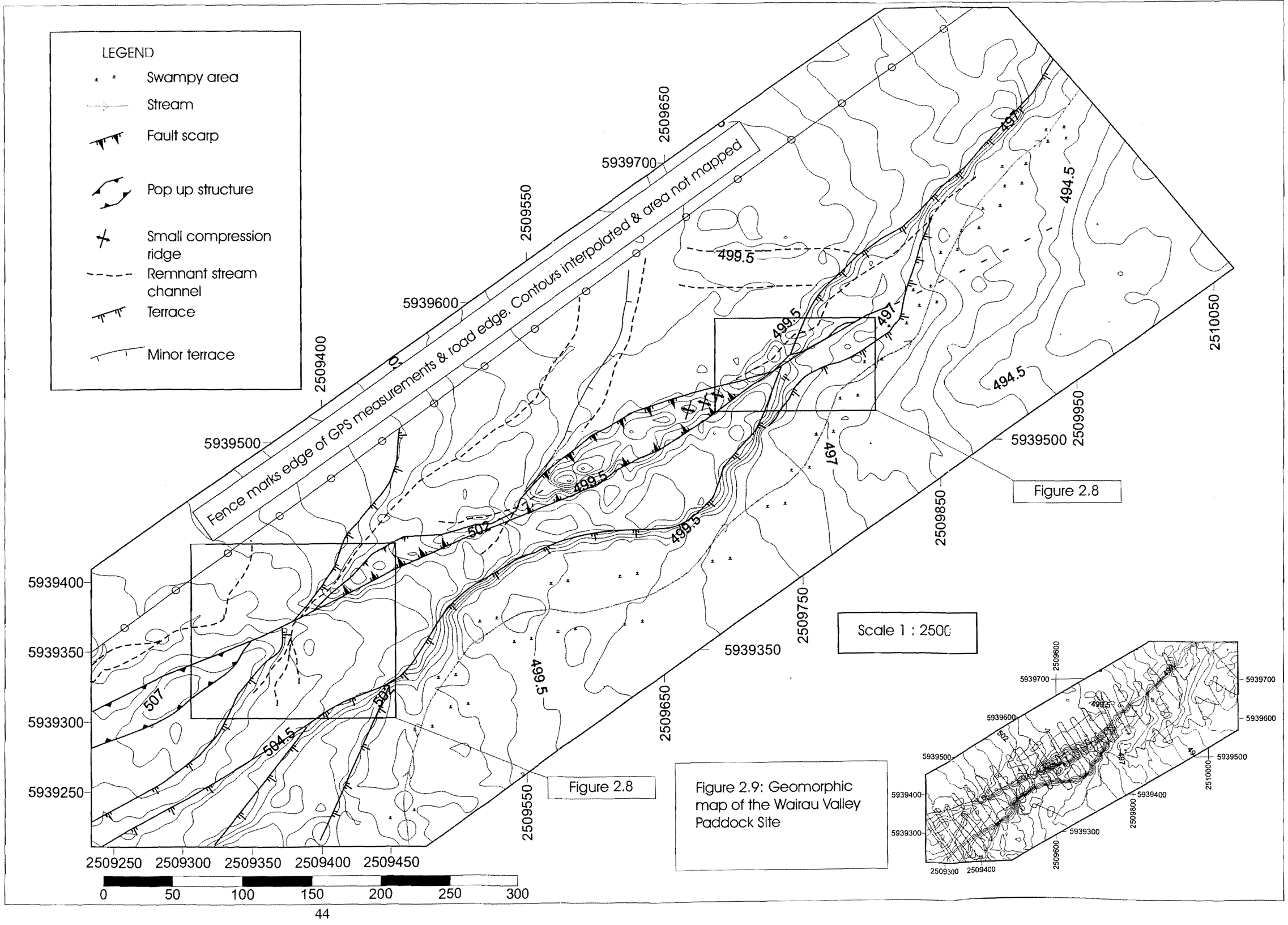

Figure 2.9: Geomorphic map of the Wairau Valley Paddock Site

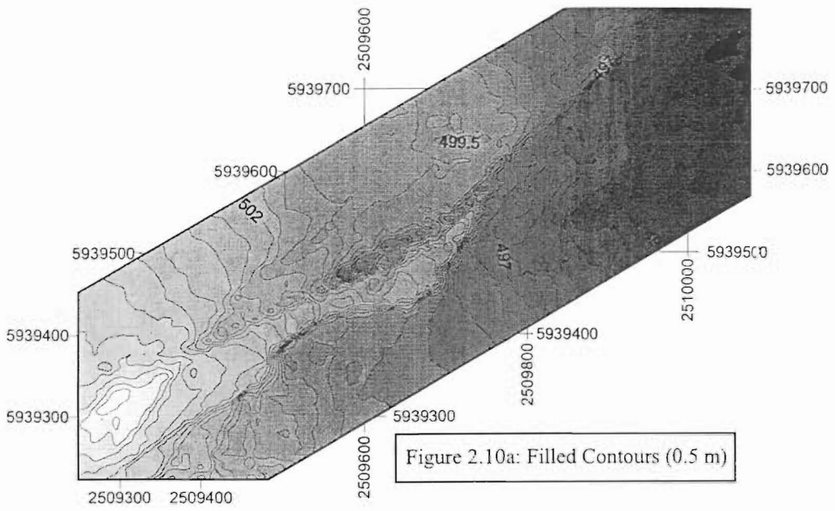

Figure 2.10a: Filled Contours (0.5 m)

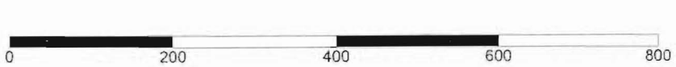

Scale 1: 800

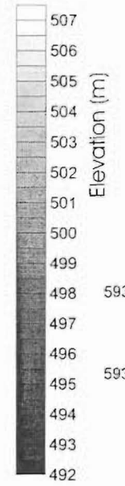

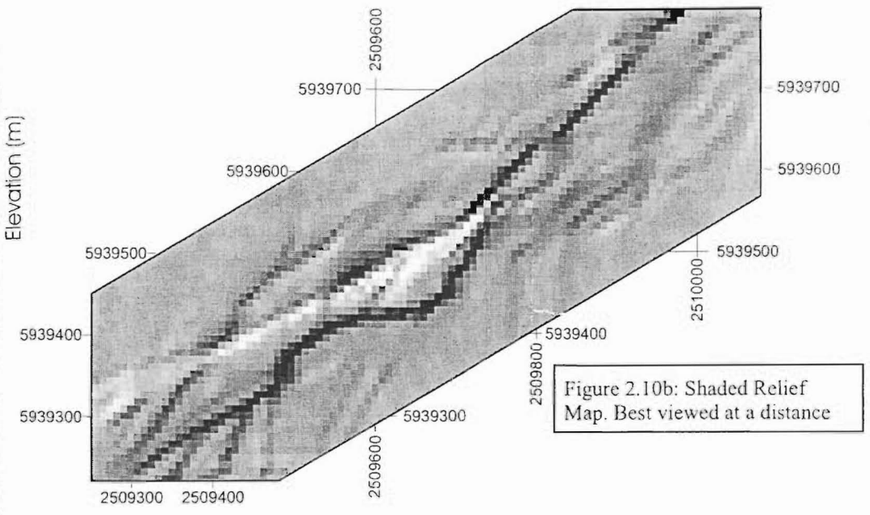

Figure 2.10b: Shaded Relief Map. Best viewed at a distance

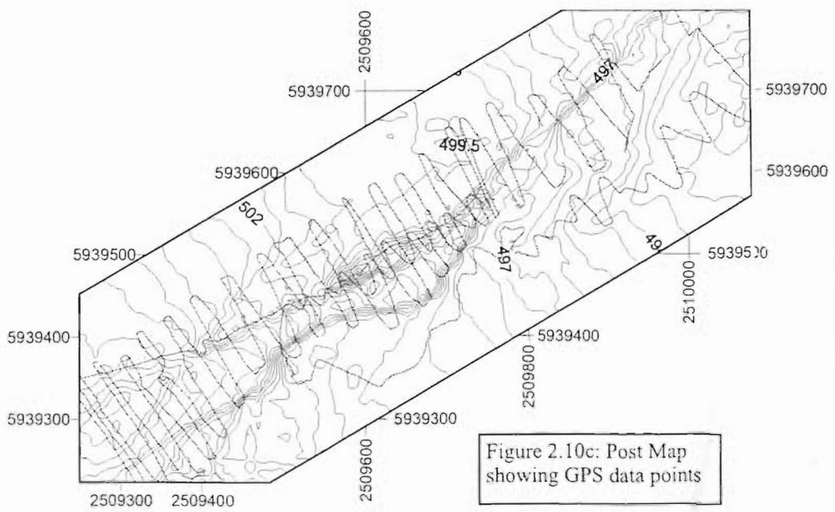

Figure 2.10c: Post Map showing GPS data points

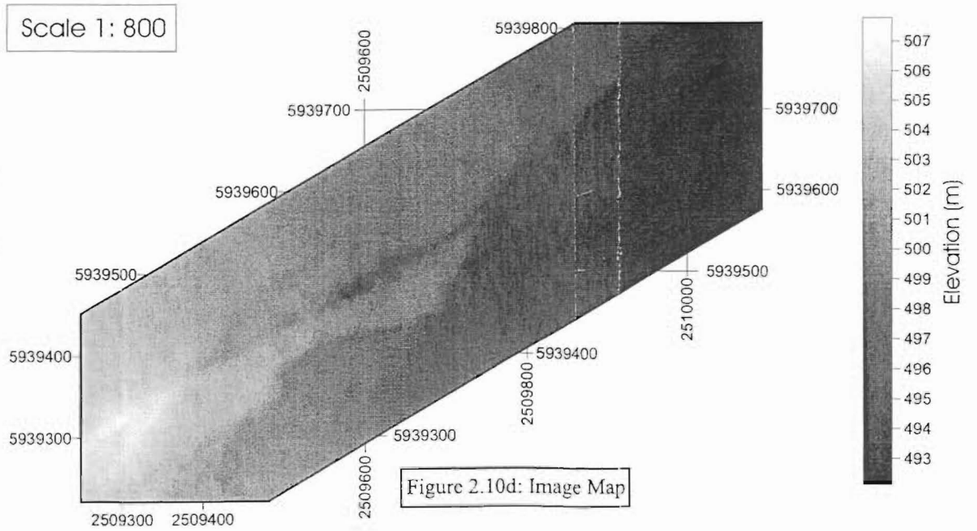

Figure 2.10d: Image Map

Figure 2.10: Surfer images of the Wairau Valley Paddock site.

The watershed between the Black Valley and Motupiko catchments is formed by the remnants of the Tophouse glacial advance loop moraine (GR 008352) (Adamson, 1964). The last stream in the Black Water catchment is deflected to the NE around a shutter ridge. This stream subsequently flows to the SW once it passes the leading edge of the shutter ridge as the topography is sloping to the west.

2.3.6.2 Two Adjacent Streams Deflected in Opposite Directions

Two adjacent streams exit the native forest behind the Woodrow Cottages (GR 015355 & GR 017356) and are subsequently deflected in opposite directions along the fault trace (Figure 2.11). In both instances a shutter ridge has been faulted dextrally creating a barrier perpendicular to stream flow. In the case of Figure 2.11b, the stream is deflected to the NE where it breaches the shutter ridge and exits the fault zone. Dextral offset of the stream to where it breaches the fault is approximately 53 metres. Upstream of the fault the stream channel is entrenched up to 10 m below the average topographic slope, as the stream exits, crossing the fault trace, incision of the shutter ridge is of the same order.

Deflection to the SW of the stream shown in Figure 2.11a is approximately 36 metres before it breaches the shutter ridge. This stream is deflected in the opposite direction to the majority of the streams along the fault. As the sense of displacement on the fault is dextral most of the streams are deflected to the NE if they enter the fault zone from the south and continue to be displaced for as long as they remain entrenched behind a topographic barrier. However, occasionally the path of least resistance for the stream is deflection to the SW (Figure 2.11a). In this particular instance the downslope (NW) side of the fault has an apex between two stream channels. As the apex passes the entrenched stream course deflection of the stream to the SW is more efficient. A large remnant channel is encountered between the streams of Figures 2.11a&b and is probably the original channel path of the stream in Figure 2.11a before it encountered the apex of the downslope surface and deflected to the left. A process of stream damming post rupture, stream ponding and stream escape via a topographic low point, subsequent accelerated

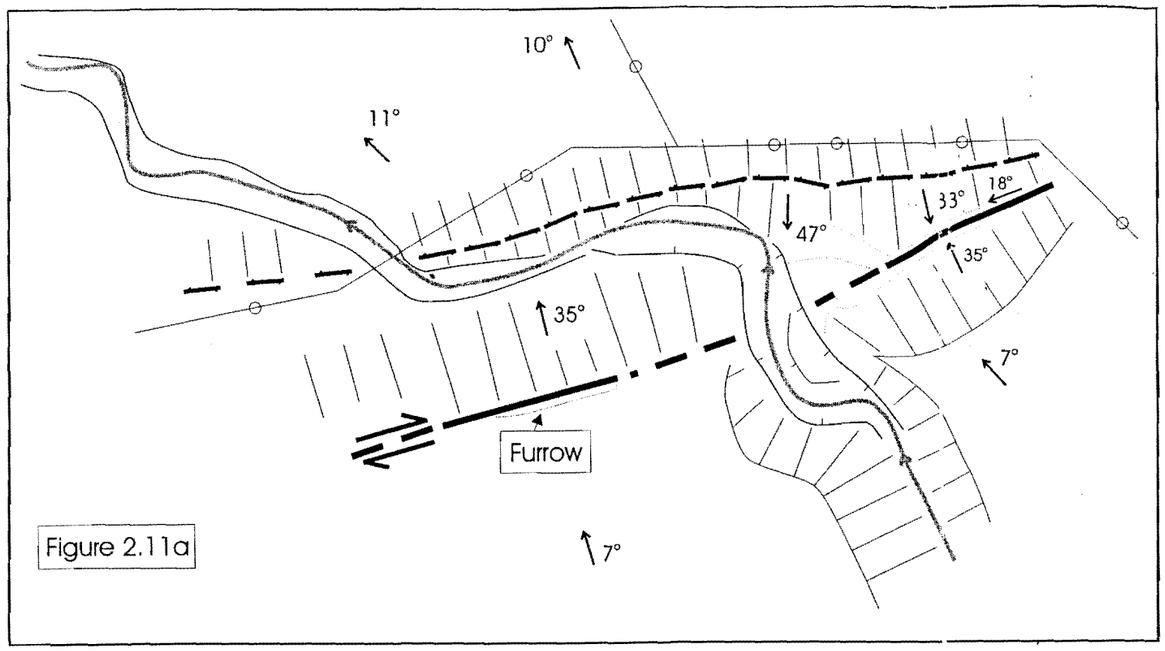

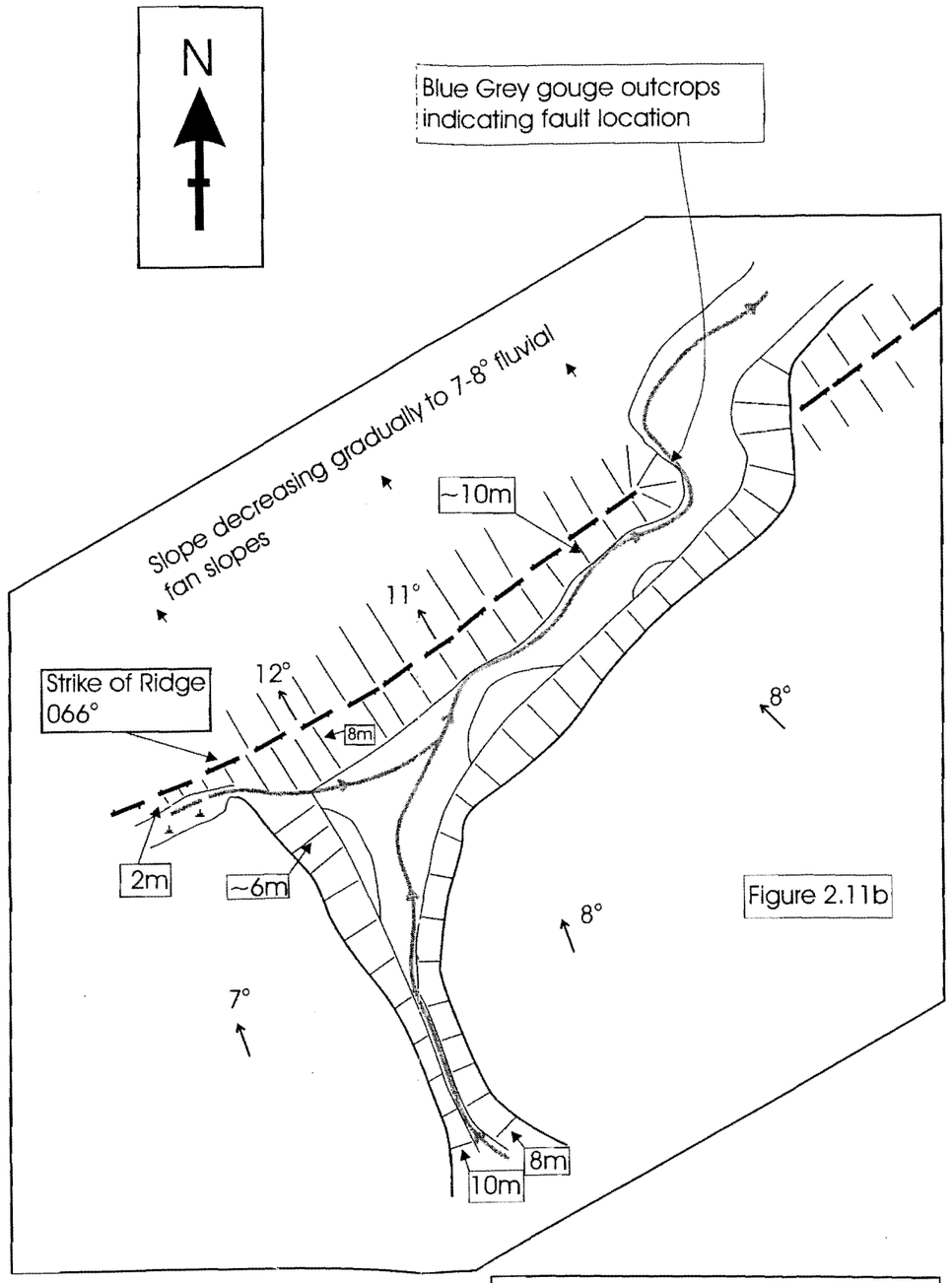

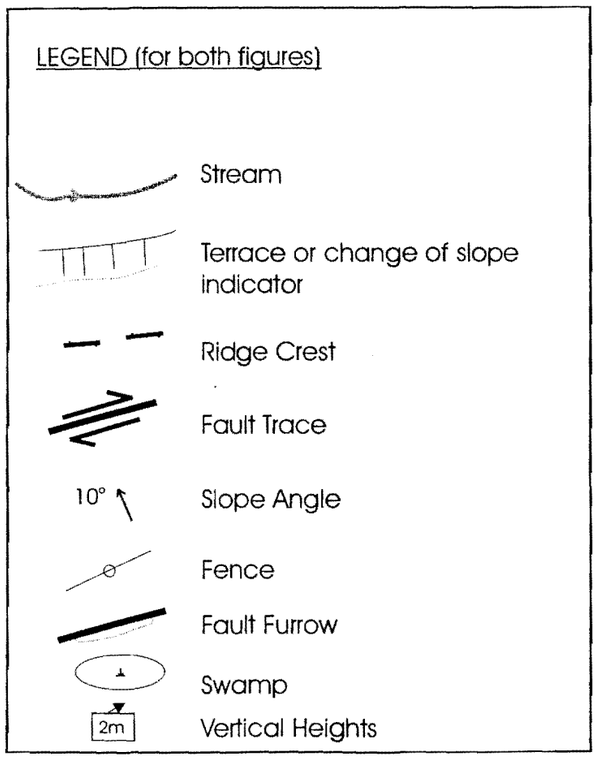

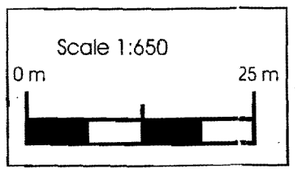

Figure 2.11: Adjacent stream channels flowing from the St Arnaud Range deflected in opposite directions by the fault behind Woodrow Cottage. See text for discussion (Section 2.3.6).

topographic incision and final abandonment of the original channel describes the evolution of Figure 2.11a. Eventually, assuming continued faulting, the exiting stream channel will re align with the upslope entrenched stream and begin to be deflected to the NE with continued faulting in a similar fashion to Figure 2.11b. In order for the deflected streams to change their course remnant lower topographic points on the shutter ridge must align with the entrenched stream or erode into the shutter ridge and eventually pierce the shutter ridge at a point similar to the stream crossing the fault in Figure 2.11b.

The next offset drainage feature NE (GR 022358) of Figure 2.11b is a classic example of a linear valley where two major streams running off the St Arnaud Range are deflected to the NE and exit via an entrenched channel towards the Motupiko River. Offset of the stream, Cedar Creek, is 704 ± 61 m (Adamson, 1964; Campbell, 1973). Active erosion of the toe of the following shutter ridge (GR 033365) provides evidence of how streams attempt to modify their course. In this case the shutter ridge is the leading edge of the drainage barrier, and hence the stream is not entrenched on exiting the fault zone. The two streams adjacent (GR 033364 & GR 035365 respectively) to this stream are virtually unaffected by the fault as they flow over relatively young fan and slope wash material, with the apparent sense of throw on the fault down slope to the NW. This local sense of apparent throw reversals creating an uphill facing scarp creates a barrier to water flow at the Northridge site (see Chapter 3). A number of small ephemeral streams are deflected NE along the fault scarp and some by up to 400 m (Section 3.2).

On the NE side of Tophouse Saddle in the Wairau Valley the frequency of fault related drainage deflections decreases as Six Mile Creek flows along the base of the ranges to the north restricting fluvial interaction with the fault. Streams flowing in the saddle are predominantly deflected down slope and along the fault trace to the NE. An example is the Old Tophouse site discussed in Section 2.3.1, (Figure 2.1). A stream with catchment on the degradational surfaces of the Wairau Valley is deflected (GR 075384) by the fault and forms a series of meanders inferring an attempt to reach a new base level in response to changing geomorphic conditions, most likely a gradient reduction due to stream lengthening, related to successive faulting episodes. Apart from this stream, which enters Six Mile Creek, there are no active stream flows between Six Mile Creek and the active

Wairau River.

2.4 SURFACE AGE CONSTRAINTS

2.4.1 Weathering Rind Dating

No it does not show th

To determine a slip rate of the fault a measurable offset and age marker are required. Unfortunately, no radiocarbon dates were available for geomorphic surfaces in the Wairau Valley. The fault transects a flight of degradation terraces that decrease in height and young towards the active Wairau River (Figure 2.9). A number of Torlesse cobbles are exposed on these terrace surfaces. Therefore, weathering rind dating (WRD) of these surfaces was attempted following the method described by McSaveney (1992).

A premise of weathering rind dating is the resetting of the rinds on transport to a new geomorphic surface. This involves mechanical weathering (ie bedload rolling) abrading to a fresh surface, effectively setting the weathering time scale to zero. Deposition of the boulders and exposure to sunlight initiates the weathering process. Without boulders resetting to a clean surface there is potential for an inherited WRD age. In addition to inherited ages, WRD can record multiple modal peaks representing significant events related to the surface. In this study modal peaks could represent an earthquake rupture event causing slumping on scarps and tossing boulders, or a temporal re establishment of a stream channel, exposing new rocks to the surface; in both instances fresh rocks are exposed at the surface.

2.4.2 Sample Locations

Location of the sampling areas was governed by two criteria, firstly the sample objective, whether it be for a terrace tread date or fault rupture related dates, and secondly the availability of samples exposed on the surface. Geographical extent of the sample sites at the Wairau Paddock site is shown in Figure 2.12, and Table 2.1 briefly describes the objective for sampling the WRD areas. Aside from Sample 9 the primary aim of the

WRD sampling was to determine a geomorphic evolution of the most recent ground rupture events; secondly, to determine a slip rate over this short period; and finally, if possible, to further constrain an ultimate and any preceding rupture dates derived from trenching.

2.4.3 Age Determination

WRD Sample Number	Number of Chips collected	Objective for Sampling	Oldest Modal Rind Thickness (mm)	Age of Feature (Years B P)	Other Modal Rind Thickness (mm) and Age (Years B P)
1	49	Tread age for T1	5.2	8500 ± 1300	4.2 – 5300 4.7– 6750
2	31	Tread age for T2	5.2	8500 ± 1300	0.9 – ~ 600
3	29	Tread age for T3	5.1	8100 ± 1200	-
4	28	Tread age for T4	4.1	5050 ± 700	3.1 – 3000 3.5 – 3700
5	27	Tread age for T5	3.8	4350 ± 450	1.9 – ~1450[F] 3.3 – 3350
6	9	Channel age, cut into T4 (C)	-	-	-
7	23	Fault rupture events (F)	4.1	5050 ± 700	1.9 – ~1450[F]
8	20	Offset terrace riser age (TR)	1.9	1450[F] ± 150	2.8 – 2500 3.4 – 3500
9	23	Terrace riser age, for time constraint at Pylon Terrace	5.8	11000 ± 2000	4.6 – 6450

([F] denotes age possibly related to fault rupture)

Table 2.1: Weathering rind date sample summary of ages

The WRD sample results are collated in the table below, Table 2.1 (see Appendix I and Figure 2.13 for frequency distribution graphs and Figure 2.12 for sample locations and brief discussion). Appendix I provides an outline of methods used to attain the WRD dates.

According to field relationships the samples should increase in age from the lowest elevation (youngest) terrace tread to the highest (oldest) terrace tread. The order of

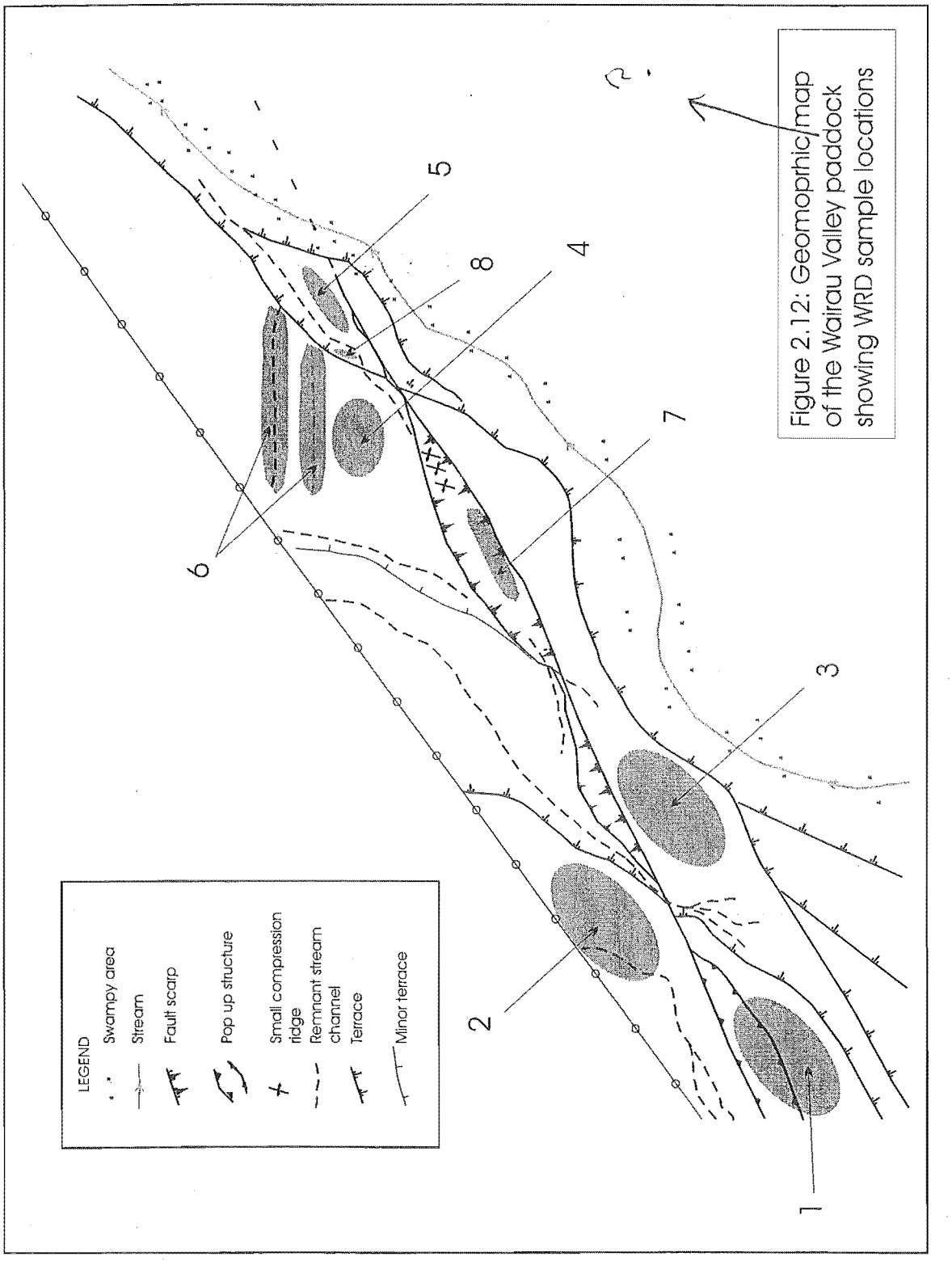

Figure 2.12: Geomophic map of the Wairau Valley paddock showing WRD sample locations

samples from youngest to oldest should correspond to the sample sites in Figure 2.12. Terrace tread ages should decrease from WRD 1 & 2, to 3 & 4 with the youngest 5. WRD 6, 7 & 8 target specific sites. WRD ages ought to correspond to terrace tread dates ie WRD 4 is cut by 6, and WRD 7 & 8 are derived from WRD 3. WRD 9 is separate from sample sites 1-8 (see Figure 2.3 at the Pylon Terrace site), and is from an older terrace.

2.4.4 Discussion of WRD Ages

The WRD data collected from the Wairau Valley has some limitations, mainly as a function of small sample size. Lack of available samples prevents robust age constraints, but the data collected does provide general information. General information available and limitations are outlined below:

a) All samples were complex distributions and clearly polymodal
b) Because of this much larger samples would be required to undertake any rigorous statistical procedures advocated in McSaveney (1992) to establish significant and reproducibility of peaks
c) Despite severe limitation on consequent investigation, the data are the only available basis for establishing any age constraints and the distribution are non-random because
    I. The populations cluster within upper and lower bounds
    II. Older and higher terraces have older modes and a longer age record defined by the variance in rind thickness, then younger low surfaces as would be expected
    III. Some modal peaks are replicated in several records and may represent disturbances affecting surfaces of different dated ages as would be predicted for the site.

The oldest terraces in the Wairau Paddock are Terraces 1 and 2 (T1 & T2) (Figure 2.9 & 2.12), corresponding WRD dates give the oldest surface age, of 8500 ± 1300 yr BP. Sample size for WRD 1 & 2 dates is larger than WRD 3-8, and therefore these are the

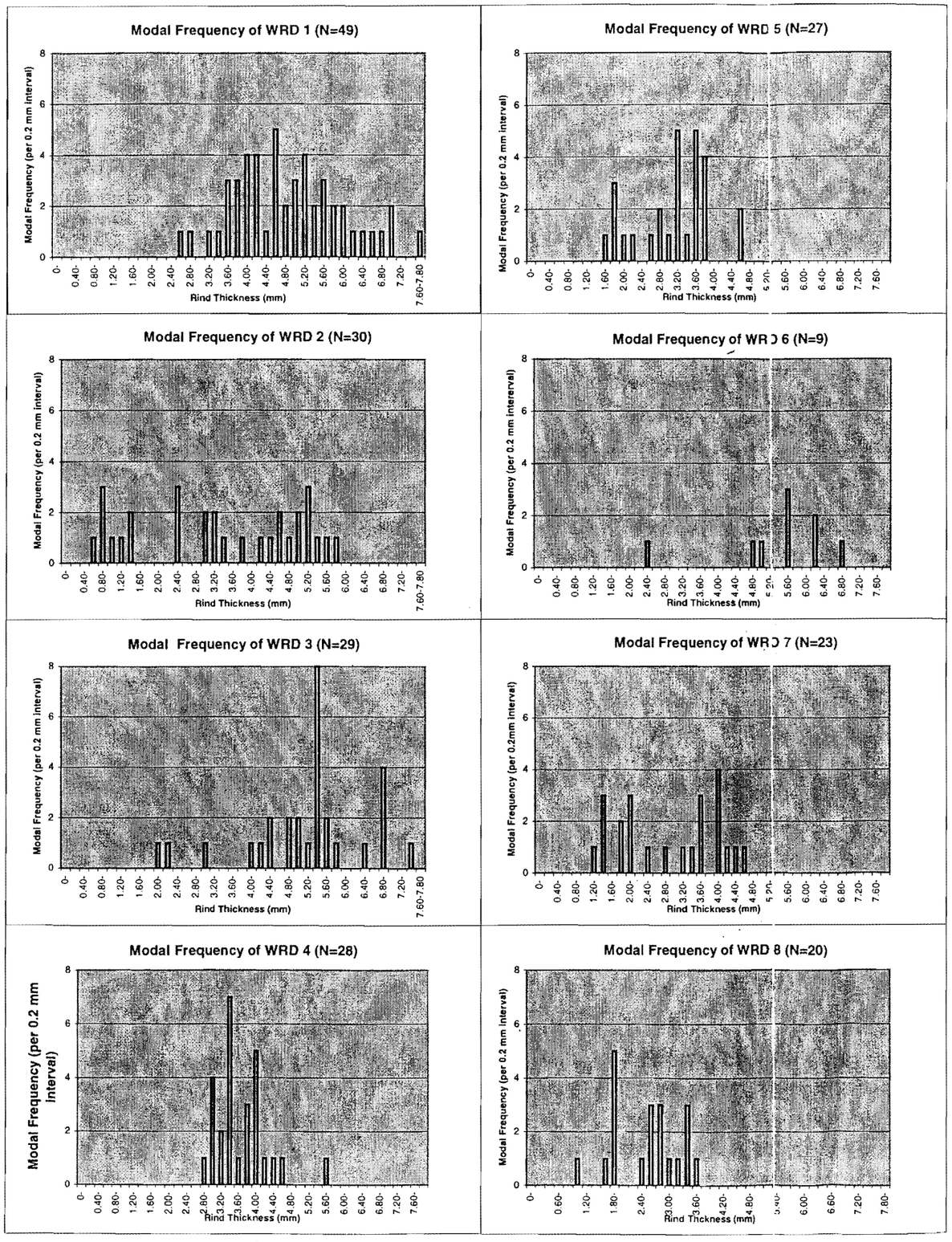

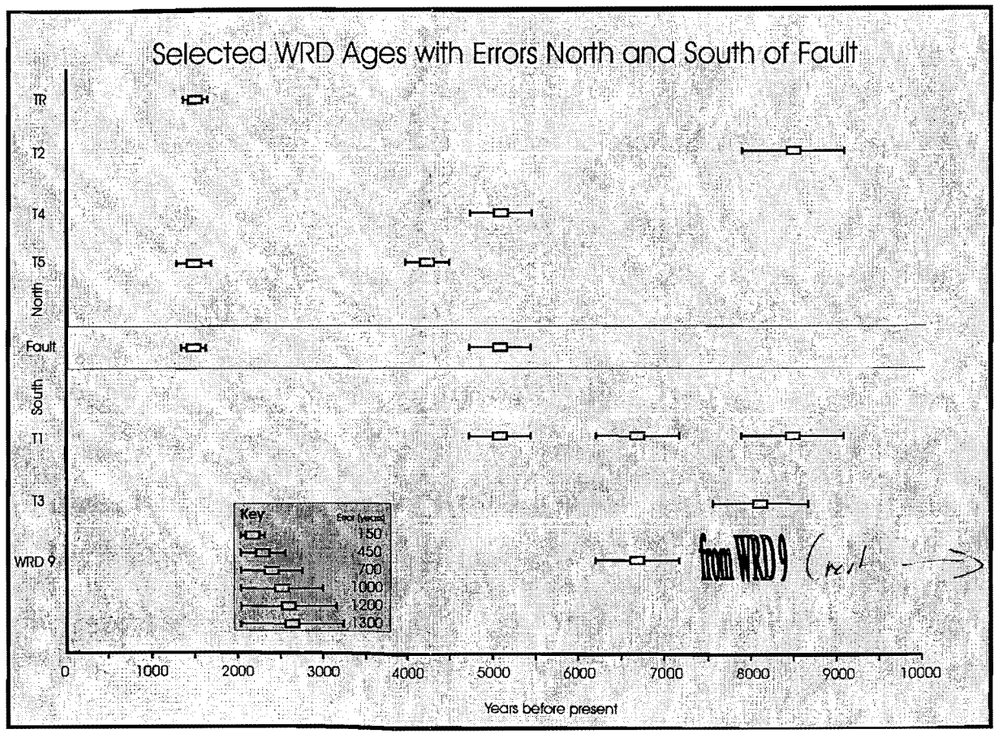

Figure 2.13: Cumulative frequency graphs for the Wairau Paddock site (Left) and a graph of surface age verses time with associated WRD errors of ~8% as per McSaveney (1992) (Above).

most robust ages for the Wairau Paddock. An episode of downcutting caused abandonment of T1 & T2 to form Terraces 3 & 4 (T3 & T4) some time after 8500 ± 1300 yr BP. This downcutting is probably related to an earthquake rupture (discussed in later Sections). Other peaks in the WRD 1 & 2 modal signature will be discussed below.

T3 & T4 are matching terraces offset by the fault. WRD 3 & 4 samples have ages of 8100 ± 1200 yr BP and 5050 ± 700 yr BP respectively. Obviously these dates are not a perfect match. Reconciling the ages is possible by considering fluvial processes associated with large braided rivers such as the Wairau River. Meanders of the river clearly cut into older surfaces eroding away banks upstream. Erosion of the older banks by river meanders often causes bank collapse depositing 'slugs' of sediment into river. A slug of sediment may then be deposited at a point bar immediately downstream before it has travelled far. If this is abandoned and not reworked residual older clasts may be preserved.

Below T3 & T4, Terrace Five (T5) is the youngest faulted terrace tread before younger treads and river channels inundate the fault trace towards the active Wairau River. A WRD terrace tread age of 4350 ± 450 yr BP, younger than T3&4, which agrees with geomorphic relationships. T5 is north of the fault trace, south of the fault trace samples were scarce.

The three remaining dates from WRD 6-8 at the Wairau Paddock site were feature specific sample sites: a remnant channel (C), the fault scarp (F) and a terrace riser (TR) respectively. WRD 6 lacks sufficient samples to indicate an age of the cut channels, although it appears the samples could be remnants of an older terrace, similar in age to T1 & T2 and quite possibly the opposite side of a river channel forming T1 & T2. Sourced from T3, a north-facing scarp provides a polymodal graph from the fault scarp samples (WRD 7) indicating different rupture events. Ages of 5050 ± 700 yr BP and of about 1450 ± 150 yr BP could represent rupture events. WRD 8 ages from the youngest offset terrace records an event at 1450 ± 150 yr BP.

Three samples sites are most susceptible to ground rupture exposing fresh boulders to the

surface. These are T5, F, & TR (WRD 5, 7 & 8). Each WRD cumulative frequency graph has a modal peak of about 1450 ± 150 yr BP. This modal peak could represent a rupture event on the Wairau Fault. Zachariasen et al, (2001) provide an age bracket for the last event on the Wairau Fault to the NE of between about 1400 – 2600 yr BP. Assuming the trench data from Zachariasen et al, (2001) is part of the same earthquake rupture segment, a modal peak of about 1450 ± 150 yr BP is consistent.

Another modal peak for WRD 7 (F), of 5050 ± 700 yr BP is similar in age to peaks in T1, of 5300 ± 800 yr BP, and T4, of 5050 ± 700 yr BP. Representation of a mode of similar age from three sample locations indicates a possible rupture event about 5050 ± 700 yr BP. Two localities, T1 and Pylon Terrace (Figure 2.3), have similar corresponding modal peaks of about 6750 ± 1000 yr BP. WRD data from T1 is bimodal except for the distinctive peak at 6750 ± 1000 yr BP. Similarly Pylon Terrace has a distinctive peak at the same time, separate from the older modes (Appendix I). One reason to suspect an earthquake at this time is that both sample sites could quite easily facilitate fresh exposure of cobbles, via the pop up structure in T1 and the ravelling on the terrace riser at Pylon Terrace.

Assuming T5 records only one rupture event, an age of 4350 ± 450 yr BP for the terrace surface, this indicates that the penultimate rupture occurred prior to 4350 ± 450 yr BP. A comparison of this age with the penultimate rupture date of Zachariasen et al, (2001), between about 2600-3300 yr BP, disagrees with the timing of the penultimate rupture at the Wairau Paddock site, while it does agree with a rupture sometime since about 4700 yr BP.

Completely separate from WRD 1-8, WRD 9 (see Appendix I) samples were from a large terrace riser (Figure 2.3). A WRD age of 11 000 ± 2000yr BP is the most significant modal peak older than the younger terraces to the NE. The WRD 9 sample is from a 10 m high terrace riser, therefore ravelling of fresh boulders with substantial ground shaking associated with a ground rupture on the fault could provide evidence of ground rupture events. WRD 9 should provide a relatively precise account of previous ground ruptures on the fault. However, modal frequencies for WRD 9 indicate only a

short period of scarp instability, instead of periodic peaks representing ground rupture. A possible scenario is proposed whereby a terrace riser records a few events in its infancy, when it is susceptible to surface ravelling and degradation, then later ground ruptures are not recorded as forest and bush cover becomes firmly established.

2.4.5 Summary

Despite a rather noisy signal, detailed investigation of the WRD data helps define the geomorphic evolution of the Wairau Valley Paddock site. A small peak present in three sample sets indicates a ground rupture event probably occurred about 1450 ± 150 yr BP, which coincides with the last rupture between approximately 1400 – 2600 yr BP from the Wairau Valley trenches of Zachariasen et al, (2001). The penultimate rupture bracket of Zachariasen et al, (2001) of about 2600 – 3300 yr BP was not recognised at the Wairau Paddock site.

All WRD dates except one, WRD 3, have dates that are compatible with geomorphic field relationships. The oldest offset terrace pair, T1 & T2 are approximately 8500 ± 1300 yr BP. Younger terrace treads have ages of 5050 ± 700 yr BP, and the youngest tread experienced one ground rupture prior to 4350 ± 450 yr BP. An older event of 6750 ± 900 yr BP is recognised in both WRD 1 & 9 (T1, Figure 2.12 and Pylon Terrace, Figure 2.3 respectively). These sample sets are separated geographically by approximately one kilometre. Both have separate distinctive peaks implying an abrupt disturbance, as opposed to, for example, a prolonged period of erosion. WRD 9 samples from the Pylon Terrace site provide an age of 11 000 ± 2000 yrs BP for the offset terrace riser.

2.5 SLIP RATE DETERMINATIONS

2.5.1 Lake Rotoiti to Tophouse Saddle

Adamson, (1964) recorded offsets of glacial and fluvial topographic features with Late Pleistocene offsets, outlined in Table 2.2. A slip rate from the Late Pleistocene of about 3 mm/yr increasing to about 5 mm/yr is determined by Campbell (1973; 1992). A slip rate discrepancy arises with extrapolation of a constant slip rate beyond the Late Pleistocene (Campbell, 1973). This study however is interested in the slip rate relevant to seismic potential at the present time, and the probable change in the tempo of tectonism is not discussed further (see Campbell, 1973 & 1992 for reference).

STAGE	FORMATION (Suggate, 1965)		OFFSET TOPOGRAPHICAL FEATURES (Campbell, 1973)		Displacement (m)	
					Horizontal	Vertical
OTIRAN	SPEARGRASS	Stadial moraines	Rotoiti II	Peninsula lateral moraine	46 ± 12	3.5 ± 1.2
			Rotoiti I	Main outer terminal moraine	58 ± 9	4.5 ± 1.5
			Black Valley II	Peninsula medial moraine	67 ± 15	9.7 ± 4.5
			Black Valley I	Outer terminal moraine, Black Valley	85 ± 12	12 ± 4.5
			Birchdale	Birchdale moraine- Wairau Saddle offset of Cedar Creek	277 ± 37	28 ± 3.5

Table 2.2: Offset topographic features and displacements between Lake Rotoiti and Tophouse Saddle from the Late Pleistocene (after Adamson, 1964; Campbell, 1973; Campbell, 1992)

2.5.2 Tophouse Saddle to the Wairau Valley

Features displaced across the fault in the Wairau Valley were measured at five localities (summarised in Table 2.3). At the Old Tophouse site a displaced terrace is offset 75 ± 10 m. Tape measurement and erosion of the leading edge of both ends of the terrace by an active stream prevents a more accurate offset measurement. No other features could be reconciled across the fault trace at the Old Tophouse site. No samples suitable for WRD dating were found at Old Tophouse and no carbonaceous material was found in outcrop, thus preventing any physical dating of the offset surface. In spite of this a relative age can be estimated as the offset terrace is probably a remnant or slight modification of the original 18 000 yr BP outwash surface associated with the last glacial maximum. Thus a maximum age for the onset of displacement is 18 000 years. Therefore the slip rate determined at the Old Tophouse site is 4.2 ± 1 mm/yr.

Location	Offset Feature (s)	Horizontal Separation (m)	Relative Vertical Separation (m)	Age of Surface (years)	Slip Rate (mm/yr)
Old Tophouse	Large Terrace Riser	75 ± 10 m	15 ± 5 m (SE up)	18 000 yrs (max)	4.2 ± 1.0 mm/yr (3.6-4.7 mm/yr)
Pylon Creek	Terrace Risers and Channel	53 ± 3 m ^{T1} 54 ± 3 m ^{T2} 46 ± 5 m ^{C}	Minor, (SE up)	18 000 yrs (max) 11 000 yrs (min)	2.9 mm/yr 3.0 mm/yr 2.6 mm/yr 4.8 mm/yr 4.9 mm/yr 4.2 mm/yr 4.0 ± 1.2 mm/yr
Pylon Terrace	Terrace Risers	50 ± 5 m ^{T1} 46 ± 2 m ^{T2}	Not Discernable	11 000 yrs (9200-13500 yrs)	4.5 mm/yr 4.2 mm/yr 4.2 ± 1.0 mm/yr
Matagouri Terrace	Terrace Riser	19 ± 2 m	1.75 ± 1 m (SE up)	?	?
Three Weddings Terrace	Terrace Riser	4.4 ± 0.5 m	Minor, (SE up)	?	?
Average slip rate for Old Tophouse, Pylon Creek & Pylon Terrace					4.2 ± 1.4 mm/yr

Table 2.3: Summary of offset geomorphic features across the fault trace in the Wairau Valley

Three offset features were measured using an EDM at the Pylon Creek site. Unfortunately extensive land cultivation has subdued the geomorphic features altering the originally distinct terrace edge to more of a flexure. Once again no datable carbonaceous material was found at the site, however, as the Pylon Creek site is situated on degradational terraces of the 18 000 yr old outwash surface, a maximum age is provided for the terrace emplacement. 18 000 yrs BP must be considered an absolute maximum age of the surface as close to 10 m of degradation has occurred relative to the Old Tophouse surface. WRD samples from the terrace riser at Pylon Creek NE along fault strike at the Pylon Terrace site provide a minimum age for the Pylon Creek site of 11 000 yr BP. The offset channel (C1 from Figure 2.2) was omitted from slip rate determinations as it was considered slightly spurious because of extrapolation of the channel centre to the fault, compounded by difficulty in accurately locating the centre of the channel. A slip rate of 4.0 ± 1.2 mm/yr incorporates data from the two offset terraces at the Pylon Creek site.

At the Pylon Terrace site two offset terraces were measured using the EDM. The larger offset is complicated by a small fault plane controlled land slump, and therefore probably does not accurately represent a true horizontal separation. However offset of the smaller terrace, is unaffected by land slumping and is undisturbed right to the fault scarp, allowing an accurate horizontal displacement measure. A WRD date of 11 000 yr BP from the undisturbed major terrace riser provides a minimum age for the smaller offset terrace. No potential carbonaceous material was encountered. A slip rate of 4.2 ± 1.0 m is determined at the Pylon Terrace site.

Slip rates were not determined at the Matagouri Terrace and Three Weddings sites, as surfaces at these sites are considered too young to represent a smoothed cumulative slip, because the frequency of individual rupture events can bias slip rate estimates. In addition, sufficiently accurate age determination of the terrace treads cannot be established.

An average slip rate from the data at Old Tophouse, Pylon Creek, and Pylon Terrace

sites is 4.2 ± 1.4 mm/yr. This slip rate data correlates well with the slip rate data of Adamson (1964), Lensen (1968; 1976) and Zachariasen et al (2001) on other sections of the fault. Slip rates along the fault are discussed in more detail in Section 4.4.

2.6 Deflected River Channels and Fault Related Tilting

2.6.1 Deflected River Channels

At two locations along the fault trace in the Wairau Valley evidence suggests fault related surface bulging has temporarily deflected the meandering flood plain course of the main Wairau River or tributary channels from crossing the fault. Evidence at both the Matagouri Terrace site and the Pylon Terrace site indicates a fluvial channel has attempted to cross the fault, but bulging on the SE side of the fault greatly deflected the stream course causing it to slip off (see Figure 2.14). The immediately subsequent river channel had the ability to cross the fault. The replication of the same distinctive sequence of landforms suggests that bulging and deflection immediately preceded an abrupt drop in base level and the generation of a significant terrace. It is suggested that a rupture event may have preceded the base level drop and the river then planed across the fault trace with an increase in stream power and strain release. In both cases the channels crossing the fault are more orthogonal to the fault. The length of the visible offset terrace on the SE side of the fault is on the order of metres, as opposed to much longer deflected terraces and offset terrace matches on the NW side of the fault (eg Figure 2.5, Matagouri Terrace & Figure 2.3, Pylon Terrace).

2.6.2 Matagouri Terrace

A detailed study has been made of the surface morphology of the Matagouri Terrace site because it illustrates complex interaction between river behaviour and small scale deformation features along the fault trace, and raises a number of issues. The site

Deflected River Terrace Evolution

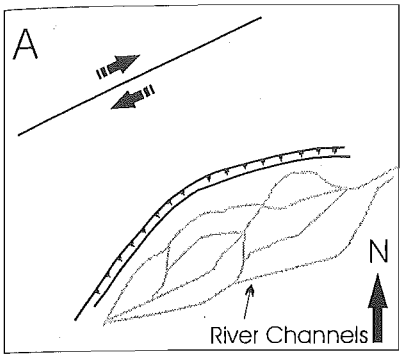

Figure 2.14 A & B: (A) Situation prior to fault-river interaction. (B) Lateral planation or erosion begins, the river terrace approaches the fault. The river is unable to continue this lateral migration as precursory fault rupture bulging on the SE side of the fault prevents lateral migration of the river channel (C).

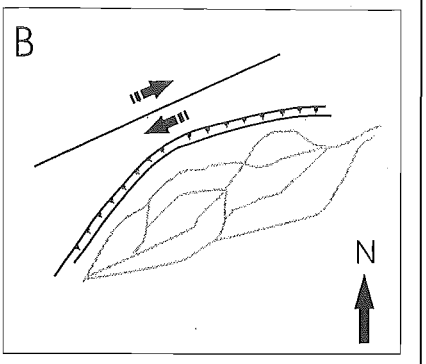

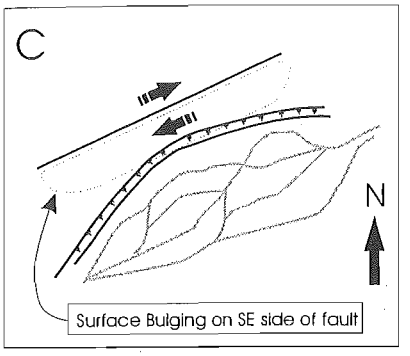

Figure 2.14 C&D: Bulging on SE side of fault contemporaneous with river channel migration prevents lateral migration of the river channel across the fault (C). Strain and bulging are released with subsequent fault rupture, which inturn induce an episode of downcutting and increasing stream power. Increased stream power combined with cessation of bulging allows the river to cross the fault in the transition zone between the mole tracks and small pull apart fault structure (D).

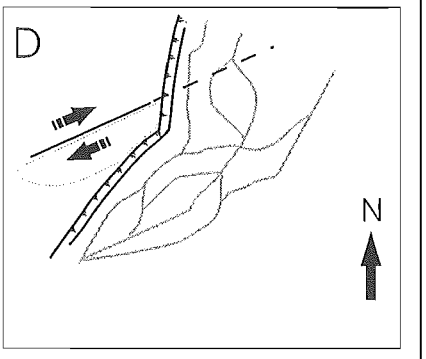

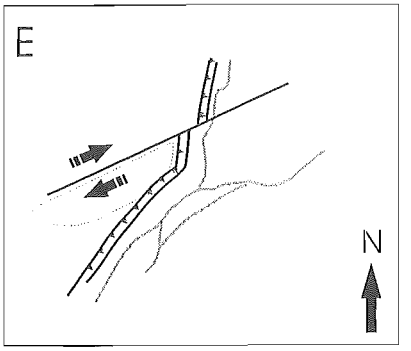

Figure 2.14E (Above): River abandonment, small streams causing minor erosion, especially of the fault and the leading edge of northern terrace.

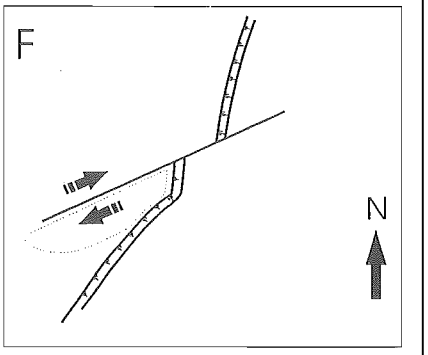

Figure 2.14F (Above Right): Possible pre rupture fault bulging causing stream abandonment and subsequent rupture, repeated bulging and rupture to present situation.

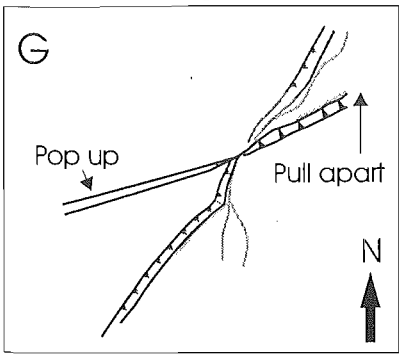

Figure 2.14G (Left Below): Present situation with older curved terrace truncated by younger terrace which is in turn truncated by the fault dextrally, matching the eroded terrace on the N side of the fault

Figure 2.14: Schematic evolution of the deflected river terrace and fault interaction at the Matagouri Terrace site

involves a positive pop up feature on the higher surface and a small pull apart basin on the terrace below, immediately to the east. These features were clearly evolving during the occupation of these surfaces by the river, and the amount of strike-slip faulting which took place during, and since, the time the river occupied the lower surface is quantified by the offset terraces at the Matagouri site and the Three Weddings terrace offset on the terrace scarp forming the eastern boundary of this surface. Following a description of the methods used to generate a digital terrain model of the surface, the following aspects are addressed for discussion:

I the evidence for the deflection of the river by general uplift along the fault trace, particularly with respect to the pop-up on the high surface;

II the evidence for the timing of opening and subsequent inversion of the eastern end of the pull-apart basin in the context of cumulative slip in what is interpreted as three slip events;

III the effects of offset topography in masking deformation across the broad width of the fault zone outside the immediate fault trace.

Many differential GPS points were collected over the Matagouri Terrace site, providing a series of points in space that were later modelled in the Surfer program (Figure 2.15, in Map Pocket). A shaded contour map (Figure 2.15a) from interpolation of the GPS points clearly illustrates a zone of higher (pop up) and lower (pull apart) elevation (white and grey-black respectively). Two wireframe maps (Figures 2.15 b&c) provide a 3-D view of the site, with Figure 2.15 b emphasising the curved deflected terrace and Figure 2.15 c looking along fault strike accentuating the offset terrace, especially the smaller length of the offset terrace on the south side relative to the north. Figures 2.15 d-f, a post map indicating each GPS location, location of transect lines, and a geomorphic map of the main features respectively, help to understand the data processing for the contour, wireframe and transect figures of the Matagouri Terrace site. Surface transects across the fault scarp were used to elucidate on uplift related to the fault using the Grapher program (Figures 2.15 g-i).

The terrace bounding the Matagouri surface on the SE side is really a compound feature formed at the SW end by a curved meander remnant that cut into, but not across the high elevated fluvial surface of the pop-up (lighter region in Fig 2.15 a, view along scarp in Figure 2.15b and shown by terrace symbols in Figure 2.15f). This segment is truncated by a later pass of the river with a much more northerly course which does cross the fault, the junction with the meander segment being marked by a sharp cusp. The river clearly cuts across the fault and is matched by the now offset extension of the same terrace on the north side. Modification of the terrace immediately adjacent to the fault, and the method of extrapolation to measure the strike-slip offset of 19 ± 2 m, is described in Section 2.3.4 and Figure 2.6a. The course of the river at this time is clearly shown by the channel incised along the base of the terrace scarp (Figure 2.15 c). Flooding and braided channels produced a rather irregular topography forming the lower terrace surface, and it is notable that it is this hummocky surface on the south side of the fault which produces some anomalously thick modal peaks from WRD samples, possibly indicating that material has not been extensively reworked.

The pull-apart basin is a marked depression, shown as the light blue area NE of the fault trace in Fig 2.15f. It is unfilled by any thickness of sediment, with the floor now lower than the river channel. Fully developed opening must therefore post-date occupation by the river. Subsidence of 1.75 ± 1 m below the adjacent surface is therefore generated by no more than 19 ± 2 m of strike-slip. This subsidence may have extended along strike far enough to affect and modify the terrace scarp over the extrapolated section either by collapse or by concentrating localised groundwater spring sapping and run-off drainage.

A view along the fault trace is usually suggestive of a general rise in topography towards the trace from both sides, and tilting of terrace surfaces away from it. Topographic sections across the trace do not always support this perception for two reasons (see Figures 2.15 g, h & i).

a) Strike-slip offset of topography does not match corresponding surfaces in a cross-section

b) Local effects such as the small pull-apart produce superimposed sagging on both up and downthrown sides of the fault scarp. These effects are illustrated by the three cross sections, A, B and C.

Section A crosses the pull-apart basin and in the exaggerated profile it can be seen that the topography rises from both sides but is rounded off by sagging into the basin through extensional faulting in the footwall and lack of support under the hanging wall.

Section B appears to show very little topographic change across the fault scarp, but comparison of the section line with the map shows that the downthrown northern side is on the older Matagouri terrace surface while the upthrown side is below the bounding terrace on the lower side. The terrace height compensates nearly exactly for the throw on the fault scarp.

Section C more closely illustrates the real rise in elevation across the fault zone, possibly exaggerated by the local effects of the pop-up and asymmetric trimming by the river.

2.6.3 Pylon Terrace

At Pylon Terrace a similar, deflected curved river channel is truncated by a younger river channel (T1), which is subsequently offset by the fault trace (Figure 2.3). Although older and more evolved, the Pylon Terrace deflected terrace mimics the Matagouri Terrace. At the Pylon Terrace the distinction between pop up and pull apart structures is emphasised, as the faulted surface is older. As at Matagouri Terrace, the deflected river terrace at Pylon Terrace is part of a broad terrace meander which is truncated slightly downslope of the meander apex before the new channel crosses the fault in the transition zone between the pop up and pull apart fault structures.

2.6.4 Deflected River Channels Discussion & Summary

A common theme appearing with the location of deflected river channels (see Figure

2.14) and the fault trace is that in both cases almost immediately SW along fault strike, or upslope in this case, there are pop up structures indicating some contribution of minor thrusting, a concentrated zone of bulging, or a space accommodation feature on a predominantly strike-slip structure with a fault dip inclined off vertical, or a minor dip slip component. Complimenting the pop up structures at both localities is the transition, along fault strike and downslope of the deflected river terraces, to a minor pull apart or inverted flower fault structure. It is plausible that this transition zone provides the impetus or opportunity for the river to cross the fault as bulging at this time is reduced. Truncation of the older terrace by the younger terrace crosses the fault trace near the point of inflection on the older deflected curved terrace (Figure 2.14).

An interesting question arises as to discerning the timing of events surrounding bulging near the fault trace. Conceivably a sequence of events could involve bulging on the SE side of the fault preceding fault rupture, contemporaneous with increased terrace degradation of the river channel causing the river to slip off the tilting surface. The ensuing fault rupture releases built up strain, effectively ceasing continuation of fault related bulging. Readjustment of the river base level in effect elevates stream power and ongoing lateral planation allows the river to cross the fault at the next meander migration downstream of the elevated pop up on the fault trace, and coincident with the transition zone between pop up and along strike pull apart system.

2.7 SUMMARY

Fault characteristics between Lake Rotoiti and the Wairau Valley are similar. A narrow zone of deformation exhibits dextral horizontal offset combined with minor, though pervasive, uplift to the SE. Small-scale fault features are identified in the younger degradational terraces of the Wairau Valley, whereas SW of Tophouse Saddle the fault zone is more evolved transecting older glacial sediments or masked by alluvial fans from the St Arnaud Range.

Strike of the Alpine Fault trace in the study area is very uniform, aside from a marked

change in fault character on either side of Lake Rotoiti. Northeast of the lake the trace is dominantly valley bound with a narrow zone of deformation extending seawards to Cloudy Bay, Cook Strait. Conversely, to the SW, a range front fault trace combined with thrust wedges and internal deformation exhibits a broader zone of deformation. This change to a broader zone of deformation could represent a change in fault characteristics possibly related to a structural segment boundary.

Fluvial processes are clearly affected by the fault trace, most notably SW of Tophouse Saddle, where the fault trace dissects late Quaternary glacial sediments. Runoff from St Arnaud Range provides numerous streams. Most enter the fault zone normal to fault strike and are subsequently entrenched in channels and along the fault trace with successive fault movements. Characteristic strike-slip related landforms produced by the fault affect drainage; landforms observed in the study area include linear valleys, shutter ridges, sag ponds, scarps and linear springs.

Weathering rind dating samples from geomorphic surfaces yield approximate dates of variable reliability related to ground ruptures on the fault. At the Pylon Terrace site, a robust set of rinds indicate an age of 11 000 ± 2000 yrs BP for the prominent terrace riser offset. Dates obtained on younger terraces nearer the active Wairau River suggest a rupture event around 1450 ± 150 yr BP from smaller peaks in cumulative frequency sample plots. This date coincides with the minimum age of the ultimate rupture date of between ~1400 – 2600 years ago (Zachariasen et al, 2001). A rupture between ~2600 – 3300 yrs BP (Zachariasen et al, 2001) was not recognised with the WRD samples. A well-defined event around 6750 yrs BP is recognised at two localities and probably relates to a ground rupture event. Samples from Pylon Terrace site provide an age of 11 000 ± 2000 yr BP.

A combined slip rate of 4.2 ± 1.4 mm/yr accommodates minor variation in slip rate and age rates from the Old Tophouse, Pylon Creek and Pylon Terrace sites. At the Old Tophouse site an uplift rate of <1 mm/yr to the SE is congruous with the general upthrow on the fault to the SE. Both rates correspond to other rates found along the length of the fault since the late Pleistocene.

One very interesting aspect related to the fault evolution in this study area, especially the Wairau Valley, is the presence of deflected channels sub parallel to the fault trace, that have been subsequently truncated almost normal to the fault trace. In both instances, at Pylon Terrace and Matagouri Terrace, the younger, fault crossing terrace and channel is downslope of a fault pop up structure on the fault in the transition zone between a pop up and pull apart structure. Along the Wairau Valley the fault exhibits other examples of this behaviour, of pop up followed by pull apart structures on the fault trace (see Map 1). The relation between the deflected river channels and the fault trace appears to be that bulging on the SE side of the fault prevents (or deflects) the river from crossing the fault trace as river downcutting or lateral planation encounters resistance in the form of surface bulging. This surface bulging is possibly a precursor to fault rupture. An episode of downcutting following fault rupture is unable to erode the increased elevation of the pop up structure, but now has the power to cross the fault downstream of the obstruction in the transition between pop up and pull apart structures.

CHAPTER 3

PALEOSEISMIC INVESTIGATION OF THE ALPINE FAULT TRACE AT TOPHOUSE

3.1 INTRODUCTION

This chapter outlines paleoseismic investigations undertaken at the Northridge Farm section of the Alpine Fault near Tophouse, including a detailed description of the trench site selection process, trench stratigraphy, fault zone structure, critical trench relationships and discusses the relevance of the radiocarbon dates to the rupture history of the fault.

Maximising chances of a successful trenching exercise requires adherence to a number of criteria. Paramount to all paleoseismological studies is that the active fault trace is trenched, therefore choosing sections of a fault trace with a narrow zone of deformation is preferable. For example, a site with multiple surface fault traces may not provide unequivocal evidence for the last one or more rupture events on a selected fault strand. Also, a fault with a multi trace surface expression introduces doubt as to whether a complete rupture history can be conclusively determined. A single fault trace, however, removes any doubt that a fault trace does not record all previous rupture events, assuming the rupture passed through this section of the fault.

Another important criterion for trench site selection is the ability of the local environment to collect and preserve datable carbonaceous material, and then remain relatively unaffected by future surface erosion processes. Carbonaceous material is best preserved in a moist environment, such as a small depression (furrow) or swamp (sag

pond) (McCalpin, 1996). Although intuitive, it is worth emphasising that the material trenched be from an environment of minimal erosion, thus maximising preservation for paleoseismological investigation and interpretation, as erosive events could affect the paleoseismic record by removing critical evidence.

Mapping of the fault trace between Lake Rotoiti to the Tophouse Saddle established that the fault trace is frequently concealed by thick alluvial fan sediment originating from the St Arnaud Range (Section 2.2). Near Lake Rotoiti land development for farm and residential property has disturbed and degraded the fault scarp. Access to the fault scarp NE of the cessation of fan sedimentation (marked on Figure 1.4) is difficult as native forest, abrupt topographic changes, and subdivision housing limit access to the fault scarp for trenching by a digger.

At the Northridge locality, however, topography is subdued and previous logging operations allowed greater access to the fault scarp. Northridge farm is south of SH 63 near the Tophouse Saddle indicated on Figure 1.4. The Northridge location provided the best access for mechanised excavation on the section of the fault between Lake Rotoiti and Tophouse Saddle. Subsequent detailed mapping of the fault trace on the Northridge farm showed an almost continuous surface rupture fault scarp confirming the location of the trace and providing a number of potential trench sites.

3.2 Fault Trace Description at the Northridge Locality

Reconnaissance geomorphic mapping of the fault at the Northridge site confirmed the existence of a relatively narrow zone of ground deformation largely confined to a single surface fault trace. Figure 3.1 shows a geomorphic map of the fault trace. At two locations near the trench sites the fault plane is exposed and detailed face logs have been recorded (Figures 3.2 & 3.3). The first face log site is located approximately

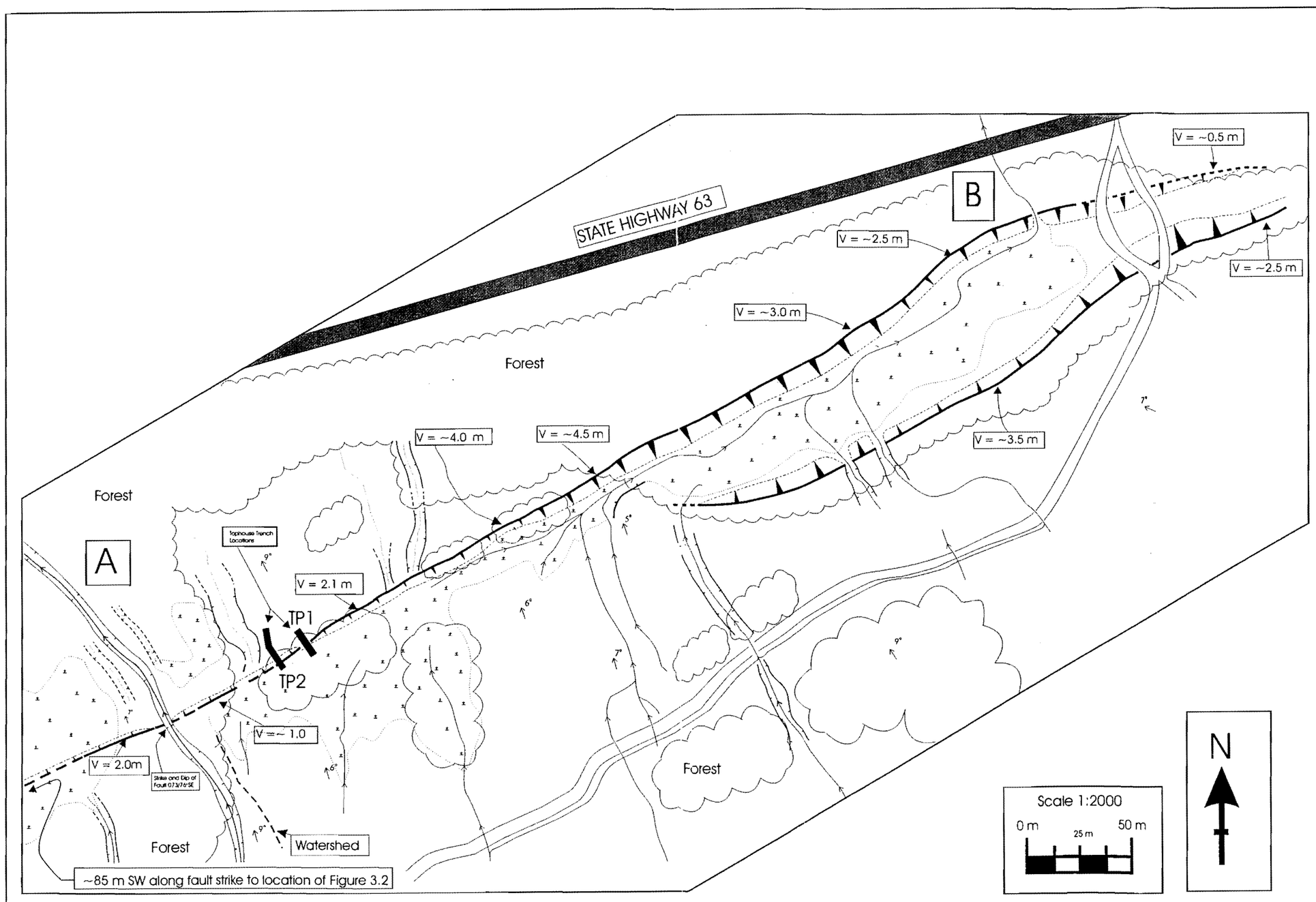

Figure 3.1: Detailed map of the Wairau Fault trace at Tophouse and Trench Locations (TP1 & TP2)

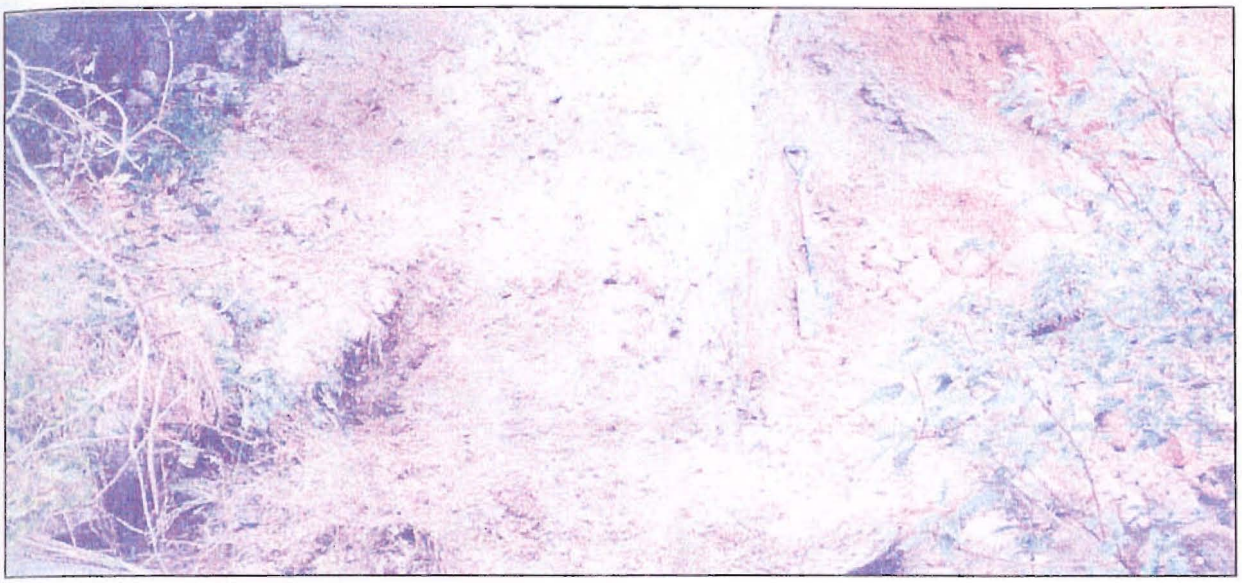

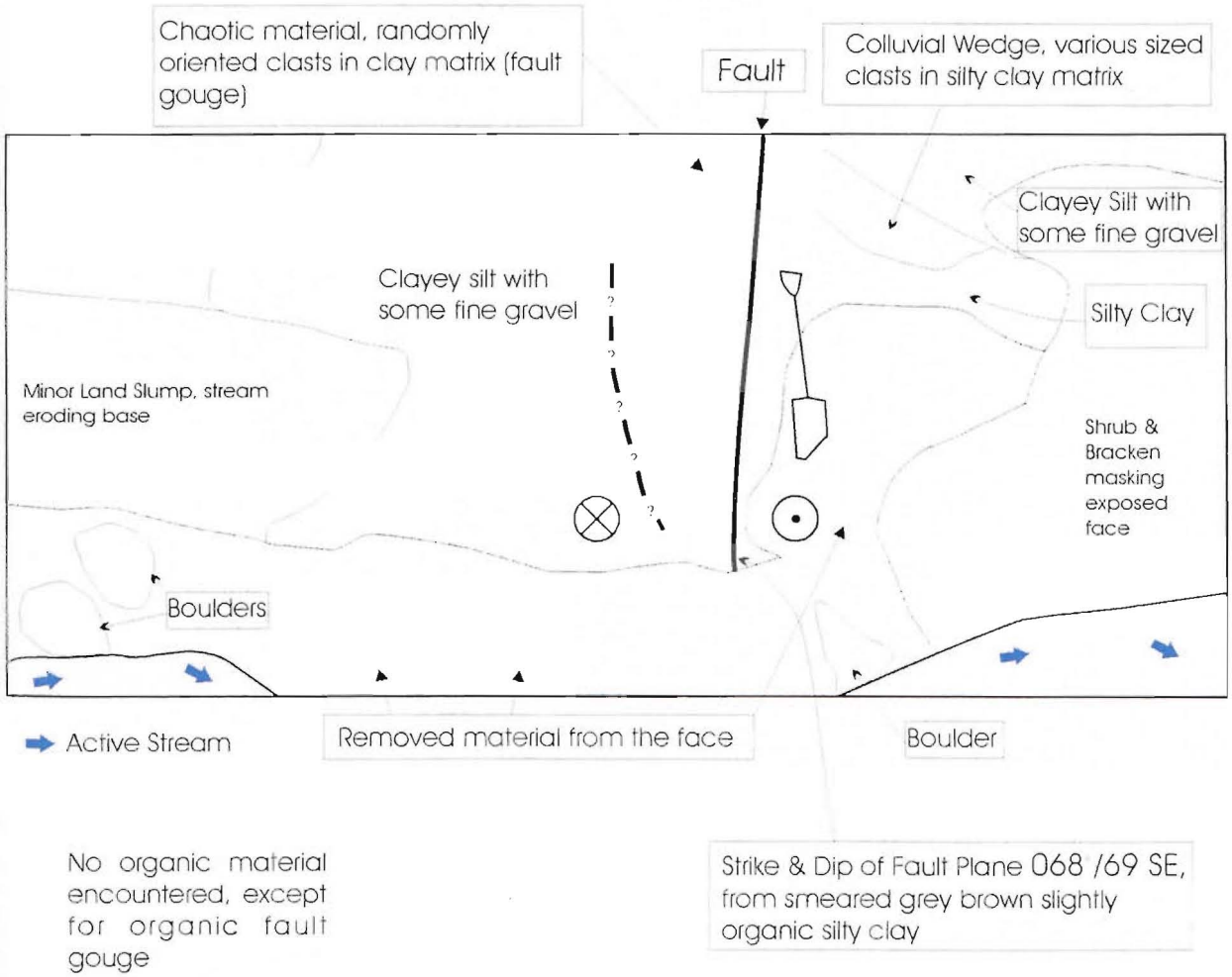

Figure 3.2: Face log of fault exposure at the base of a stream eroding the fault zone. Location shown in Figure 1.5. See 1 m long spade for relative scale.

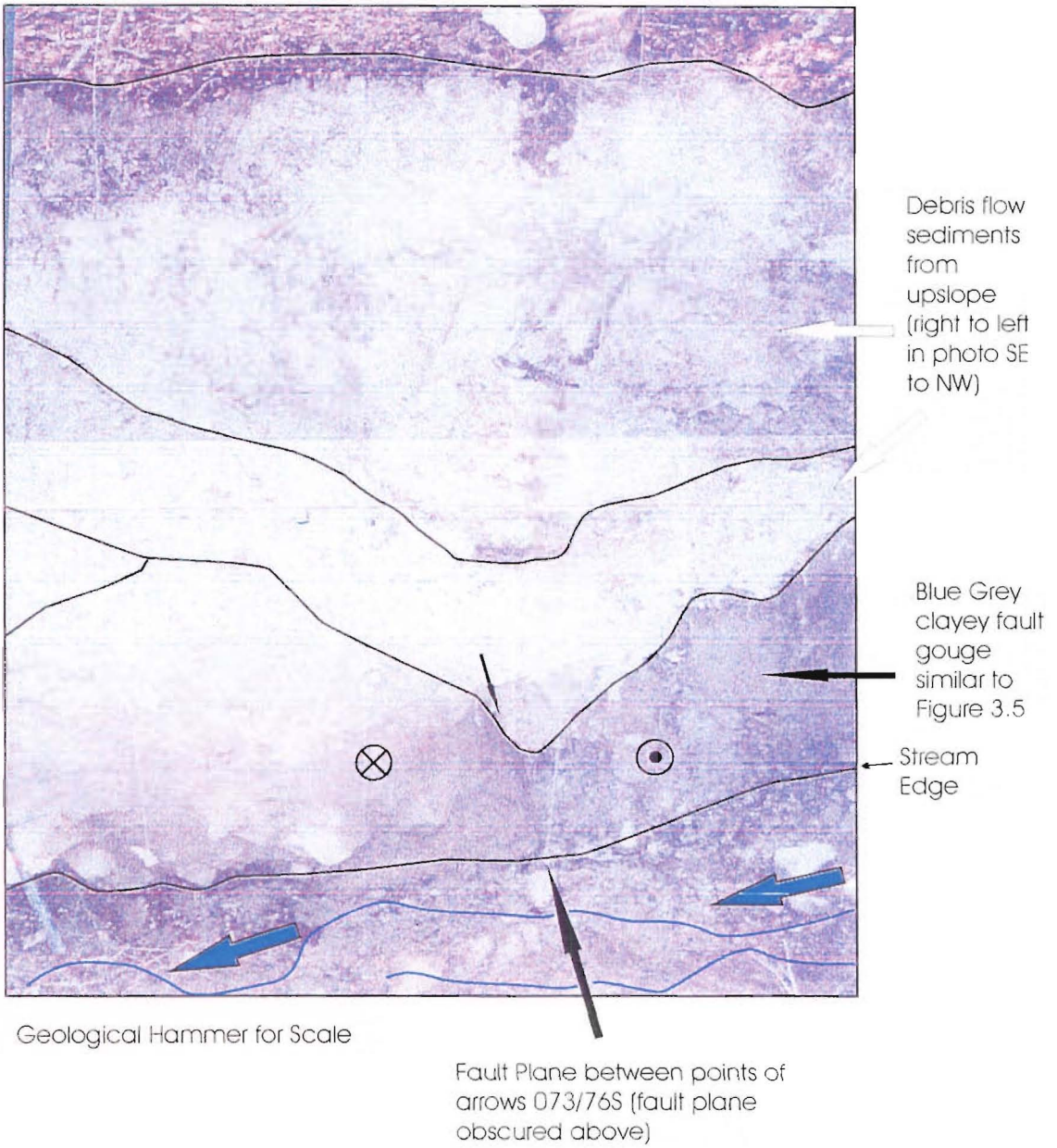

Figure 3.3: Face log of fault exposure at the base of Stream A (in Figure 3.1). Debris flow sediments obscure the fault plane besides the plane marked two black arrows. Geological hammer bottom left for scale.

85 m SW along fault strike from the SW tip of the trace depicted in Figure 3.1 (location in Figure 1.4). At this site a creek has incised into the upthrown (relative) SE side of the fault cutting into an alluvial fan surface. At this locality, vertical displacement is approximately 3 m with the fault plane orientation of 068°/69SE (Figure 3.2). A single fault trace continues to the NE, scarp height decreasing as recent local fan and swamp deposits have concealed the trace. The second face log site is an approximately 2 m high downhill facing fault trace exits in a swampy area (SW edge of Figure 3.1, denoted V = 2.0 m). At this point an incised (~2-3 m deep) stream reveals the fault plane of 073°/76SE (Figure 3.3). With the benefit of subsurface excavation (presented in following Sections 3.3 & 3.5) both fault plane measurements are considered only part of a partially concealed fault zone beneath the outcrop, however, both measures do suggest a steeply SE dipping fault plane.

A poorly defined downhill facing scarp (location at V=~1.0 m in SW of Figure 3.1) exits the forested area and decreases in height towards an inversion point where the apparent sense of upthrow of the fault is reversed. The fault scarp now faces uphill as a consequence of offset variable topography, not by reversal of throw. At this point the fault scarp faces uphill, creating a sediment and drainage obstacle, which is an ideal environment for sediment accumulation. Scarp height increases further NE along the trace, and is locally up to 4.5 m high. Streams A & B (Figure 3.1) provide the only drainage outlets. Drainage is deflected to the NE, bounded by a watershed roughly parallel to Stream A (Figure 3.1) and the fault scarp, resulting in significant local scouring of the fault scarp. This is unfortunate with respect to paleoseismic investigation as this has modified and/or destroyed potential sites for investigation, and hence the sedimentary record and the rupture history record for this section of the fault is incomplete. North east of Stream A (Figure 3.1) on the southern side of the fault a swampy area extends parallel to fault strike until the streams breach the fault via Stream B. Along this swampy strip the fault scarp has been scoured, locally to depths of about 1 metre.

Another large swampy area appears to have developed prior to Stream B breaching the fault scarp. A second fault scarp bounds the swamp along its south margin. The SE fault

trace is downthrown to the north, and increases height to the NE. The development of the swamp indicates that the faults probably define a graben structure, or, alternatively represent a right stepping right lateral strike-slip step over.

From a paleoseismic perspective the Northridge farm site offered the best sites for trenching along the fault trace from Lake Rotoiti. A well-defined fault trace allowed unambiguous fault trace location, conversely towards Lake Rotoiti fan sediments frequently conceal the trace. For much of its length at Northridge farm the fault trace is uphill facing, presenting an ideal environment for paleoseismic sediment accumulation and preservation environment. Because uphill facing scarps form effective sediment traps, they are considered an important criterion in selecting trench sites.

Relative to sections of the fault trace further SW towards Lake Rotoiti, access to the fault trace at Northridge farm is excellent. Logging in the 1960's provided the tracks to access the fault trace, however, logging is also a very destructive activity. Therefore the ease of access is a mixed blessing as this advantage may be offset by the logging operations modifying potential trench sites. It is crucial to have an undisturbed paleoseismic site, so a detailed investigation of potential trench sites paying particular attention to logging disturbance, and avoiding disturbed sites, has hopefully obviated site modification as a problem in the chosen sites. The final site selection is discussed in the following section.

Throughout the text, Tophouse Trench One and Tophouse Trench Two will referred to as TP1 & TP2 respectively.

3.3 PALEOSEISMIC INVESTIGATION OF TOPHOUSE TRENCH ONE

3.3.1 Site Selection

A number of possible trench sites were investigated thoroughly on completion of detailed fault trace mapping (Figure 3.1). Site selection processes outlined in the

previous two sections were followed, consequently two trench sites were chosen from six potential trench sites on the Northridge Farm section of the fault.

Selection of the TP1 site was relatively straightforward. A single fault trace was located from surface expression. Large beech trees remained close to the site, making it less likely previous logging has destroyed or modified paleoseismic data at the site. Immediately upslope of the trace there is a swampy area providing an environment perfect for accumulation and preservation of datable carbonaceous material. The presence of the swampy area adjacent to the fault trace also dismissed the likelihood of recent scouring activity removing part of the sedimentary record as has occurred further NE along the fault trace. The location of the swamp is a consequence of displaced irregular topography which reverses the apparent scarp face rather than a reversal of throw. Location of the trench site is shown on Figure 3.1.

3.3.2 Trench Unit Description

A log of the SW side of TP1 is presented in Figure 3.4 (back pocket). The trench log will be discussed in two sections, SE and NW of the fault zone, while the fault zone itself is discussed in the following section (Section 3.3.3). SE of the fault zone sediments are predominantly composed of fan deposited material from the St Arnaud Range. The NW section is mostly comprised of debris flow sediments and within the fault zone itself is predominantly undifferentiated highly sheared material.

Units on the SE of the fault zone have been assigned numbers 1 – 11. Basal units consist of debris flow deposits (Units 1, 3 & 5) with intervening periods of fan sand and gravel (Units 3, 4, 5) and peat deposition (Units 2 & 4). Fan and debris flow activity has occurred contemporaneously on occasions (e.g. Units 3 & 5). Above Unit 5 there is no evidence of debris flow deposition suggesting a cessation of debris flows over the trench site at the time, or change of local environment and any subsequent debris flows being diverted elsewhere.

Overlying the debris flow units is a fine peat horizon with grey-blue silty clay and sand interbeds (Unit 7) marking an episode of swamp development. A period of fan activity has followed depositing fine gravels and local sand beds (Unit 8). Slope wash derived clay rich units (Unit 9 & 10) cover the fan gravels. Carbonaceous material content increases within the clay rich units and is then prevalent in the overlying surface unit (Unit 11), a dark brown fibrous peat unit with twigs from surrounding tree litter and swamp deposits.

A thin discontinuous peat layer (nw2) separates basal debris flow units (nw1 & 3) on the NW sided of the trench. The uppermost debris flow unit (nw4) has developed an "A" horizon (nw4a) with associated "B" horizon that extends to the oxidation level marked on the trench log (Fig. 3.4). Apart from the period of minor swamp deposition (nw2) units on the NW side of the trench are silty, poorly sorted and give the appearance of being distal from their source relative to units on the SE of the fault zone. Radiocarbon evidence (discussed in Section 3.4) suggests long term shearing on the fault zone from a small branch fragment found in the shear zone, this long term shearing has juxtaposed the units of different origin.

3.3.3 Faults and Structures exposed in trench and critical relationships

F1 and F2 have been used to label the main bounding faults found in TP1. Besides the truncated unit 9 and overlying unit 11 shearing between the steeply dipping faults (F1 & F2) prevents correlation of any units within the fault zone with units on either side. The fault zone is narrow, with a surface width of ~3 m tapering to ~1 m wide at the base of the trench.

3.3.4 Summary

In TP1 there is no stratigraphic evidence to suggest direct correlation of units on either side of the fault zone. An event horizon is located between Units 10 & 11. Radiocarbon

samples were found in the fault-truncated clayey peat unit (Unit 10), and the base of the overlying fibrous peat (Unit 11) allowing the last rupture event to be bracketed. Shearing was accommodated in a narrow zone of deformation and evidence for significant long-term deformation can be identified by the juxtaposition of two different local deposition environments and the branch trapped in the shear (age ~ 12 500 years).

3.3.5 Radiocarbon Samples and Dates

Six radiocarbon samples were analysed from TP1 and the results are summarised in Table 3.1 below.

Tophouse Trench Code	Wk Number	Radiocarbon Date
W600	10245	12 418 ± 81 BP
W601	10246	* 1 787 ± 57 BP
W604	10247	14 450 ± 92 BP
W605	10248	16 830 ± 123 BP
W609	10249	13 594 ± 76 BP
W610	10250	* Post 1950

Table 3.1 Radiocarbon sample results including trench code, analysis number, and radiocarbon date with associated error. Asterisks denote sample of critical importance (discussed in Section 3.4). See Figure 3.4 for sample locations.

3.4 DISCUSSION OF RADIOCARBON DATES

Six carbonaceous samples analysed from TP1 provided radiocarbon ages that varied from about 17 000 years BP to recent post 1950 dates (see Table 3.1 & Figure 3.4).

Surprisingly, most of the radiocarbon dates are different to what was envisaged at the time of trenching, most notable is the much older than expected dates from the buried peat samples. The oldest date of 16 830 ± 123 BP (Wk 10248) was from the SE basal peat unit (Unit 2), now buried approximately 2 m below the ground surface.

The next oldest date is from peat from Unit 7 also from the SE side of the fault with an age of 14 450 ± 92 BP (Wk 10247). This date is considerably older than predicted at the time of trenching as Unit 7 is less than 1 m from the ground surface, but 1 m above Unit 2. Somehow the geomorphic environment has changed significantly since 14 450 ± 92 BP. This geomorphic adjustment could have followed a brief period of instability post the last glaciation, approximately 18 000 yrs BP (Suggate, 1988) (see discussion Section 3.5.2), as a gradual warming of the environment could help facilitate growth of beech forest similar to the natural vegetation pre-European settlement in the mid 1800's and increase stability. Forest growth would increase stability of the whole area, and especially the upper slopes which are more susceptible to instability. At present the bush line on the St Arnaud Range is at about 1400 m asl with the approximate elevation of the trench sites at 725 m. Another consideration is the possibility of an erosion event removing part of the sedimentary record as both the fault and upper units (esp. Unit 9 & 10) appear to be truncated and or eroded respectively. A combination of these three processes (local instability, forest growth and erosion) is most likely. The extent to which each process affects the stratigraphic record is difficult to establish, except the radiocarbon date of 1 787 ± 57 BP (Wk 10246) (discussed below) from Unit 10 suggests little net sedimentary deposition between 14 450 ± 92 BP and 1 787 ± 57 BP.

A thin discontinuous layer of peat situated between two debris flows on the NW side of the fault zone provides the next oldest radiocarbon date of 13 594 ± 76 BP (Wk 10249).

Dates from the three peat samples do not provide direct evidence of rupture timing on the fault, but they do prove faulting has occurred, as evidenced by the juxtaposition described above. The remaining three radiocarbon dates of 12 418 ± 81 BP (Wk 10245), 1 787 ± 57 BP (Wk 10246), and post 1950 (Wk 10250) all directly relate to the timing of rupture on the fault. Oldest of these dates, a small branch found in the shear close to F1,

of 12 418 ± 81 BP implies a rupture event post this time. There is a possibility that this branch has been recycled (captured during an episode of shearing) from a peat layer and therefore the event could be significantly younger than this date. This can be discounted fairly conclusively, however, as other peat units in the trench are dense, fine and free of branch-sized material (eg Unit 11). From this assumption the suggestion of the potential of forest cover at this particular site is reinforced, with the branch either caught in the rupture while on the ground surface or falling into a fissure immediately post rupture.

A section of beech branch from the truncated Unit 10 provides the most valuable piece of information regarding rupture history on the fault. A radiocarbon date of 1787 ± 57 BP (Unit 10) provides a maximum age since last rupture and converts to the calendric period AD 200 – AD 500. Once again, this date is much older than anticipated while trenching and, although an accurate recurrence interval is unknown at present. This date suggests that the elapsed time in the seismic cycle of the fault is longer than previously envisaged.

The youngest date from the undisturbed Unit 11 in the trench unfortunately yielded a 'post 1950 modern' radiocarbon date indicating the beech twig samples are from trees grown since AD 1950 when nuclear testing modified atmospheric C^{14} levels. On first assessment in the trench it was highly surprising that the swamp was such a young feature. Other peat units in the trench (NW side) provide evidence for this location being a swampy area in the past and indicate accumulation began at the last increment of movement and has built up behind the scarp so it was assumed that the swamp surface would be older than the C^{14} date indicates. While it was hoped that the C^{14} sample from Unit 10 & 11 would help to tightly constrain the last rupture on the fault. It could be argued that the beech twigs collected from the base of Unit 11 could have fallen and settled through the peat to the base of the unit, however, the unit (see Figure 3.4) is very fibrous and this appears unlikely. Therefore it is assumed that the date is correct and the swamp is a young feature and probably was a result of logging operations in the 1960's affecting drainage patterns in an adverse way.

3.5 PALEOSEISMIC INVESTIGATION OF TOPHOUSE TRENCH TWO

3.5.1 Site Selection

Site selection criteria for TP2 were identical to those of TP1. At this location an interesting surface feature was recognised, and interpreted as either a possible splay of the fault trace in surface expression, or alternatively warping and folding adjacent to the fault zone.

A well-defined zone of ground deformation, no evidence of local scouring, and a lack of any obvious forest disturbance all support selection of this trench site location. TP2 was excavated approximately 15 m SW along the fault trace from TP1, and intersected the same swampy area as encountered in TP1. A change in orientation of the fault trench avoided interference from a remnant stream channel and allowed further subsurface investigation of the extent of a surface feature (change in elevation above F3 & F4 in Figure 3.5 in back pocket). Faults encountered in TP2 are referred to, fault zone one (FZ1), and three additional faults (F2-F4) respectively.

3.5.2 Trench Unit Description

Figure 3.5 shows a detailed log of the NE side exposed in TP2. For the purposes of discussion, the trench log units have been divided into four sections. The SE end of the trench and the SE end wall, FZ 1 units, a central section between FZ1 and F4, and finally a NW section NW of F4.

Units in the SE section of TP2 are virtually identical to the SE section of TP1. The SE end section of TP2 reveals intervening periods of swamp deposition, fan sediment accumulation, and possible debris flow deposition of the basal unit has produced this deposition sequence (see Section 3.3.2 for further discussion).

FZ1 units are clay rich units with clasts of a range of sizes randomly positioned within a clay matrix. Some of these clasts are aligned within the generally sheared and smeared fault gouge. Original pre-faulted units are not recognised, however, the various colourations of the gouge suggest their source materials include previously faulted gouge (blue), organic peaty material (brown) and a slope wash or ponded deposit (white). The highly disturbed units incorporated in FZ1 indicated this is the locus of repeated concentrated fault displacements.

Units between FZ1 to F4 are predominantly composed of a series of colluvial wedges. The basal silty clay (Unit SC) unit lacks carbonaceous material and has very few clasts, suggesting rapid sedimentation in a fault related sag pond with intermittent sediment pulses from a number of ephemeral stream channels (eg interfingering of Units SC and CW northwest of F4). From the dearth of carbonaceous material in Unit SC forest cover seems unlikely at this site at time of deposition. The silty clay nature of the sediment also supports the inferred lack of forest cover as Unit SC is probably sourced from slope wash material entering the ponded area and settling.

A poorly sorted coarse gravel debris flow unit overlies the silty clay and marks the onset of debris flow sedimentation in TP2. Unit CGR, a poorly sorted coarse gravel, is likely to be a correlative of the debris flow sediments in TP1 which mark a period of geomorphic adjustment from sometime around 17 000 yrs BP onwards (16 830 ± 123 BP, Unit 2, TP1). This would support deposition of the older Unit SC sometime around the glacial maximum of about 18 000 yrs BP (Suggate, 1988) in a period of sparse forest cover and as indicated by the lack of carbonaceous material in the unit. Units above the debris flow are a series colluvial wedges and confirm multiple ruptures on the fault.

Units to the NW of F3 & F4 are also mostly colluvial wedge units. Exceptions include Unit GM-S with silt and clay content increasing with depth, indicative of some ponding occurring intermittently followed by fluvial activity. In addition, Unit OCW, an anomalous organic, unsorted sandy gravel unit with some clay has intruded from the base of the trench through essentially horizontal overlying units, and appears to be fully

enclosed in these younger units (eg in Unit SGX near the change of trench orientation). The most likely deposition scenario for Unit OCW is via liquefaction, either liquefaction of an organic horizon, or a liquefaction path collecting sidewall material on the way to the surface. Liquefaction induced deposition accounts for the nature of the cross cutting relationships of Unit OCW and its peculiar enclave like deposits.

3.5.3 Faults and Structures exposed in trench and critical relationships

As outlined previously numbers have been assigned to faults located in the trench, FZ1 to F4. Only one fault strand (in FZ1) penetrates to the present ground surface in the 7 m wide faulted zone. The intensity of faults and gouge material suggests that FZ1 accommodated most of the displacement that has occurred within the entire zone of faulting and ground disturbance. Another indication that FZ1 has accommodated most of the displacement is that F2-4 juxtapose similar stratigraphic units, whereas juxtaposition across FZ1 is of differing stratigraphic units.

FZ1 is comparable to the steeply dipping bounding faults of TP1. Between F1&2 of TP1 and FZ1 of TP2, an ability to distinguish stratigraphic units in this highly sheared zone proved relatively unsuccessful. FZ1 juxtaposes units of different origin, without any noticeable change in surface expression, along steeply dipping faults that suggest almost pure strike slip displacement on FZ1 fault strands. As with TP1 the main zone of rupture displacement is confined to a narrow zone of deformation.

F2 is a steeply dipping fault that appears to have faulted through Unit CGR. The fault was located via anomalously orientated clasts seen in Fig 3.5. A younger colluvial wedge truncates F2 indicating that the fault is probably a redundant or relict structure, with deformation accommodated elsewhere.

F3 and F4 are both moderately dipping faults that approach the surface then bifurcate and are subsequently truncated by younger sediments. Units either side of F3 and F4 appear to have a normal fault component (eg Unit CW on F3), however Figure 3.5 shows

both faults having a relative component of thrust coupled with a strike slip sense of shear (discussed below).

A complex series of units are juxtaposed either side of F3, suggesting displacement in various directions on the fault plane. For example, Unit SC is downdropped appreciably, whereas Unit CGR appears to have been upthrown on Unit CW on the NW side of F3. Deformation of the ground surface is apparent with an elevation change of ~1 m SE to NW above F3 & F4 (Figure 3.5). Juxtaposition of units on either side of F4 is also complex. Units SGX & CW thin appreciably and appear to have a normal sense of relative movement on the fault. A minor thrust component is often apparent on secondary splays adjacent to major strike-slip faults, this combined with the ground surface expression in TP2 (above F3 & F4) indicates a component of dip slip or thrust is accommodated on these secondary splay faults. The explanation for the apparent "normal" slip displacement for units (SGX, CW, & SC) across for example F4, is dependent on the depositional geometry of the colluvial wedges, and the strike-slip offsets accommodated by the fault through irregularly shaped unit contacts.

One partial or complete explanation for apparent reversal of the sense of throw is outlined below. Assuming local colluvial wedges taper from a point source this provides an explanation of units either side of F4, accommodating the surface expression indicating a component of oblique thrust, while still accounting for the apparent "normal" sense of shear on the faults in Figure 3.5. Figure 3.6 a&b are sketch maps of the fault and subsidiary splays for the TP2 setting. The relative sense of shear for each fault is shown, and the adjoining Figure 3.6c outlines a schematic interpretation of the fault zone at greater depth. The relative decrease in unit thickness of Unit CW (Fig 3.5) on the SE side of F4 can be explained by units from a more central colluvial wedge environment being juxtaposed dextrally from a more radial colluvial wedge (hence thinner units) environment. Units either side of F3 have juxtaposed with the major slip component being fault parallel allowing units of differing thickness to appear faulted in the opposing sense, relative to those ascribed to, and reflected by ground surface deformation.

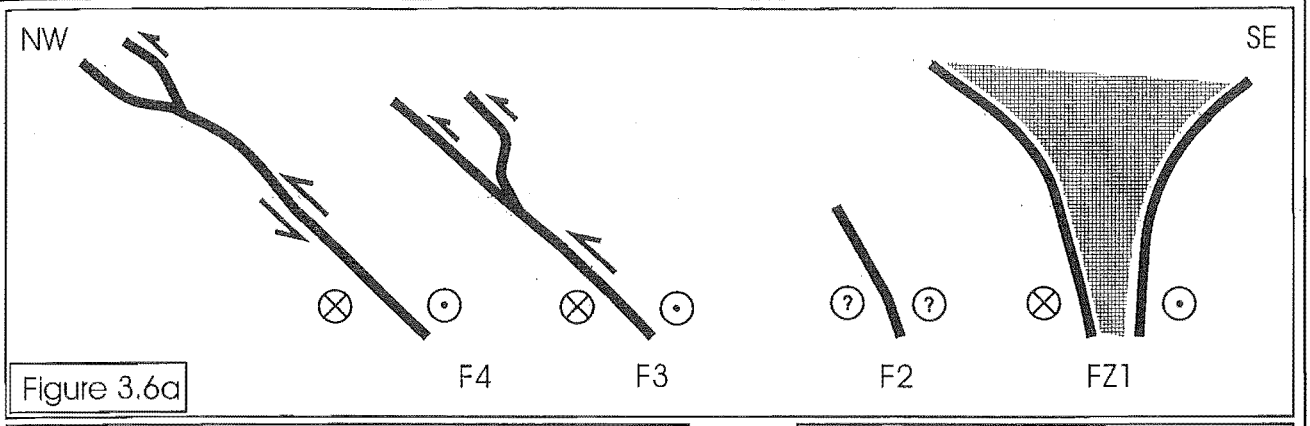

Figure 3.6a

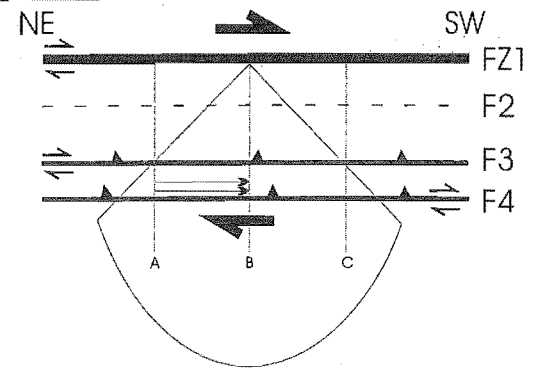

Figure 3.6b: Tapering colluvial wedge plan view above. Cross section through F4 below.

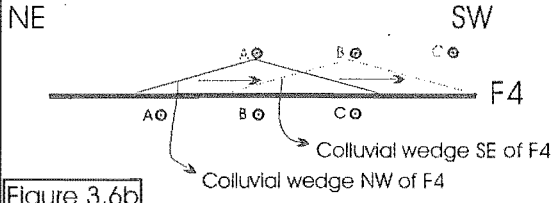

Figure 3.6b

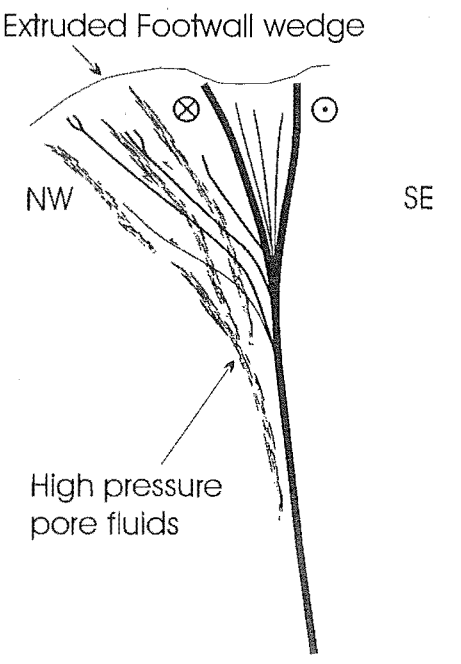

Figure 3.6c

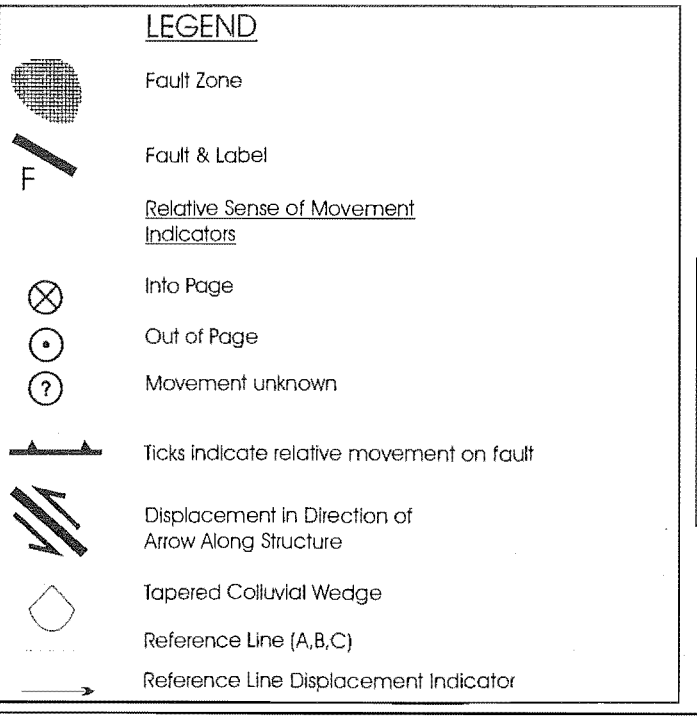

Figure 3.6: Schematic map of the faults of Tophouse Trench Two (Fig 3.6a) accompanied by a schematic tapering colluvial wedge example (Fig 3.6b). Figure 3.6c is a schematic map of the fault at depth.

3.5.4 Radiocarbon Samples and Dates

Five radiocarbon samples were collected from TP2. Four of the samples are from the SE of the trench and of inferred similar stratigraphic horizons to TP1 samples. The fifth sample W616 (see Figure 3.5) is from a thin organic horizon under colluvium and NW of the truncated F4. None of the radiocarbon samples collected from TP2 have been sent for analysis as they were from similar stratigraphic horizons to TP1 samples, which appeared promising at the time of trenching but failed to yield the anticipated dates, or assist in constraining the paleoseismic history for the site.

3.5.5 Summary

The zone of overall deformation in TP2 is wider than TP1, although the primary deformation zone (FZ1) is similar to that in TP1. Ground surface deformation relates to the subsurface structures recorded in the trench (eg F3&4). A minor element of thrust faulting coupled with a major strike-slip component is apparent on F3&4, while not apparent in TP1, TP1 is shorter and it may have failed to extend, far or deep enough to intersect faults underlying the anticlinal warp on the north side. As with TP1 there is no evidence for similar stratigraphic units spanning FZ1, therefore repeated long-term displacement is inferred.

3.6 LOCALISED GROUND DEFORMATION

3.6.1 Tophouse Trench 1

At first glance TP1 (Figure 3.4) does not appear to exhibit any appreciable localised ground deformation. However, closer inspection reveals that about two metres to the NW (Figure 3.4) along the ground surface from F1 there is a slight change in surface slope,

increasing slope gradient down and away to the NW. Under present conditions this slope change is slight. However, the swamp (Unit 11) is a very young feature (radiocarbon date post 1950) and the ground surface prior to swamp deposition must have been similar to the present base of Unit 11 for close to two thousand years (approximate age of the truncated Unit 10, Wk10246). Without the Unit 11 mantle a more apparent and pronounced ground roll was associated with the fault at this site, prior to 1950. Slight deformation of Unit nw2 could be inferred looking at Figure 3.4. Unit nw4 on the other hand does not appear deformed indicating deformation has not propagated to the surface, or, alternatively that the inferred deformation of nw2 is related to the disturbed ground surface of Unit nw1.

Without any other evidence, suggesting localised ground deformation at TP1 would be imprudent. Figure 3.7 of the NE side of TP1, less than two metres along the fault strike from Figure 3.4 reveals some local ground warping. A white clay horizon outlined in Figure 3.7b appears deformed, in between the main fault zone and the point where the surface expression changes in the NW. Unfortunately units below the white clay layer (Figure 3.7a) are difficult to distinguish and localised deformation below the clay horizon cannot be identified. A possible explanation for the deformation is the initial development of a fault-propagated fold on the back of a minor thrust splay. This fault propagated fold explanation is further discussed in Section 3.6.3.

3.6.2 Tophouse Trench 2

Deformation related to the main strike-slip fault zone is expressed by both sub-surface and surface features (Figure 3.5 & 3.8). Sub-surface features include F3 and F4, which are oblique slip structures with the dominant strike-slip component and minor thrust component (as discussed in Section 3.5.3). Compared with the juxtaposition of units either side of FZ1 movement on F3 and F4 is relatively minor, as the juxtaposed units are similar. This suggests that the structures F3 and F4 are not well established relative to FZ1 and ephemeral. F3 & 4 may reflect fault plane irregularities, or alternatively

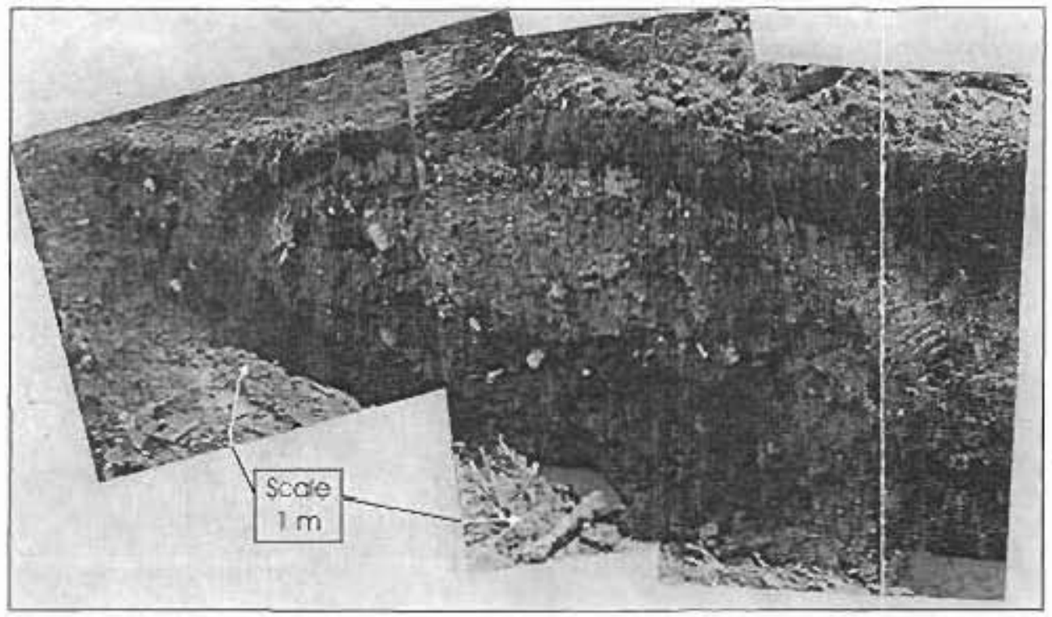

Figure 3.7a: Photomosiac of part of the NE face to Tophouse trench one

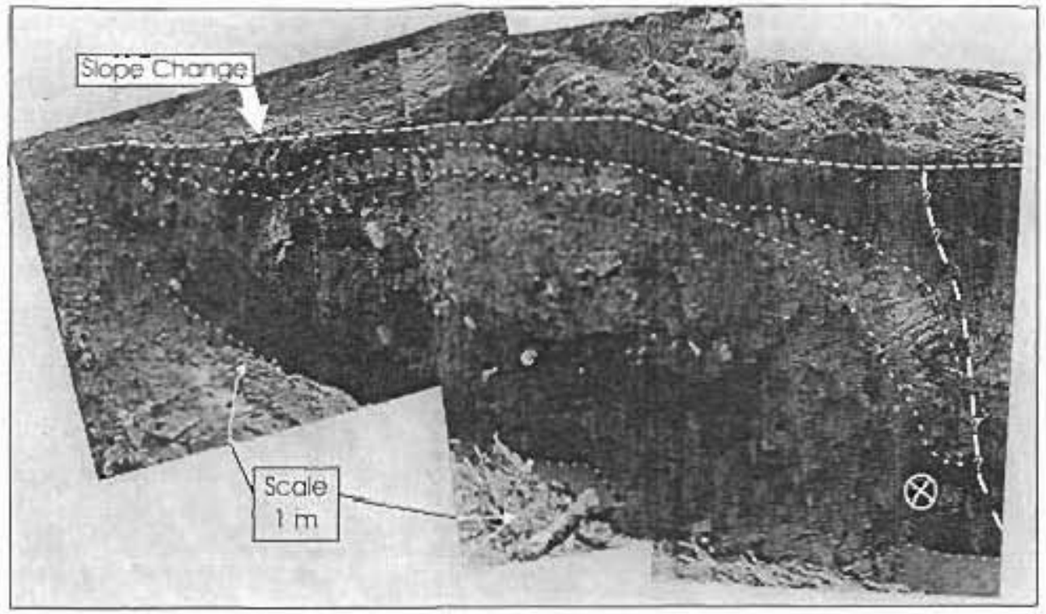

Figure 3.7b: Photomosiac of part of the NE face to Tophouse trench one with approximate unit and fault locations and relative fault movement

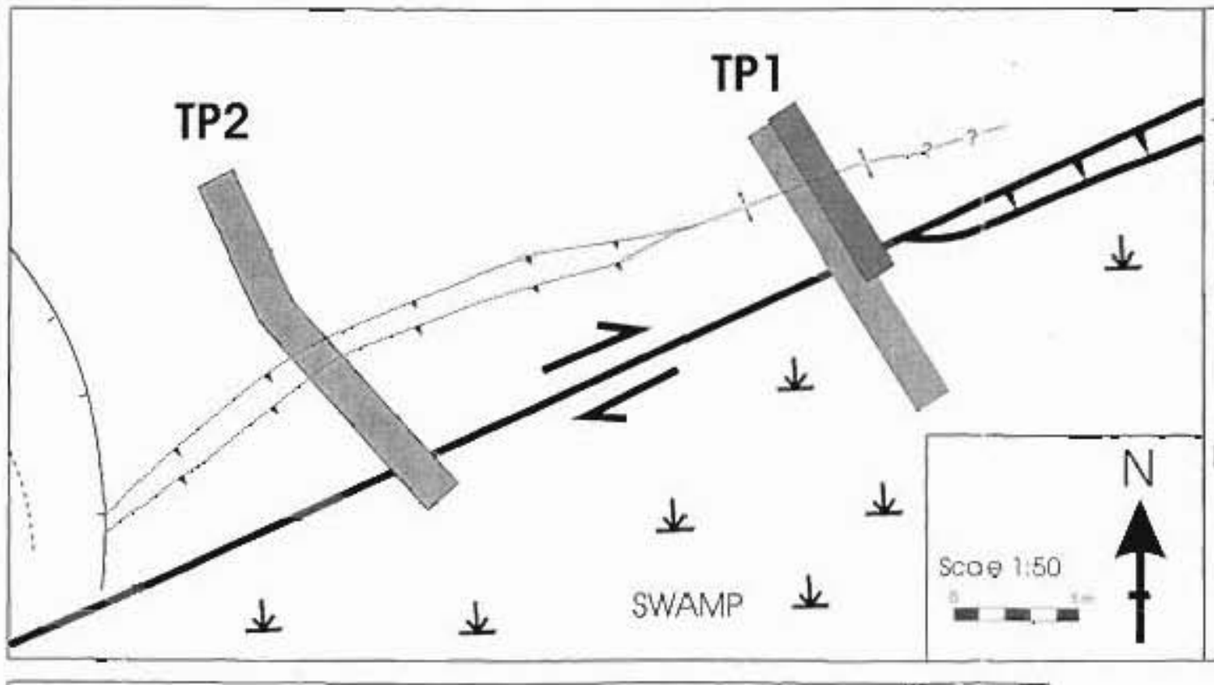

LEGEND (for plan view map)

- Channel Centre and Edge
- Location of Photomosaic above relative to trench sites
- Fault Scarp (top and base)
- Relative displacement direction along fault (arrows) and fault location
- TP — Trench locations and Trench number
- Change of slope (related to ground deformation)
- Swampy area

LEGEND (for Figure 3.7b)

- Deformed White Clay Sediment
- Edge of Fault
- Ground surface prior to
- ⊗ Motion on relative to fault zone (into page or perpendicular to trench azimuth)

Figure 3.7: Photomosaic of NE face of Tophouse Trench One (3.7a) with deformed zone marked on 3.7b. Figure 3.7c plan view showing photomosiac location.

Figure 3.7c: Plan view of trench site and Figure 3.7a&b location

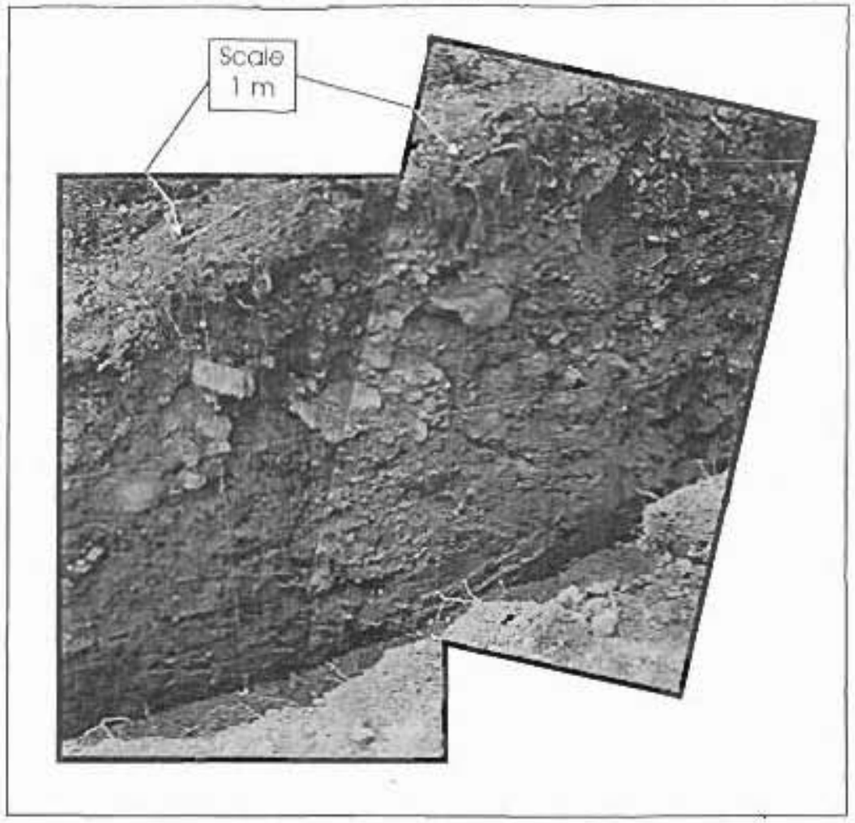

Figure 3.8a: Photomosiac of part of the NE face to Tophouse Trench Two

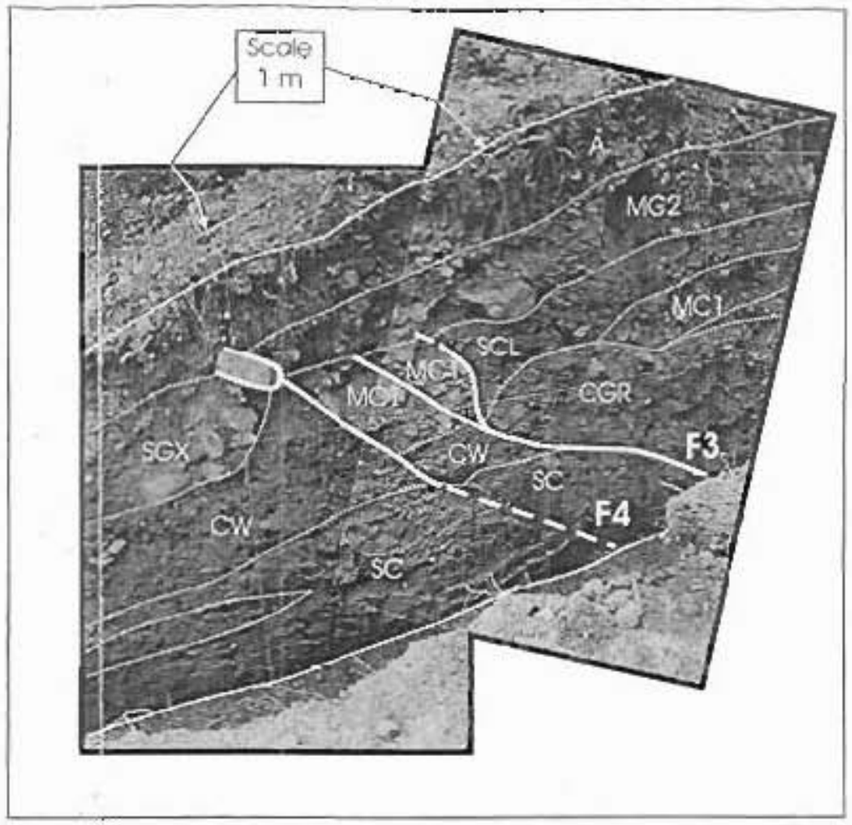

Figure 3.8b: Photomosiac of part of the NE face to Tophouse Trench Two showing Faults 3&4 and unit boundaries

LEGEND (for Figure 3.8b)

- Unit outlines
- Faults
- Top and Base of Trench
- CW — Trench Unit code
- F3 — Trench Fault code

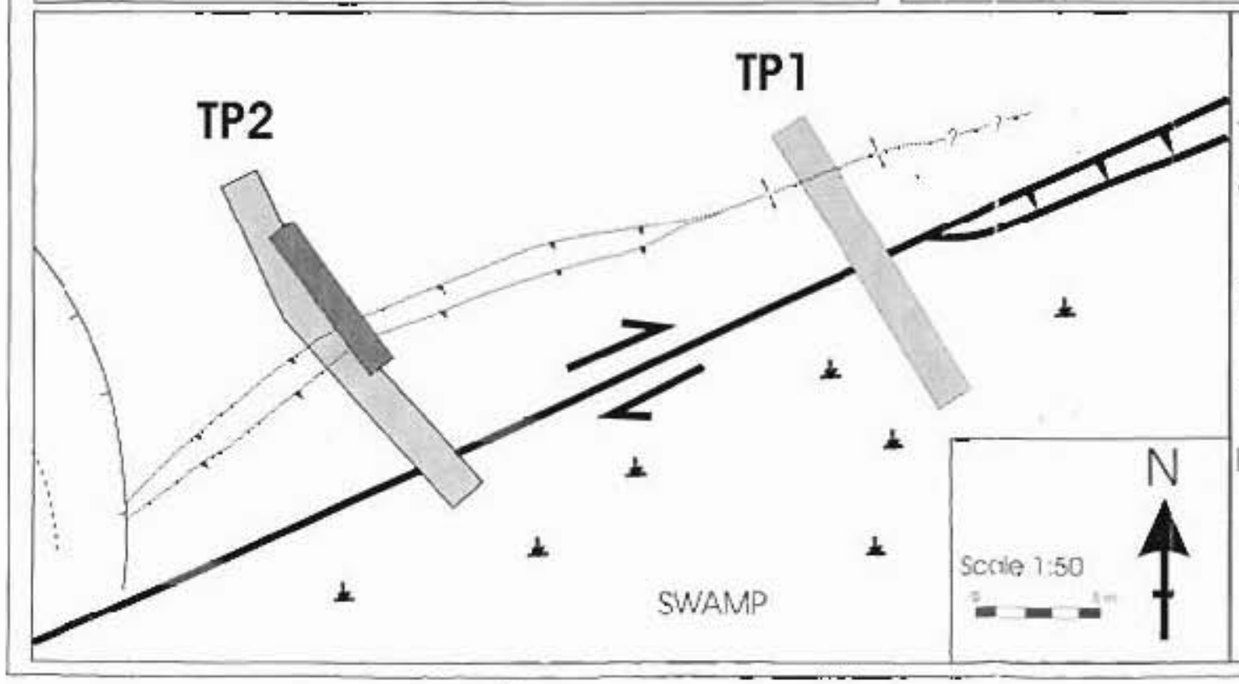

LEGEND (for plan view map)

- Channel Centre and Edge
- Location of Photomosaic above relative to trench sites
- Fault Scarp (top and base)
- Relative displacement direction along fault (arrows) and fault location
- TP — Trench locations and Trench number
- Change of slope (related to ground deformation)
- Swampy area

Figure 3.8: Close up photomosaic of NE face of Tophouse Trench Two Faults 3&4 (Figure 3.8a) with Figure 3.8b showing trench units, faults and sense of displacement indicators. Figure 3.8c is a plan view of the trench site showing the location of Figures 3.8 a&b.

Figure 3.8c: Plan view of trench site and location of Figures 3.8a&b

evidence of strain partitioning on the fault, or may be related to topographic effects with respect to fault rupture. One distinct difference from TP1, is visible structures have developed (F3&4) which suggests that either these structures are older, more developed, and deformation is accommodated on existing structures, or that there is a local fault plane asperity, concentrated about TP2.

Strike-slip juxtaposition of wedge-shaped packets of colluvium can, and may, account for all the anomalous apparent reversals of sense of throw, but an alternative mechanism may also be involved. The paradox of apparent normal faulting on a transpressive fault zone has been observed in similar settings eg at Greenburn on the Hope Fault (Langridge et al, in press) and personally observed by the author. Partitioning of strike-slip into a furrow fronted by the footwall thrust system is well known, but what is evident is that the imbricated footwall wedge is extruded as an asymmetric pop up or flake. Because the wedge moves out from under the hanging wall the fault or faults on the upper side are technically normal faults in terms of movement sense even though the structure is compressional. Evidence of fluidisation and elevated pore pressure associated with wedge extrusion observed in the Greenburn trench are paralleled at this site.

3.6.3 Ground Deformation Summary

Localised deformation on a fault zone subject to ruptures of this size is not uncommon (Sylvester, 1988), however, it is interesting that within metres structures and features accommodating this deformation vary markedly. Partitioning of slip helps explain the juxtaposition of the units near F3&4. The assumption of slip partitioning is reinforced by otherwise unexplained surface features in both trenches, and the apparent bulging of the NE side of TP1. A gradual decrease in deformation coincides with the reversal of the fault scarp (see plan view Figure 3.7).

Ground deformation in the vicinity of the Tophouse trenches is related to the major strike-slip fault zone. In both trenches, the strike-slip component of deformation is

dominant and accommodated over a narrow zone. The minor thrust flaps are on the free slope side of the fault and are related to minor stress perturbations related to the major strike-slip displacements, which appears to reduce and fade with the initiation of the major fault zone scarp reversal.

3.7 SUMMARY

Paleoseismic evidence from the Tophouse trenches brackets the timing of the last rupture event on the Wairau Fault at Tophouse to sometime between AD200 and AD 1840. A small branch fragment from the shear zone (TP1 - Wk 10245) provides evidence of an earlier rupture event about 12 500 years ago.

Both trenches suggest repeated displacements have been accommodated over a narrow zone of deformation. Minor "flower" structures accommodate displacement of predominantly strike-slip nature with some localised minor slip partitioning producing minor oblique thrust faults, minor folding and earth deformation. Minor structures associated with the faulting generally develop on the free downslope side of the fault, evolving and dying out over short distances. Termination of the minor thrusts and anticline to the NE coincided with the reversal of the sense of throw on the main fault scarp.

Streams and channels have been deflected appreciably by the fault scarp running roughly perpendicular to general ground slope. This is especially the case where the scarp is uphill facing, deflecting streams to the NE towards one of only two locations where streams have breached the main fault scarp, near the trench sites.

Radiocarbon dated peat layers from TP1 indicate a change in the geomorphic environment over the last 20 000 years. Debris flows interspersed with thin peat layers suggest a relatively unstable geomorphic environment post the last glaciation and prior to widespread reforestation. There is no evidence of carbonaceous material in Unit SC from TP2, this unit is inferred to be older than the basal peats of TP1 and coincides roughly

with the last glacial maximum of about 18 000 years BP (Suggate, 1988). Sedimentation appears to be relatively stable at this locality at least since the beginning of the Holocene and location of the small beach tree branch in the fault zone suggests establishment of a forest prior to about 12 500 years ago.

An age bracket of this time span (AD 200 - AD 1840) does not accurately constrain the timing of the most recent rupture event, critical when assessing future seismic hazard of the fault. The rupture bracket does, however, provide a valuable reference point, and will help in understanding the paleoseismic history of the fault when used in conjunction with other paleoseismic studies on the fault.

PALEOSEISMIC DATA COMPARISON WITH ALPINE FAULT SECTIONS TO THE NE AND SW

4.1 INTRODUCTION

Of crucial importance when assigning the location of fault segment boundaries is the timing of the most recent ruptures and slip rate determinations at different geographic locations along the length of a fault (McCalpin, 1996). The case for the Alpine Fault is no differentbut, as the Alpine Fault is a range-bounding fault in an area of active tectonism and high erosion, identification of geomorphic fault features not masked by aggradation or fan sedimentation, with suitable and accessible trench locations provides its own set of challenges.

This chapter collates relevant paleoseismic data from various authors along the length of the Alpine Fault and combines this existing information with data from this study. Placing the information from this study in a regional context is a step forward in the development of the paleoseismic record of the fault, further supplementing improvements to the accuracy of seismic hazard assessment for the region.

4.2 Dates of Major Earthquake Rupture in the Southern, Central and Northern Sections of the Alpine Fault

4.2.1 Southern & Central Section

Division of the fault into sections by Berryman et al (1992) places a boundary between the North and Central sections around the crossing of the Taramakau River over the Alpine Fault trace. A robust paleoseismic record has been determined for the southern, central and part of the northern section over the last 1000 years or so (Figure 1.3) (Berryman et al, 1998; Bull, 1996; Cooper & Norris, 1990; Wright, 1998; Yetton, 1996, 2000; Yetton et al, 1998). This record provides evidence of rupture at some point along the above fault sections at AD 1717, AD 1620 ± 10, AD 1440 ± 10, AD 1210 ± 30 and around AD 940 ± 50 (rupture dates from two or more matching dates from the authors above). A rupture recorded at Waitaha River, AD 1580 ± 10 by Wright (1998) is not recorded in trench dates elsewhere, although revised dates of Bull (Wright 1998 & Norris et al, 2001 pers.comm. Bull 1998) point to a rupture date at this time. Wright (1998) suggests the AD 1580 ± 10 event is a smaller earthquake rupture event capable of local disturbance though not recorded in trench data.

4.2.2 North Section

Yetton (2002) recently completed an extensive paleoseismic investigation of the North Alpine Fault section at Blue Grey River, Maruia River, and the Matakitaki River. This work in conjunction with previous paleoseismic investigations (Yetton et al, 1998; Yetton, 2002) on the northern end of the Central Alpine Fault section and part of Northern section provides crucial information about the behaviour of the Alpine Fault in this region. Most importantly this work provided evidence of, and tightly constrained, the northern termination of the AD 1717 event, termed the Toaroha event, to between Haupiri River and Crane Creek (Yetton 1996, 2000; Yetton et al, 1998). The penultimate

event, termed the Crane Creek event (Yetton, 1998) extended through Haupiri River and is recognised further NW along the fault trace. Yetton (2002) combines recent trench investigations from the Blue Grey, Maruia, and Matakitaki River trench sites and has constrained the last rupture period to AD 1600-1700 for this section of the North Alpine Fault.

4.3 Dates of Major Earthquake Rupture in the Wairau Section of the Alpine Fault

4.3.1 Tophouse Trenches

Our paleoseismic investigations in the trenches at Tophouse found evidence for two ground ruptures, firstly approximately 12 500 years ago, and secondly the most recent rupture between AD 200 and AD 1840. No other evidence directly related to individual fault ruptures, however, dates from offset peat horizons suggest multiple ruptures on the fault in the intervening period. The youngest bracket, AD 1840, is the time of European settlement in New Zealand, hence an historic date and does not physically constrain the last rupture date on the fault. The age from the truncated Unit 10does provide evidence of rupture since AD 200 on this section of the Alpine Fault. At present the other date directly related to fault rupture of approximately 12 500 years ago does not contribute a significant constraint on the fault rupture history as the present paucity of data prevents this. In future this date may help constrain a recurrence interval for the fault.

Indirect weathering rind dates tentatively suggest a ground rupture event around 1450 ± 150 yr BP. WRD dates also tentatively constrain the penultimate rupture event to prior to 4350 ± 450 yr BP. Another event is recognised around 6750 ± 1000 yr BP at two separate locations.

4.3.2 Wairau Valley Trenches

Paleoseismic investigations near the Wairau Valley settlement by Zachariasen et al,

(2001) provide evidence of faulting. Three episodes of faulting are recognized; of most importance to the Tophouse trenches is the most recent rupture event and the only rupture event comparable with timing constraints at Tophouse. Radiocarbon dates of charcoal from Wadsworth trench indicate the most recent rupture is constrained to the calendric period between AD 700 and 760 BC, summarised in Table 4.1 below. However close inspection of the dates and re-interpretation of the self-ages suggests that the actual youngest date the fault could have ruptured is before AD 1000. This date allows for the self-age of 300 years from the difference between NZA 11643 & NZA 12461 therefore extending the youngest possible age of last rupture to about AD 1000 (Yetton 2002). Therefore, the new adjusted bracket constraining the last rupture on the fault at Wadsworth trench is between AD 1000 and 760 BC.

Sample Code and Unit Code	^{14}C Date	Calendric Date Range	Comments
NZA 12461, Unit 49	1530 ± 55 BP	AD 470 to AD 700	Unfaulted colluvium, self age limited to less than 300 years by the definite self age of NZA 11643 below
NZA 11643, Unit 49	2025 ± 60 BP	BC 130 to AD 168	Unfaulted colluvium, implied minimum of 300 years self-age because this date is at least 300 years younger than NZA 12461
NZA 11642, Unit 55	2531 ± 55 BP	BC 760 to BC 364	Youngest faulted unit

Table 4.1: Radiocarbon ages and calendric ages from samples that bracket the last fault rupture on the Wairau section of the Alpine Fault in the Wadsworth trench of Zachariasen et al (2001). Table modified from Yetton (2002).

Zachariasen et al, (2001) tentatively recognised other rupture events occurring between ca 2600-3300, before ca 4700 yr and possibly another event since 5600 yr.

4.3.3 Paleoseismic Summary of the Wairau Section of the Alpine Fault

Radiocarbon dated fault rupture brackets at two locations on the Wairau section of the Alpine Fault, of between AD 1840 - 200 AD and AD 1000 - 760 BC at Tophouse and Wairau Valley trenches respectively, provide evidence of rupture in the late Holocene. However both the rupture brackets are broad and do not tightly constrain the last rupture. If you consider that both trench locations are part of the same fault segment and that the respective rupture brackets overlap, then it is possible to further constrain the most recent rupture event. A rupture bracket between AD 200 and AD 1000 constrains the last rupture on the Wairau section on the Alpine Fault combining dates from Tophouse and Wairau trenches. Modal peaks from weathering rind dates tentatively indicate the time of the last rupture around AD 550 (1450 ± 150 yr BP). .

4.4 Slip Rate Distribution and Single Event Displacements

4.4.1 Central & Northern Sections

The confluence of the MFS (the Hope Fault of the MFS) with the Alpine Fault significantly decreases the fault parallel slip rate transfer to the north (Norris & Cooper, 2001). South of the coalescing of the MFS on the Alpine Fault, 27 ± 5mm/yr of right lateral strike slip is accommodated on the Alpine Fault combined with a maximum 8-12 mm/yr fault normal component west of the Mt Cook region (Norris & Cooper, 2001). Consistent dextral single event displacements of c 8 m are encountered south of Haast (Norris et al, 2001; Sutherland & Norris, 1995). Fault parallel slip is reduced by nearly a third north of the Hope-Alpine Fault intersection, at the junction with other faults of the MFS more slip is undoubtedly dissipated progressively northward from the Alpine Fault.

Evidence to indicate dissipation of slip rate further north along the North Alpine Fault

section is described below. Three slip rates are recorded on the North Alpine Fault to date (Berryman et al, 1992; Yetton et al, 1998 & Yetton 2000; Yetton, 2002). Near the Taramakau river Berryman et al (1992) estimated a fault parallel slip rate of about 8-12 mm/yr from dextral offsets of 11-13 m, vertical components of up to 7 m and weathering rind ages of 1100-1300 yrs, with an estimated single event displacement of ~6 m dextral and 3 m vertical offset. Norris & Cooper (2001) analysed the uncertainties of the slip rate and provided a best estimate of 10 ± 2 mm/yr fault parallel and 6 ± 2 mm/yr fault normal for the offset near the Taramakau River.

Northwest along fault strike at Haupiri River a fault parallel slip rate of 6.5 ± 2.5 mm/yr was estimated from an offset terrace tread (Yetton et al, 1998; Yetton, 2000). Once again Norris & Cooper (2001) refined the slip rate slightly to agree with their common uncertainty analysis of Alpine Fault slip rates to ≥ 6.3 ± 2 mm/yr fault parallel and ≥ 2.5 ± 0.5 mm/yr fault normal components.

Recently Yetton (2002) reported slip rates from offset small tributary streams of Crooked Mary Creek NW of the Haupiri River site. The offset streams ran over moraine surfaces, the exact age of this moraine is unknown and tentatively assigned to the Late Otiran glaciation of about 18 000 years BP of Suggate's (1990) nomenclature (Yetton, 2002). A slip rate of 7.7 ± 1 mm/yr was determined as a best estimate over the last 20 000 years or so near the Blue Grey and Maruia Rivers. Yetton (2002) reported single event displacements at Maruia and Blue Grey Rivers of ~1.3 m horizontal and a consistent 0.25 m vertical, and ~1.0 ± 0.3 m horizontal and 0.2 – 0.4 m vertical respectively.

No geomorphic features allowed slip data from the area around the Matakitaki trench sites, to be determined although a well-defined channel was recognised to be offset dextrally by 6 ± 1 m (Yetton, 2002). Yetton (2002) considered the age of the displaced terrace to be of the order of thousands of years because of its relative height above the current river level, with the possibility that there could be up to 6 rupture events. Field relations suggest that the only confident inference from the site is that the last single event displacement at the Matakitaki site was less than 3 m (Yetton, 2002).

4.4.2 Wairau Section

Numerous authors have recorded slip rates along the Wairau Section of the Alpine Fault (Lensen 1968; 1976; Campbell 1973; Grapes & Wellman 1986; Kneupfer, 1992; Yetton 2002). A right lateral sense of slip dominates along this essentially straight fault trace, with a minor component of vertical displacement evident (Lensen 1968; 1976; Campbell 1973). Lensen (1968) reports variation in sense of vertical movement along fault strike and local reversal of vertical movement over time at Branch River.

Glacial features offset by the fault were measured by Adamson (1964) and Campbell (1973) described the change in slip rate needed to accommodate these offset features. Reconciliation of the features involves a decrease in slip rate over the late Quaternary, to a slip rate of about 3-5 mm/yr dextral and <1mm/yr vertical correlating with the Holocene and late Pleistocene offset features. An attempt to increase the accuracy of slip rate data, especially the vertical component of slip using GPS measurement failed, as in most cases tree canopy interrupted satellite signals. Also severe degradation of the geomorphic markers occurred, most notably between the offset Black Valley I terminal moraine on the NE outskirt of St Arnaud where the refuse tip has been filled (NW of fault) and excavation has recommenced in a quarry (SE of fault).

Slip rate data from this study from offset fluvial terraces in the Wairau Valley provides a slip rate of 4.2 ± 1.4 mm/yr. The large error associated with the slip rate is related to the paucity of good age constraints, one weathering rind date of 11 000 yr BP combined with relative ages related to the last glacial maximum aggradation surface. Matching offset features were recognised at three sites and offsets decrease towards the active Wairau River. The youngest faulted terrace riser was offset 4.4 ± 0.5 m.

Branch River crosses the Wairau Fault almost perpendicular to the fault trace. A series of river terraces provide excellent geomorphic displacement markers and provide crucial fault evolution data (Lensen, 1968; 1976). Maximum displacement of the highest terrace at the Branch River site is on the order of 70 m (Lensen, 1976), with displacement

progressively decreasing with each younger geomorphic surface. Lensen (1976) analysed the progressive terrace displacements and concluded the single event displacements were 5.2-6.7 m per rupture event.

Lensen (1976) estimated the age of the highest terrace at Branch River as approximately 18 000 years, corresponding to the major aggradation terraces of similar age in the Buller Valley (Suggate 1988, 1990). Both Lensen (1976) and Suggate (1988) correlate the major aggradation surfaces with the maximum of the last Otiran stadial advances, about 18 000 years BP (see section 1.5.2) and not the more recent and less extensive stadial advance of about 14 000 years BP. A long-term slip rate of 3.8 mm/yr is determined at Branch River by correlating the 70 m offset terrace with the 18 000 year old aggradation surface (Lensen, 1976).

A study by Kneupfer (1992) dated terrace surfaces at Branch River using weathering rind dating and calculated a slip rate of 3-5 mm/yr. Correlation of the Lake Rotoiti oldest moraine (ie Back Valley I moraine of Adamson, 1964) with an age of 18 000 ± 2000 yrs corresponds to a slip rate of 3.7 ± 1.4 mm/yr fault parallel and ~0.5 mm/yr vertical (uplift on SE side).

Zachariasen et al (2001) estimate a slip rate at Wairau Valley of a displaced channel of 4-5 mm/yr on the assumption that the stream ponding began post displacement of the channel by the fault. Radiocarbon dates in the Dillon trench from below ponded sediments and in the ponded sediments provided age controls.

Studying the fault near the coast at Cloudy Bay, Grapes & Wellman (1986) propose an alternative slip rate of 6.7 mm/yr. Two channels acted as displacement markers, offset 10 m dextrally and upthrown 2 m to the NW, across a surface interpolated to be 1500 yrs old from radiocarbon dated shorelines. Grapes & Wellman (1986) comment that Lensen (1976) discounts the likelihood that the highest Branch River terrace is not associated with the ultimate glacial stadial advance (~14 000 BP), and suggest an early post-glacial age of 10 000 yrs for the Wairau surface, which would increase the slip rate at Branch River to about 7 mm/yr.

4.5 Discussion of a Possible Fault Segment Boundary

A clear distinction is made between the terms fault segment and fault section. According to McCalpin (1996) an earthquake segment is defined by historic rupture limits. In many instances, especially in New Zealand with our short historic observation period the faults under discussion have not ruptured historically therefore cannot be assigned as earthquake segments. Behavioural fault segments may be assigned by multiple well-dated paleoearthquakes, changes in slip rate, variation in recurrence intervals, sense of displacement, or fault complexity (McCalpin, 1996). A fault section on the other hand is defined from one geographic location to another based on geomorphic evidence. Berryman et al (1992) assigned a fault section boundary around Lake Rotoroa on the basis of geomorphic expression and fault behaviour. No direct paleoseismological data constrained this boundary.

4.5.1 Discussion of Rupture Dates

As outlined in Section 4.2, rupture dates on the Southern & Central sections of the Alpine Fault are well constrained. The last rupture of the southern fault sections, in AD 1717, terminated before Ahaura River and is not recorded in any paleoseismic investigations to the north (Yetton, 2000; Yetton, 2002; Yetton et al, 1998). This contrasts to the penultimate event, AD 1620 ±10 yr which is recorded in the Ahaura River trenches. Radiocarbon dates from trenches to the NE as far as the Matakitaki River bracket the AD 1620 ±10 yr rupture, although not specifically or unequivocally assigning the rupture event encountered in the trenches to that of AD 1620 ±10 yr. Dates of ruptures prior to the AD 1620 ±10 yr event are not recognised in the trenches NE of Ahaura River.

Individually the Tophouse and Wairau Valley trenches do not tightly constrain a rupture bracket for the last rupture on the Wairau Section of the Alpine Fault. However, on the assumption both trenches are part of the same fault rupture segment and the same rupture

is recorded in both trenches a conservative rupture bracket of AD 200 – AD 1000 is determined. With the best estimate from trench data from Matakitaki SE to Blue Grey River a rupture bracket is defined as between AD 1600 – AD 1700 (Yetton, 2002) and the rupture bracket of Tophouse and Wairau Valley, AD 200 – AD 1000, (this study & Zachariasen et al, 2001) there is a temporal disparity of at least 600 years (Figure 4.1 & Figure 4.2). As the AD 1000 upper limit from Wairau Valley is conservative the actual age difference is greater than 600 yrs. Paleoseismic trench data therefore defines an earthquake rupture segment boundary between the Matakitaki trenches in the SW to the Tophouse trenches in the NE.

4.5.2 Slip Rate Discussion

All available slip rate data from the Northern and Wairau Section of the Alpine Fault are outlined in Table 4.2 below. The slip rate data are from the Late Pleistocene to present day and provisionally divided geographically by the fault section boundary near Lake Rotoroa of Berryman et al (1992). Apart from the slip rate data of Grapes & Wellman (1986) slip rates from the Wairau Section of the fault lies between 3-5 mm/yr. Conversely, the slip rate data to the SW on the North Alpine Fault section although variable, is significantly larger than to the NE. An average slip rate on the order of 8 mm/yr on the North Alpine Fault as opposed to a conservative average slip rate to the NE of 4 mm/yr suggests there is a fault segment boundary impeding slip transfer to the NE. Since the last glacial maximum, 18 000 yr BP (Suggate, 1988), matching offset geomorphic features to the southwest would be offset about 140 m (8 mm/yr) compared to about 70 m (4 mm/yr) with the differing slip rates. Placing a fault segment boundary on Alpine Fault slip rate data alone would be between Crooked Mary Creek, 7.7 ± 1 mm/yr (Yetton, 2002), and Lake Rotoiti, 3-5 mm/yr (Campbell, 1973). This location does not constrain dissipation of slip to any singular feature such as faults branching into the MFS or faults to the north eg the Flaxmore Fault, Speargrass Fault zone and the Waimea Fault.

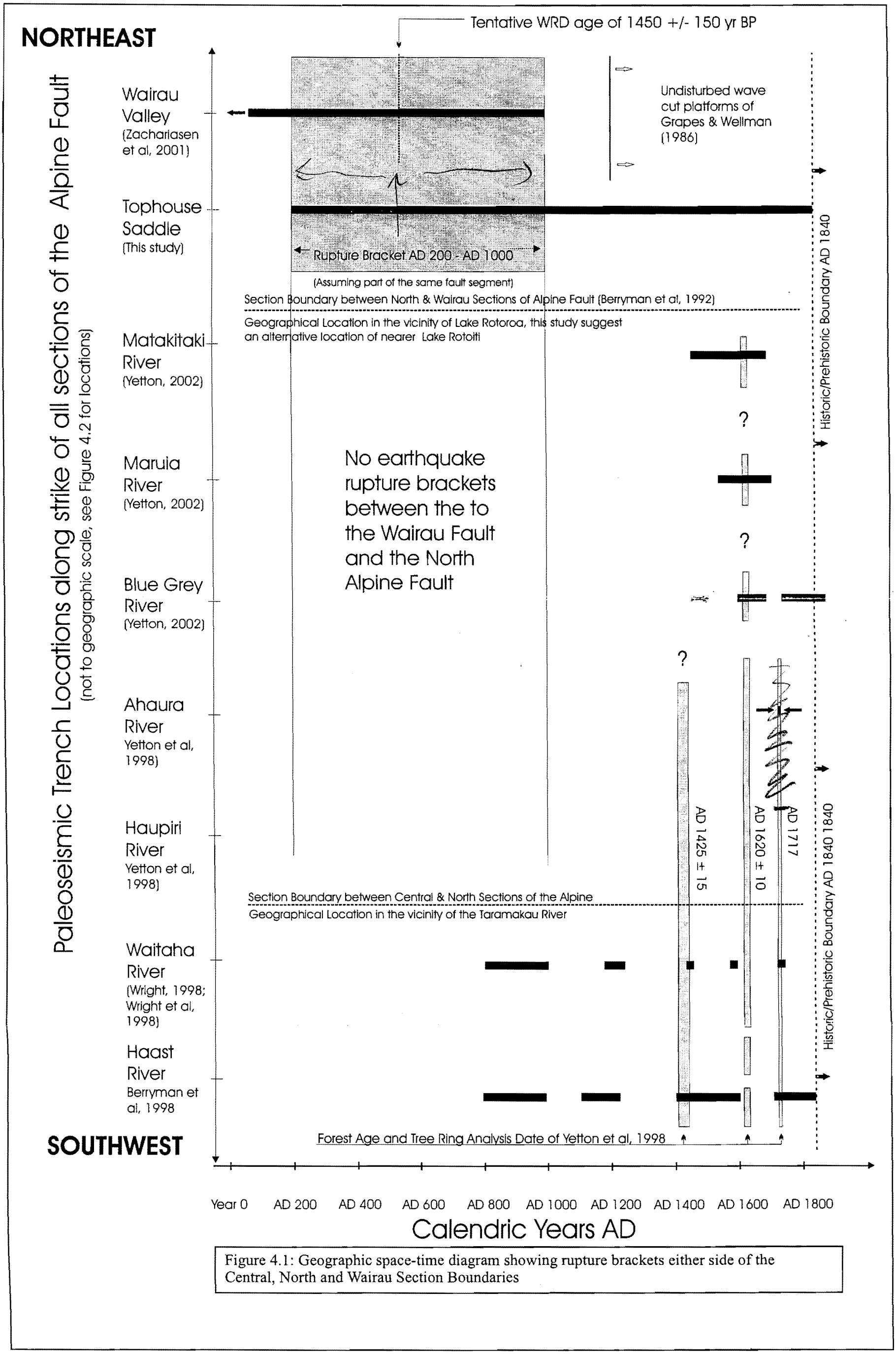

Figure 4.1: Geographic space-time diagram showing rupture brackets either side of the Central, North and Wairau Section Boundaries

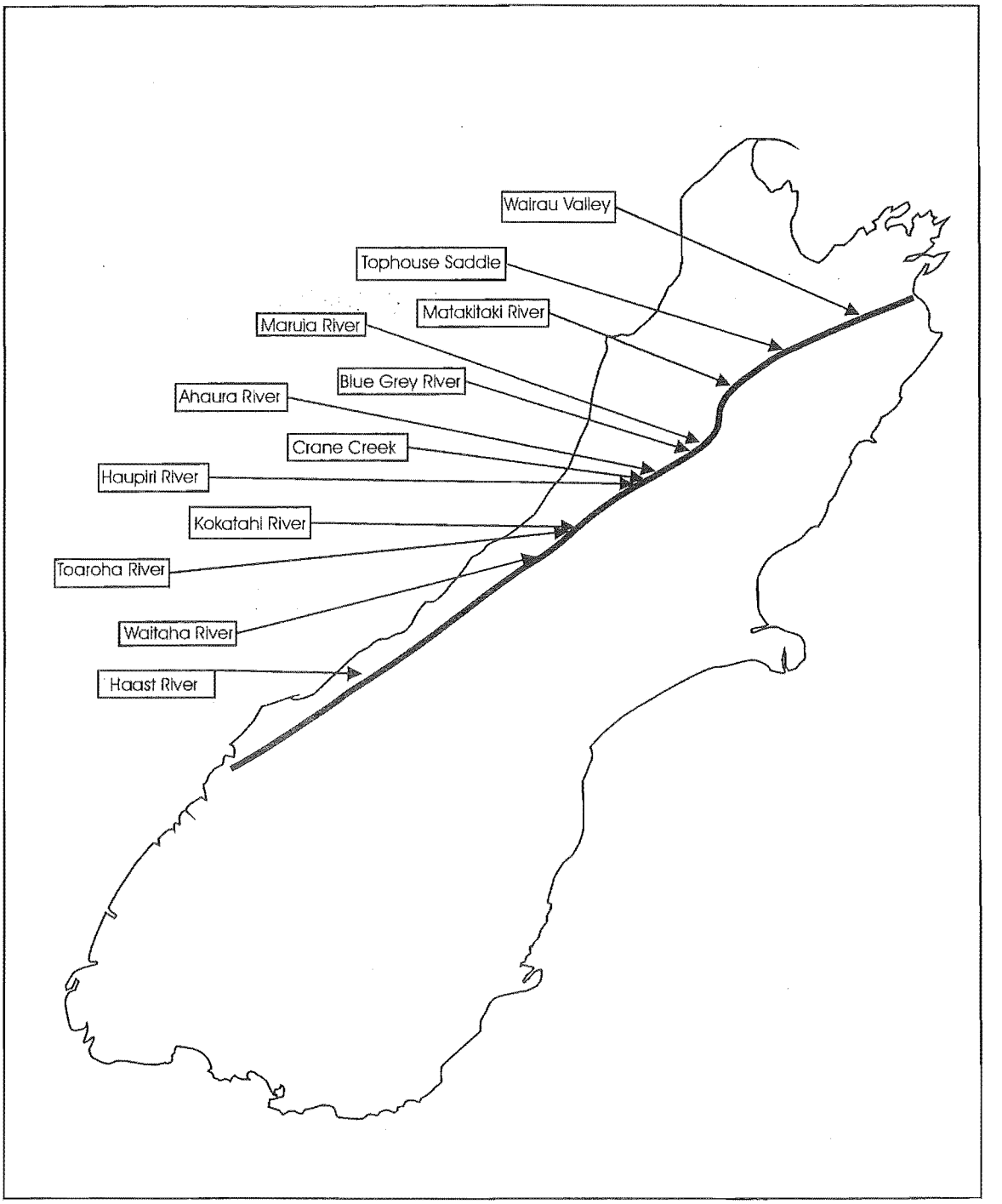

Figure 4.2: Geographical locations of trench sites along the Alpine Fault

Table 4.2: Slip Rate Summary Table from Holocene and Late Pleistocene geomorphic features along the North & Wairau Sections of the Alpine Fault

Author & Location	SLIP RATES ON THE NORTH ALPINE AND WAIRAU SECTIONS OF THE ALPINE FAULT	
	Wairau	North Alpine
Grapes & Wellman (1986) NE end of Wairau Fault, near Cloudy Bay	6.7 mm/yr	-
Zachariasen et al, (2001) Dillon Trench, Wairau Valley.	4-5 mm/yr	-
Lensen (1968) Branch River	3.8 mm/yr	-
Kneupfer (1988) Branch River	3-5 mm/yr	-
This Study, Lower Wairau Valley	4.2 ± 1.4 mm/yr	-
Campbell (1973) Tophouse Saddle to Lake Rotoiti	3-5 mm/yr	-
Yetton (2002) Crooked Mary Creek	-	7.7 ± 1 mm/yr
Yetton et al, (1998); Yetton (2000) Haupiri River	-	6.5 ± 2.5 mm/yr
Berryman et al, (1992) Near Taramakau River	-	10 ± 2 mm/yr

4.5.3 Single Event Offsets

Single event offsets vary markedly over the North and Wairau sections of the Alpine Fault. Near the Taramakau River significant vertical offset in combination with dextral offsets, 3 m and 6 m respectively. Single event displacements on the order of 1.3 m horizontal and 0.25 m vertical are reported by Yetton (2002) at Maruia and Grey Rivers. At the Matakitaki River no definite single event offsets recorded, although the last event is probably less than 3 m dextral displacement and is quite conceivably a combination of

more than one rupture event of smaller displacements (Yetton, 2002).

One single event displacement was recognised in this study in the Wairau Valley, of 4.4 ± 0.5 m. At Branch River single event displacements of 5-7 m and other locations along the fault trace described by Lensen (1968; 1976) indicates this offset in the Wairau Valley is smaller than the average single event offsets.

Assuming the Taramakau single event offset is related to a larger earthquake rupture emanating from the Southern and Central sections of the Alpine Fault, the single event displacement can be discounted as having a bearing on locating the segment boundary between the North and Wairau sections of the fault. Single event offsets are about 1.3 m horizontal and 0.25 m vertical for approximately 50 km of strike length on the North Alpine Fault and contrast the significantly with larger single event offsets encountered in the Wairau Valley of about 5 m horizontal and minimal vertical component. Considering the smallest single event offset encountered in the Wairau Valley is 4.4 ± 0.5 m, even assuming the most conservative offset of 3.9 m is still twofold larger than the single event encountered to the SW of Matakitaki River. Sieh (1978) reports offset related to a single rupture event on the San Andreas varying considerably along fault strike and will tend to decrease towards the end of the faulted segment. Therefore, it could be deduced that defining a fault segment boundary on the basis of single event displacements is arbitrary particularly if there is not an abundant array of comparable data along the potential segment length. In this case there are several lines of evidence indicating a rupture segment boundary somewhere between the Matakitaki River and the Wairau Valley.

4.5.4 Segment Boundary Limits

Based on rupture dates from the discussion above, we can be reasonably confident in the assumption that there is a segment boundary somewhere between the Matakitaki River trenches and the Tophouse trenches. Rupture brackets, AD 1455 – 1700 (Yetton, 2001) and AD 200 – 1840, for the Matakitaki and Tophouse trenches respectively overlap and could conceivably be the same event. However, combining dates from along strike of the

same segment further constrains the brackets and provides a distinct temporal gap between events at Matakitaki and Tophouse. To the SW the best estimate of rupture at Matakitaki is between AD 1600 – 1700 (Yetton, 2001), while further to the NE a rupture is determined between AD 200 and AD 1000 (this study and combined with data of Zachariasen et al, 2001). The upper date of the NE trench data bracket is conservative as it takes into account self age of the radiocarbon sample collected by Zachariasen et at (2001) who estimated the age to be ~1400 years ago (~AD 600).

4.5.5 Possible Segment Boundary

Assigning a segment boundary between the Matakitaki and Tophouse trenches involves determining characteristics of the fault capable of arresting a propagating rupture. Numerous fault segment characteristics are observable on either side of Matakitaki River and Tophouse but in between access and outcrop are limited.

The extensively faulted and dissected nature of Torlesse rocks to the south, and the intersection of several major NE-SW striking fault zones to the north of the Alpine Fault provide ample opportunity for earthquake rupture energy to dissipate, although assigning a location specific boundary is complicated (Figure 4.3, map pocket). Structures encountered between Matakitaki River and Tophouse are discussed below in an attempt to elucidate the location of the fault segment boundary.

The orientation of strike of the Alpine Fault from Matakitaki River to Tophouse is the most important structural feature capable of affecting location of the segment boundary. From Matakitaki River to Tophouse there is a general swing in strike from approximately 050° to approximately 065° with the hinge at Lake Rotoiti. As the dominant sense of displacement on the fault is dextral slip this swing in strike forms a releasing bend on the Alpine Fault. Releasing bends, or dilational fault jogs are known to arrest fault rupture (Sibson, 1985). An example from the Imperial Valley 1979 earthquake (Sibson, 1985) is of similar scale to the releasing bend found on the Alpine Fault between Matakitaki River and Tophouse.

Intersection of faults bleeding off slip from the Alpine Fault can cause fault segment boundaries (McCalpin, 1996). The active Waimea Fault intersects the Alpine Fault trace at Tophouse, is deflected SW along the fault and dies out before Lake Rotoiti. From offsets on the Waimea Fault, Johnston (1990) indicates slip rates are about a third of the Alpine Fault. Activity on the Waimea Fault decreases northward from the intersection with the Alpine Fault (Johnston, 1982a: 1982 b: 1983). This decrease in activity suggests slip on the Waimea Fault is fed from the Alpine Fault and dissipates progressively northward. Another major structural boundary, the Flaxmore and Kikiwa Faults and the Speargrass Fault Zone intersects the Alpine Fault at the base of Mt Robert Range, immediately SW of Lake Rotoiti. The preceding three faults have had minor recent traces indicative of late Holocene activity relative to the Alpine and Waimea Faults (Johnston, 1990). It is worth noting that the Speargrass Fault Zone does mark a major deep crustal feature in it association with the Median Tectonic Line. The nature of the topography is such at surface activation may not be clearly evident and this structure may be capable of playing a more important role in strain redistribution than its surface expression indicates.

The behaviour of the fault trace expression within the topography changes at Lake Rotoiti. In the Wairau Valley the fault trace is often submerged by Wairau River and valley bound by ranges of similar elevation. With progression SW, the fault trace passes through the Tophouse Saddle, continues along the valley to Lake Rotoiti before emerging and following the base of Mt Robert Range. The fault trace varies from a predominantly singular linear trace with a narrow zone of deformation to a series of thrust slivers extending beyond the line of strike-slip, with a broader zone of deformation respectively (Adamson, 1964).

Differential uplift on the Wairau section of the Alpine Fault is minor and fluctuates along the length of the fault from Cloudy Bay (Lensen, 1976). Near Cloudy Bay Grapes & Wellman (1986) describe the fault as upthrown to the north. Near Wairau Valley township the fault trace bifurcates and has a slight north side up component (Zachariasen et al, 2001). Lensen (1968) at Branch River reports the vertical displacement on the fault has reversed over the last 20 000 yrs with the most recent upthrow on the south side of

the fault, and at other locations the fault small upthrow varies. Lensen (1968) suggests small changes in strike change the relatively upthrown side of the fault where the principal shortening direction is close to a critical value. Progressively SW from the Three Weddings terrace (Figure 2.8) in the Wairau Valley to Lake Rotoiti (Adamson, 1964) upthrow is consistently to the SE indicating a change in behaviour on the fault. It is notable that the Wairau River has consistently slipped off the western side below the Tophouse Saddle at the point where it emerges from the ranges to the south and is deflected along the fault controlled Wairau Valley. It is this eastward migration which has created and preserved the terrace sequence described in this study. Consistent SE upthrow on the fault could represent the effects of uplift and crustal thickening of a deformation front evolving in response to the ramping and telescoping associated with the Alpine Fault restraining bends (Campbell & Rose, 1996; Campbell, 1991).

Mapping of the structure in Torlesse rocks south of the fault Adamson (1964); Johnston (1990), McLean (1987) and Rose (1987) have shown that a complex pattern of faults, but with a dominant NE-SW strike, dominate the structure and they show clear evidence of recent traces and extensive crush zones. Some of these follow older Cretaceous suture zones of melange and high strain fabrics where packets of Mesozoic rocks of various ages have been juxtaposed. One such example, the Sunset Saddle Fault (McLean, 1987) can be traced from the St Arnaud Range SW into Sunset Saddle across the Spencer Mountains, west of Lake Tennyson. Collectively these structures are capable of taking up significant internal strains in the blocks between the major transfer faults of the MFS.

In the same general context, it is worth noting that in the bends area in the vicinity of the Matakitaki site, the restraining bend structure has generated a complex system of thrust blocks developed from footwall splays on the Alpine fault, which also show evidence of Holocene activity. It is very possible that ruptures propagating into this area are either partitioned into these splays, or may be totally accommodated by one of them accounting for the small displacements noted.

4.6 FAULT RUPTURE SCENARIOS AND MAGNITUDE ESTIMATES

4.6.1 Coseismic Rupture of the North Alpine and Wairau Faults

There is potential for both the North Alpine and Wairau Faults to rupture in unison as part of a larger rupture event. The long elapsed time since the last event on the Wairau Fault could mean that it is reaching culmination of its seismic cycle and with present paleoseismic information we can only define a rupture segment boundary for the last event. Yetton (2002) postulated that ruptures on the North Alpine Fault are governed more by ruptures on the Central Alpine Fault than strain build up. It is probable that the Alpine Fault ruptures in a single rupture event (Yetton et al, 1998). However, historic evidence on the North Anatolian Fault in Turkey suggests earthquake rupture on large faults can rupture frequently on smaller segments appearing to behave as a single longer rupture event (Ambraseys, 1970). Two earthquakes within months of each other on the Alpine Fault similar to the North Anatolian Fault (Ambraseys, 1970) could not be discriminated by present paleoseismological techniques on the Alpine Fault. Yetton et al, (1998) and Wright (1998) suggest that for the case of the Alpine Fault, a rupture would propagate as a single event, as the Alpine Fault trace is more linear than the more complicated, highly segmented North Anatolian Fault.

If a large rupture event occurred similar to those indicated by present paleoseismic data on the Central Alpine Fault (eg Wright, 1998; Yetton et al, 1998) there is a possibility of coseismic rupture with the adjoining fault sections to the north. Magnitude estimates in excess of M = 8.0 are calculated for the AD 1620 ± 10 yr rupture event (Yetton et al, 1998) which is tentatively assigned the Matakitaki rupture bracket of AD 1600 to AD 1700 (Yetton, 2002). Whether the Central and North Alpine Fault rupture coseismically or independently is open to interpretation, Yetton (2002) while one event is possible, more probable is the strain transfer from a Central Alpine Fault segment setting off a North Alpine Fault rupture, either slightly pre-, or post-, a larger Central Alpine Fault rupture. Strain transfer could present itself in the form of clustering of earthquake ruptures, on the Central Alpine, North Alpine and Wairau Faults. Therefore as the

Wairau Fault is nearing the end of its seismic cycle a rupture on the Central and North Alpine Faults could initiate the rupture process over a short period of time.

4.6.2 Magnitude Estimates

Historical earthquake magnitudes are determined from seismological instruments (eg M_L, M_S & M_B) that reach a saturation point. Saturation levels are related to released seismic energy, whereby the seismological instruments are unable to record the highest frequencies generated by the earthquake rupture, therefore creating a false upper earthquake magnitude limit. In contrast to this direct measurement of energy release, prehistoric earthquake magnitude estimation relies on correlation of earthquake magnitude to physical fault parameters. As seismic moment is a direct measure of radiated energy accompanying earthquake rupture, rather than a response of a seismograph to an earthquake it is considered to be a more accurate measure of the size of an earthquake (Hanks & Wyss, 1972). Hanks & Kanamori (1979) developed a relation between seismic moment (M_O) and the physical parameters of fault a fault rupture by:

$$M_O = G\bar{u}A$$

Where G = rigidity modulus (assumed ca 3.0 x 10^{11} dyne/cm^2, Aki 1966), $\bar{u}$ = average displacement on the whole fault plane, A = area of the fault plane subject to displacement (fault length multiplied by down dip fault depth).

Without conversion to a comparable magnitude scale seismic moment values are meaningless with respect to local, surface and body wave magnitudes (M_L, M_S & M_B). Hanks & Kanamori (1979) convert seismic moment to a moment magnitude (M_W) via the relation:

$$M_W = 2/3 \log M_O - 10.7$$

Empirical relations from a compilation of historic worldwide earthquake data allow

estimation of earthquake magnitude from rupture parameters (Wells & Coppersmith, 1994). Regression equations of Wells & Coppersmith (1994) for surface rupture length and rupture area parameters on strike-slip faults are outlined below:

$$M_{SRL} = a + b * \log (SRL)$$

Where a and b are strike-slip coefficients 5.16 and 1.12 respectively, SRL is surface rupture length (km). The regression equation relating rupture area to strike-slip fault parameters is:

$$M_{RA} = a + b * \log (RA)$$

Where a and b are 3.98 and 1.02 respectively, and RA is rupture area (km^2).

Another regression analysis of fault magnitudes from historic earthquakes by Anderson et al (1996) incorporate slip rate data into magnitude estimates. This differs from previous estimation techniques, and according to Anderson et al (1996) provides a more accurate earthquake size prediction by including a slip rate component. The equation of Anderson et al (1996) is presented below:

$$M_W = A + B \log L + C \log S$$

Where A = 5.12, B = 1.16, L = length of fault rupture (km), and S = slip rate (mm/yr).

4.6.3 Fault Parameters

Magnitude estimations outlined in the previous section are related physical fault parameters and not a response energy radiated and recorded on a seismograph, therefore, assuming a characteristic earthquake model (eg Schwarz & Coppersmith, 1984) similar prehistoric earthquake magnitudes will probably occur in the future. Fundamental to magnitude estimation in strike-slip environments is rupture length, as it the most variable. Other parameters are depth to the base of the seismogenic zone, fault dip, and

average displacement per event. Physical fault parameters for the Wairau Section of the Alpine Fault are outlined below or assumed from regional examples.

As part of a nation wide seismicity study Anderson & Webb (1994) indicate a depth of about 15 km or less to the base of the seismogenic zone below the Wairau section of the Alpine Fault. Microseismicity studies in the northern South Island of Arabasz & Robinson (1976) encountered most crustal earthquakes above 15 km depth, seismicity deeper than about 20 km appears to be intimately related to the underlying subduction zone. The recent MFS Tennyson earthquake is one of the closest earthquakes to the Wairau Fault in recent times, Anderson et al, (1993) analyse the depth of the Tennyson earthquake as part of a regional study and define the focus to a depth of 8 km (± 3 km) with a similar strike to the Wairau Fault of 055° ± 10. To reconcile strain rates observed across the MFS Bibby (1976) stipulated that earthquakes must be deeper than 10 km deep (ie locking depth) to allow smooth distribution of strain across MFS.

This indirect and regional information suggests the depth to the seismogenic zone of the Wairau section of the Alpine Fault is ca 15 km deep, which matches the depth used by Stirling et al (1999) for magnitude estimates as part of a national probabilistic seismic hazard model. The above discussion assumes a vertical fault plane, surface fault plane measurements indicate a steep (~70°) dip to the SE, this increases down dip fault plane distance to the seismogenic zone to ca 16 km (from 15km/sin (fault dip)).

Average slip per event estimate for the Wairau Fault at Branch River is 5.2 – 6.7 m of Lensen (1968), however, incorporating the single event displacement from the Wairau Valley of 4.4 ± 0.5 m indicate some along strike variation. To account for this a conservative range of 4-7 m average displacement per event is used for magnitude estimates. Slip rate determination from various studies on the Wairau Valley compares well, therefore the slip rate of from this study 4.2 ± 1.4 mm/yr is adopted for magnitude estimation.

A number of rupture lengths are proposed below to account for the limitations of accurately defining a SW fault rupture segment boundary of the Wairau Section of the

Alpine Fault (assume the Wairau Section is part of a whole earthquake rupture segment unless stated otherwise):

(I) Matakitaki River to Cloudy Bay, Blenheim. Probably an over-estimate of the onshore fault rupture length as it is the maximum extent of the rupture segment boundary defined by the Matakitaki trench dates.

(II) Tophouse to Cloudy Bay, Blenheim. Probably an underestimate of onshore fault rupture length as the Tophouse trenches define the minimum end of the rupture segment boundary towards the Matakitaki River trenches.

(III) Lake Rotoiti to Cloudy Bay, Blenheim. Best estimate of actual onshore fault rupture length.

(IV) Half the length of (iii) on the conservative assumption that there is a segment boundary between Lake Rotoiti and Cloudy Bay. Division of the rupture length in two is arbitrary.

(V) From Ahaura River to Cloudy Bay, Blenheim. Maximum earthquake magnitude scenario for rupture propagation over the length of the North and Wairau sections of the Alpine Fault (Ahaura River is assumed SW termination of North Alpine rupture events of about 1.3 m displacement).

There is no indication that any component of the slip rate on the Wairau Fault is aseismic, as no deformation is apparent where sealed roads have crossed the fault. Also liquefaction sediments are recognised in Tophouse Trench Two (Figure 3.5) indicating movement on the fault is associated with earthquake rupture. In addition, a GPS survey of the Marlborough Fault Zone indicates 90-95 % of the relative plate motions between the Australian and Pacific plates are accounted for by crustal velocities, indicating the relative plate motion is accommodated via episodic earthquake processes (Bourne et al 1998).

4.6.4 Rupture Magnitudes

Moment magnitudes are calculated using the parameters outlined in Section 4.6.2. $M_W^{(2)}$, M^A, M^B and $M_W^{(3)}$ are presented in Table 4.3 where the variation of the differing calculation techniques is averaged to provide a useful magnitude estimation.

Magnitude estimates range between M = 7.1 and M = 7.6. This range is the minimum and maximum on land ruptures on the Wairau section of the Alpine Fault, with the maximum M= 7.6 assuming coseismic rupture with the North Alpine Fault.

Previous magnitude estimates on the Wairau Section of the Alpine Fault by Yetton (2002) of M = 7.5-7.6 are consistent with the above magnitude estimates (Table 4.3). Yetton (2002) calculated magnitudes for the on land section of the Alpine Fault similar to this study, in contrast to Stirling et al, (1998) who estimated a much greater magnitude of M= 7.8 – 7.9 including extension of the Wairau Fault into Cook Strait.

Table 4.3: Summary of estimated earthquake magnitude potential for various fault rupture parameters on the Wairau Fault.

EARTHQUAKE SOURCE (see below for locations)	LENGTH (L) (km)	RUPTURE AREA (A) (km^2)	SINGLE EVENT DISPLACEMENT (m)	SEISMIC MOMENT (Mo) [1] (x 10^{26} dyne/cm^2)	MOMENT MAGNITUDE				MAGNITUDE AVERAGE
					$M_{w\,(2)}$	M^{SRL}	M^{RA}	$M_{w\,(3)}$	
I	140	2100	4-7	2.52 4.41	7.65	7.55	7.35	7.5	**7.5**
II	100	1500	4-7	1.8 3.15	7.55	7.4	7.2	7.3	**7.4**
III	110	1650	4-7	1.98 3.47	7.6	7.45	7.25	7.4	**7.4**
IV	60	900	4-7	1.08 1.89	7.4	7.2	7.0	7.1	**7.2**
V	175	2625	4-7	3.15 5.51	7.7	7.7	7.45	7.6	**7.6**

[1] multiplied by 1 x 10^{12} (converting kilometre and metre for dyne/cm^2)

[2] Moment Magnitude - Hanks & Kanamori (1979) (M_w = 2/3 log Mo – 10.7)

[3] Moment Magnitude - Anderson et al (1996) (M_w = 5.12 + 1.16 log L – 0.20 log S)

(where L (Length) is km & S (Slip rate) is mm/yr)

(I – V) rupture length determined in previous section

4.7 DISCUSSION

Paleoseismic data gathered from the Wairau Fault (this study and Zachariasen et al, 2001) and at the Matakitaki River (Yetton, 2002) defines an earthquake rupture boundary between Tophouse and the Matakitaki River. In the absence of further paleoseismic information, assuming that this rupture boundary arrests rupture propagation at every rupture is imprudent. The identification of the rupture brackets for the last ground ruptures does imply the rupture boundary was operational for the last known surface ruptures on the Wairau and North Alpine Faults.

The precise location of the rupture segment boundary lies somewhere between Matakitaki River and Tophouse, however, defining a boundary to a location, or to a single structural feature, is problematic. Seismic energy could dissipate on any number of structures on either side of the Alpine Fault between Matakitaki River and Tophouse. For instance, dissipation of seismic energy on the Sunset Saddle Fault (McLean, 1987) and associated crush zones south of the Alpine Fault, or alternatively, on the Waimea Fault (Adamson, 1964; Johnston, 1990) to the north could arrest rupture propagation. A swing in strike of the Alpine Fault from Matakitaki to Tophouse from about 050° to about 065° forms a releasing bend often associated with rupture arrest (Sibson, 1985) could also arrest rupture propagation. The paucity of paleoseismic data between Matakitaki River and Tophouse prevents assigning a segment boundary on the basis of fault behavioural features, such as slip rate and fault complexity (McCalpin, 1996).

Assigning a rupture segment boundary on the basis of the information above is arbitrary, but, a number of coincidental features suggest the location is SW of Lake Rotoiti at the base of the Mt Robert Range. These features include, the swing in Alpine Fault strike creating a releasing bend, the intersection of the Flaxmore, Kikiwa and the Speargrass Faults, southwest of the intersection of the Waimea Fault at Tophouse where it is dragged into the Alpine Fault Zone. The change in the character of the fault with progressive upthrow to the SE beyond Tophouse towards Matakitaki River and change in fault location from predominantly valley bound and linear to range front forming thrust

slivers, may reflect a change in fault geometry at depth and also the topographic contrast with the point at which the fault truncates the major structural depression of the Moutere Basin. Evidence that the rupture segment boundary is west of Lake Rotoiti is the offsets on the Peninsula and moraines around the lake are comparable to and an integral part of the late Pleistocene slip-rate curve.

4.7.1 Recurrence Intervals

A first order recurrence interval can be calculated with the information from this study. Previous recurrence intervals encountered on the Wairau Fault are between 1000-2300 years (Berryman et al, 1992) and about 1100-1900 years (Zachariasen et al, 2001). Division of the single event offset minimum and maximum values provides a first order recurrence interval of between 650 and 1750 years (from 4.4 ± 0.5 m and slip rate of 4.2 ± 1.4 mm/yr) for the data collected in the study area. Weathering rind dates place some constraints on recurrence interval, ruptures are indicated at about 1450 ± 150 yr BP, 5050 ±800 yr BP and 6750 ± 1000 yr BP, suggesting a recurrence interval from the first order estimate is a touch small, A period of 1800 years may have passed since the last ground rupture on the Wairau Fault, which correlates to about 7.5 m of strain accumulation, much larger than this study's single event displacement suggesting earthquake rupture is imminent.

4.8 SUMMARY

Trenching data from Zachariasen et al (2001) and this study defines a rupture on the Wairau Fault between AD 200 and AD 1000. The upper bound is a conservative estimate accounting for self-age of radiocarbon dating of charcoal, therefore the last rupture event on the Wairau Fault is probably closer to AD 200. A clear temporal disparity exists between the last rupture bracket for the Wairau Fault, AD 200 to AD 1000, and for the rupture bracket of the North Alpine Fault, of AD 1600 to AD 1700 (Yetton, 2002). This indicates a rupture segment boundary exists between the Matakitaki River and Tophouse trench sites.

A rupture segment boundary on the North Alpine and Wairau Faults is located between Matakitaki River and southwest of Tophouse and was in operation for at least the last fault rupture. Evidence from trenching, slip-rates, single event displacements and fault characteristics constrain the rupture segment boundary limits. Defining the exact location of the rupture segment boundary is elusive, as no obvious single structural feature affects the fault, although numerous structural features could dissipate seismic energy. Circumstantial evidence suggests a rupture segment boundary at the base of Mt Robert Range, SW of Lake Rotoiti, but it is not likely to take the form of an abrupt termination

Displacements on the Wairau Fault probably occur as single rupture events, although present paleoseismic information does not categorically confirm this assumption. The existence of a rupture segment boundary cannot be discounted between Tophouse Saddle and Cloudy Bay, particularly if the slip-rates of Wellman and Grapes are valid. The suggestion of no rupture segment boundary is based on the concept of strike-slip fault evolution (Wesnousky, 1988), a long slip history, a linear trace, and cumulative displacement of offset markers pertaining to a smoothing of the fault plane and not physical trenching evidence. Further paleoseismic investigation, and comparison to data from this study and Zachariasen et al, (2001) is needed to enhance understanding of rupture history on the Wairau Fault, and whether or not the estimates of higher slip rates at the coast are substantiated.

Magnitude estimates on the Wairau Fault for a rupture segment between Cloudy Bay and Lake Rotoiti range from M = 7.3-7.7, with the average magnitude estimate M= 7.4. Magnitude estimates for the minimum and maximum rupture lengths of the defined rupture segment boundary are M= 7.4 and M = 7.5 respectively. Magnitude estimates using rupture area (M^{RA})are consistently smaller than other methods, therefore, excluding M^{RA} estimates increases magnitude estimates for a Wairau Fault rupture event to about M = 7.5, consistent with rupture estimates of Yetton (2002). For the unlikely event that a rupture segment boundary exists along the Wairau Fault a slightly smaller magnitude of M = 7.1 is expected. Coseismic rupture of the North Alpine and Wairau

Fault would result in a larger magnitude of M = 7.6. In conclusion, a magnitude estimate from a variety of estimation techniques for a rupture event on the Wairau Fault is M = 7.4 ± 0.25.

CONCLUSIONS

5.1 INTRODUCTION

No known historic earthquake rupture has occurred on any section of the Wairau Fault, the northerly extension of the Alpine Fault. Field evidence suggests the Alpine Fault ruptures in large episodic earthquakes capable of widespread destruction. Until recently no paleoseismic information was available for the Wairau Fault. Zachariasen et al, (2001) completed paleoseismic investigations near the Wairau Valley settlement and in conjunction with this study a better understanding of the rupture history of the Wairau Fault is emerging. Some slip rate data existed on the Wairau Fault before this investigation began, most notably the comprehensive study at Branch River (Lensen, 1968). Other offset landforms are recognised, but placing an age constraint is difficult. Tentative correlation of glacial surfaces elsewhere does provides some, albeit general, age controls.

Progressive southward migration of the Hikurangi margin has reduced the slip rate of the Wairau Fault, effectively reducing slip accommodation on the Wairau Fault (Adamson, 1964; Berryman et al, 1992). Previously the Wairau Fault accommodated the majority of interplate slip, demonstrated by the cumulative offset of the Brook Street and other terranes. A change in plate motion vector is expressed by migration of the Hikurangi margin southward, contemporaneous with oblique continental collision initiating the formation of the Southern Alps. Even if the Wairau Fault is considered a relict of its

former self, it is still in excess of 100 km long, with a slip rate of 3-5 mm/yr and is capable of generating a large magnitude earthquake. The objective of this study was to constrain the timing of the last earthquake rupture event on the Wairau Fault, with the intention of better forecasting future seismic hazard on the fault. Also incorporated in the investigation is the interaction between the Wairau Fault and sections of the Alpine Fault further south.

5.2 FAULT CHARACTERISTICS

A slip rate of 4.2 ± 1.4 mm/yr is calculated from a series of offset fluvial terraces in the Wairau Valley. The large error associated with the slip rate reflects the lack of precise age constraint of the offset terraces and accurate location of the offset features as erosion and cultivation have modified the features close to the fault trace. The slip rate of 4.2 ± 1.4 mm/yr agrees well with the general consensus for the slip rate on the Wairau Fault of between 3-5 mm/yr (Lensen, 1968).

Unfortunately only one single event displacement was recognised in the study area of 4.4 ± 0.5 m on the youngest offset terrace in the Wairau Valley. This event is less than those recorded at Branch River by Lensen (1968) where single event displacements were in the 5-7 m range. Considering single event displacements can vary over the length of a fault the encountered single event offset 4.4 ± 0.5 m is considered realistic with respect to the Branch River offsets. Although no other single event displacement can be separated out, this value can be compared with the 19 ± 2 m offset of the terrace riser at the Matagouri Terrace site which is thought to be the product, of three events as indicated by clast rejuvenation modes in the weathering rind record at the site.

The fault trace in the study area is a linear feature offsetting landforms dextrally with minor SE uplift most recognisable where the fault crosses older glacial sediments

forming large fault scarps, linear valleys and entrenched streams. A general strike of about 065° is defined by a linear scarp, deflected slightly by topography through the Tophouse Saddle, indicating a dip to the SE. This dip is in accordance with the dip of the fault plane observed in two stream beds incised through the scarp in the study area (Chapter 3). Local tilted wedges are recognised between Lake Rotoiti and the Wairau River, but are more abundant in the less evolved juvenile fault trace crossing the degradation terraces in the Wairau Valley. In the Wairau Valley a linear fault trace links a series of pop up and pull apart structures. Coupling between a pop up followed by a pull apart structure NE along the fault trace in the Wairau Valley appears to reflect a conveyor style migration of coupled collapse and inversion also seen at the Matagouri and Pylon Terrace sites.

In the Wairau Valley, the Matagouri and Pylon Terrace sites indicate intricate interaction between the fault and the river channels of the Wairau River in the past. At both locations there is evidence that channels of the Wairau River, flowing from the south, have been deflected by the fault during an episode of downcutting or lateral planation. A detailed differential GPS survey of the Matagouri Terrace revealed evidence for surface bulging on the SE side of the fault. This bulging is also apparent at the Three Weddings terrace offset. It is suggested that surface bulging on the SE side of the fault is a precursor to fault rupture, which prevents the river channel crossing the fault trace. Subsequent rupture releases strain, which in turn decreases surface bulging lowering the energy required for the river to cross the fault. Alternatively the general lowering of base level generates sufficient stream power for the next meander to sweep across the fault, favoured by evidence that the fault zone retains positive elevation marked by relict uptilting of adjacent surfaces. The length of the younger fault crossing terraces on the south side of the fault is consistently shorter than to the north. At both sites the younger terraces cut the fault trace along strike and downslope of the pop up structure in the transition zone between pop up and pull apart. Elevation of the pop up structure still provides enough resistance to river flow to remain, whereas the pull apart structures are depressions so the river is able to cross.

5.3 Comparison of Tophouse Paleoseismic Data with Alpine Fault Sections North and South

Radiocarbon dating of carbonaceous material in the Tophouse trenches provides evidence of a surface rupture event after AD 200. The historic/prehistoric boundary constrains the rupture bracket slightly to AD 200 – AD 1840. A maximum period of 1800 yrs since last rupture indicates the Wairau Fault could be reaching culmination of its seismic cycle. A radiocarbon dated branch caught in the shear zone suggests a rupture event about 12 500 years ago, although this is not conclusive. Subsequent ruptures over the intervening period are inferred by the highly disturbed shear zone and dated offset peat horizons in the Tophouse trenches, but cannot be bracketed to define individual events.

Data from Zachariasen et al, (2001) in conjunction with Tophouse data further constrains the last rupture bracket on the Wairau Fault assuming contemporaneous rupture at both sites. A combined last rupture bracket for the Wairau Fault is AD 200 – AD 1000, the radiocarbon self age associated with the upper bracket suggests rupture closer to AD 200. By comparison with the North Alpine Fault to the SW, the last Wairau Fault rupture bracket is temporally disparate. Best estimates for the North Alpine and Wairau Faults are AD 1600 – AD 1700 and AD 200- AD 1000 respectively. So for the last rupture event, at least, a rupture segment boundary was in operation between the Matakitaki River and Tophouse trenches. The precise location of the rupture segment boundary is unclear. However, a number of structural features on the Alpine Fault and intersection of structural features north and south of the fault tentatively suggest a rupture segment boundary at some point from immediately SW of Lake Rotoiti at the base of the Mt Robert Range.

At present, paleoseismic data prevents assigning an earthquake rupture boundary for more than the last rupture. This poses an interesting question regarding the nature of the interaction between the Wairau Fault and Alpine Fault sections further south. This study demonstrates that at least part of the Wairau Fault behaves independently from the southerly extensions of the Alpine Fault. The elapsed time in the current seismic cycle on the Wairau Fault is long enough for significant strain accumulation. Although the recurrence interval on the Alpine Fault sections further south, is an order of magnitude shorter, the elapsed time there suggests that they are approaching the end of the current seismic cycle. The possibility exists that each rupture segment could rupture independently, or induce stress transfer from one segment to another. Fault rupturing, either independently in spaced succession or temporally could induce either earthquake clustering, or rupturing synchronously across segment boundaries.

5.4 MAGNITUDE ESTIMATES

Relative to the approximation in estimates of fault magnitude, the effect of varying the choice of segment boundary to within a few kilometres has a barely noticeable effect on the calculation. Assigning a rupture segment boundary minimum estimate, at Tophouse, as opposed the preferred location immediately SW of Lake Rotoiti alters the rupture magnitudes minimally. An earthquake rupture segment boundary was definitely operational for the last rupture at some location between the Tophouse and Matakitaki River trench sites.

Fault parameters assigned to calculate magnitude estimates produced an average value of $M = 7.4 \pm 0.25$ for the onland section of the Wairau Fault. Estimated magnitude of a possible, although unlikely, smaller earthquake rupture segment in the Wairau Valley is

M = 7.2. Assigning a rupture length to this estimation is arbitrary as no segment boundary can be demonstrated with present paleoseismological information, however it still remains a possibility. A larger magnitude estimate of M = 7.5 for an earthquake rupturing between Cloudy Bay and the Matakitaki River accounts for the largest average magnitude estimate of this study on the Wairau Fault, but does not take into account any offshore extension. A slightly larger magnitude estimate of M = 7.6 results for rupture propagation of the Wairau Fault coseismically with the Alpine Fault. As the North Alpine Fault provides evidence of smaller single event displacements, rupture on the Wairau Fault could feasibly set off a rupture on the North Alpine Fault. If this does occur the strain transfer from the Wairau Fault to North Alpine Fault could initiate rupture on the North Alpine Fault over a relatively short period of time.

5.5 FUTURE STUDIES

Fundamental to any future seismic hazard assessment on the Alpine Fault is the accurate identification of fault segments, especially the Wairau Fault, as the present paleoseismic record is still relatively sparse. Field evidence suggests the Wairau Fault is capable of severe earthquakes, either independently, or in conjunction with sections of the Alpine Fault further south. The primary concern of any future paleoseismological investigation must be to tightly constrain the age of the last rupture. Secondly, it is necessary to elucidate the existence of rupture segment boundaries along the Wairau Alpine Fault. Ruptures are not necessarily constrained by fault segment boundaries, although they can dissipate energy at a segment boundary (eg Cowan, 1990). A crucial element in seismic hazard analysis is the identification of rupture propagation and arresting zones as they usually define the length of a rupture, which is critical when assessing seismic magnitude.

To further constrain the present age bracket of the last rupture, further trenching is

suggested, primarily between Tophouse and Cloudy Bay, as identifying segment boundaries is crucial. Although, any site capable of tightly constraining the last rupture would be valuable. Southwest of Tophouse, possible trenching sites include the swampy area immediately NE of Kerr Bay, Lake Rotoiti, behind the Department of Conservation camping ground (GR 964334). Excavations on the Brunner Peninsula are a possibility but would have to be hand dug.

Alternative paleoseismic techniques are a possibility. Dendrochronolgy dates for the Alpine Fault further south were very successful. As most of the forest in the study area is mixed beech with a lifespan of approximately 300 years dendrochronological studies are not appropriate. One paleoseismic technique worth mentioning is the use of diatom stratigraphy recording earthquake ruptures. Hill et al, (2001) used this method to good effect in Lake Jasper, Awatere Fault. A potential site along the Wairau Fault is the sag pond in the Wairau Valley (GR 091392). Abundant rockfalls and landslides occur along the Mt Robert Range, and the projected ages place critical events outside the lichenometry dating range. Weathering rind dating, supported by strategic duplication using cosmogenic exposure age dating may provide a chronology of shaking events, some of which may possibly be linked unequivocally to the Wairau Fault.

5.6 Concluding Comments

The Wairau Fault is clearly less active than either the Alpine Fault or more southern members of the MFS.

It is still clearly capable of generating a damaging earthquake of an estimated M 7.4 ± 0.25 that would cause very severe damage to St Arnaud, the new developments on the scarp at Tophouse and all the settlements along the Wairau Valley. Of the large centres, Blenheim is close enough to the Wairau Fault to be severely affected as are State

Highway 1, the railway, and the infrastructure associated with local intensive rural horticultural industries. Propagation across Cook Strait and effects on the Kapiti Coast remain problematic. Propagation into the Matakitaki and Northern Alpine Fault would also affect major access routes to the northern South Island via the Lewis Pass.

Without better constraints on recurrence intervals, calculating the probability of the timing of the next event is not feasible, but it should be noted that the length of elapsed time since the last event suggests that further investigation is warranted.

Secondary to the objective of exploring the seismicity of the Wairau Fault, some other aspects of the study are worth noting.

Observations on the interaction of the river and fault zone suggest that further exploration of process and response, particularly with respect to the timing of ground deformation within the fault zone, relative to rupture events and river behaviour, may yield some useful insights into the faulting process.

The excellent preservation of topographic detail in settings such as the Wairau terraces provide sites for the study of the evolution of small scale structures which have developed at the restraining and releasing bends as analogues of processes operating on a larger scale. This is of specific interest with respect to indications of an apparent conveyor process opening and closing basin structures.

Finally, it is clear that paleoseismic studies should not be restricted to a concentration of attention on the fault trace only, and treating the problem in terms of rigid blocks and discrete segments in which all strain is assumed to be accommodated on the primary fault alone. It is important to recognise that a range of deformation processes can be operating synchronously within the adjacent blocks, capable of transferring displacement off, or onto the fault, without necessarily defining abrupt segmentation.

REFERENCES

Adams, J. (1980) Paleoseismicity of the Alpine Fault seismic gap. *Geology* 8:72-76.

Adamson, J.K. (1964) The Alpine-Wairau and Waimea Fault system in the Lake Rotoiti area. Unpublished MSc thesis, University of Canterbury, Christchurch, New Zealand.

Aki, K. (1996) Generation and propogation of G waves from the Niigata earthquake of June 16, 1964; Part 2, Estimation of earthquake moment, released energy, and stress-strain drop from the G wave spectrum. Bulletin of Earthquake Research Institute; 44, 73-88.

Ambraseys, N. (1970) Some characteristic features of the Anatolian fault zone. *Tectonophysics* 9,1 143-165.

Anderson, H.J & Webb, T. (1994) New Zealand seismicity: patterns revealed by the upgraded National Seismograph Network. *New Zealand Journal of Geology and Geophysics* 37, 477-493.

Anderson, H.J., Webb, T. & Jackson, J., (1993) Focal mechanisms of large earthquakes in the South Island of New Zealand: implications for the accommodation of Pacific-Australia plate motion. *Geophysical Journal International* 115, 1032-1054.

Anderson, J.G., Wesnousky, S.G. & Stirling, M.W. (1996) Earthquake size as a function of fault slip rate. *Bulletin of the Seismological Society of America,* 86: 683-690.

Arabasz, W.J. & Robinson, R. (1998) Microseismicity and Geological Structure in Northern South Island, New Zealand. *New Zealand Journal of Geology and Geophysics* 19, 569-601.

Bakun, W.H. & McEvilly, T.V. (1984) Recurrence Models and Parkfield, California, Earthquakes. *Journal of Geophysical Research* 89: 3051-3058.

Berryman, K., Beanland, S., Cooper, A.F., Cutten, H.N., Norris, R.J. & Wood, P.R. (1992) The Alpine Fault, NewZealand: variation in Quarternary structural style and geomorphic expression. *Annales Tectonicæ* VI: 126-163.

Berryman, K., Cooper, A.F., Norris, R.J., Sutherland, R., & Villamor, P. (1998) Paleoseismic Investigation of the Alpine Fault at Haast and Okuru. *Geological*

Society of New Zealand and New Zealand Geophysical Society, Joint Annual Conference, Christchurch, New Zealand: 44.

Bourne, S.J., Arnadottir, T., Beavan, J., Darby, D.J., England, P.C., Parsons, B., Walcott, R.I. & Wood, P.R. (1998) Crustal deformation of the Marlborough fault zone in the South Island of New Zealand; geodetic constraints over the interval 1982-1994. *Journal of Geophysical Research, B, Solid Earth and Planets* 103 (12): 30 147-30 165.

Bull, W.B. (1996) Prehistorical earthquakes on the Alpine fault, New Zealand. *Journal of Geophysical Research* 101:6037-6050.

Campbell, J.K. (1973) Displacement data form the Alpine Fault at Lake Rotoiti and its relevance to glacial chronology and the tempo of tectonism. Ninth congress of the International Union for Quaternary Research; abstracts. 9, 57-58.

Campbell, J.K. (1991) Styles of deformation associated with the Marlborough Fault System. In: Structural transition from Alpine Fault Hikurangi Margin in space and time (Programme & Abstracts). *Geological Society of New Zealand miscellaneous publication 56.*

Campbell, J.K. (1992) The Wairau and Alpine Fault: structure and tectonics of the s-bend junction. In: Geological Society of New Zealand and New Zealand Geopyhsical Society 1992 joint annual conference; field trip guides. Ed. Campbell, J.K. Geological Society of New Zealand. Christchurch, New Zealand.

Campbell J.K. & Rose, R. (1996) Oblique tectonics and the restraining bend on the Alpine Fault. *Geological Society of New Zealand Miscellaneous Publication 91A.* Geological Society of New Zealand 1996 Annual Conference, Dunedin.

Carter, L., Lewis, K.B. & Davey, F. (1988) Faults in Cook Strait and their bearing on the structure of central New Zealand. *New Zealand Journal of Geology and Geophysics*, 31 431-446.

Carter, R.M. & Norris,R.J. (1976) Cainozoic history of southern New Zealand: an accord between geological observations and plate tectonic predictions. *Earth Planet Science Letters*, 31: 85-94.

Cole, J.W. (1990) Structural control and origin of volcanism in the Taupo Volcanic Zone, New Zealand. Bulletin of Volcanology 52: 445-459.

Cooper, A.F. & Norris, R.J. (1990) Estimates for the timing of the last coseismic displacement on the Alpine Fault, northern Fiordland, New Zealand. *New Zealand Journal of Geology and Geophysics*, 33: 303-307.

Cooper, A.F., Barreiro, B.A., Kimbrough, D.L. & Mattinson, J.M. (1987) Lamprophyre dyke intrusion and the age of the Alpine fault, New Zealand. *Geology.* 15: 941-944.

Cowan, H.A. (1990) Late Quaternary displacements on the Hope Fault at Glynn Wye, North Canterbury. *New Zealand Journal of Geology and Geophysics*, 33: 285-293.

Cowan, H.A. (1991) The North Canterbury earthquake of September 1, 1888. *Journal of the Royal Society of New Zealand*, 21/1: 1-12.

Cowan, H.A. (1992) Structure, seismicity and tectonics of the Porters Pass-Amberley Fault Zone, North Canterbury, New Zealand. Unpublished Ph.D thesis, University of Canterbury, Christchurch.

Cowan, H.A.& McGlone, M.S. (1991) Late Holocene displacements and characteristic earthquakes on the Hope River segment of the Hope Fault, New Zealand. *Journal of the Royal Society of New Zealand*, 21/4: 373-384.

Davey, F.J., Henyey, T., Kleffman, S., Melhuish, A., Okaya, D., Stern, T.A., Woodward, D.J. (1995) Crustal Reflections from the Alpine Fault zone, South Island, New Zealand. *New Zealand Journal of Geology and Geophysics* 38, 601-604.

DeMets, C., Gordon, R.G., Argus, D.F. & Stein, S. (1994) Effect of recent revisions to the geomagnetic time scale on estimates of current plate motions. *Geophysical Research Letters,* 21: 2191-2194.

DuFrense, J. (1989) Tramping in New Zealand. Lonely Planet Publications, Victoria, Australia (2nd ed).

Grapes, R. H. & Wellman, H.W. (1986) The north-east end of the Wairau Fault, Malborough, New Zealand. *Journal of Royal Society of New Zealand* 16, 245-250.

Grapes, R., Little, T., Downes, G.L. (1998) Rupturing of the Awatere Fault during the 1848 October 16 Marlborough earthquake, New Zealand: historical and present day evidence. *New Zealand Journal of Geology and Geophysics* 41 (4): 387-399.

Hanks, T.C. & Kanamori, H. (1979) A moment magnitude scale. *Journal of Geophysical Research* 84, 2348-2350.

Hanks, T.C. & Wyss, M. (1972) The use of body-wave spectra in the determination of seismic-source parameters. *Bulletin of the Seismological Society of America* 62, 561-589.

http://www.nzine.co.nz/life/rotoiti.html ; Lake Rotoiti in Nelson Lakes National Park. Website.

Johnston, M.R. (1982a) Part Sheet N27 – Richmond. Geological map of New Zealand 1:50 000. Map (1 sheet) and notes (32 p.). Wellington, New Zealand, Department of Scientific and Industrial Research.

Johnston, M.R. (1982b) Part Sheet N28 BD – Red Hills. Geological map of New Zealand 1:50 000. Map (1 sheet) and notes (48 p.). Wellington, New Zealand, Department of Scientific and Industrial Research.

Johnston, M.R. (1983) Part Sheet N28 AC – Motupiko. Geological map of New Zealand 1:50 000. Map (1 sheet) and notes (40 p.). Wellington, New Zealand, Department of Scientific and Industrial Research.

Johnston, M.R. (1990) Sheet N29-St Arnaud. Geological Map of New Zealand 1:50 000. Map (1 sheet). Wellington, New Zealand. Department of Scientific and Industrial Research.

Kieckhefer, R.M. (1979) Sheets M31D, N31A, N31C and parts of M32A and M32B Leader Dale(1st edition) and Sheets O32C and O32A Lake McRae (1st edition) "Late Quaternary Tectonic Map of New Zealand. 1: 50 000 3 Maps & Text (28p). Department of Scientific and Industrial Research.

Keller, E.R. (1986) Investigation of active tectonics; use of surficial earth processes. In Active Tectonics: Studies in Geophysics (R.E. Wallace, chairman), pp. 136-147. National Academy Press, Washington, DC.

Knuepfer, P.L.K. (1988) Estimating ages of late Quaternary stream terraces from analysis of weathering rinds and soils. *Geological Society of America Bulletin* 100, 1224-1236.

Knuepfer, P.L.K. (1992) Temporal variations in latest Quaternary slip across the Australian-Pacific plate boundary, northeastern South Island, New Zealand. *Tectonics* 11/3, 449-464.

Koons, P.O. (1990) Two-sided orogen: Collision and erosion from the sandbox to the Southern Alps, New Zealand. *Geology*, v 18, 679-682.

Langridge, R.M., Campbell, J., Hill, N., Pere, V., Estrada, B., Pettinga, J. & Berryman, K. (in press) Preliminary Paleoseismic results for the Conway Segment of the Hope Fault at Greenburn Stream, South Island, New Zealand *Journal Annali di Geofisica.*

Larson, K.M., Freymueller, J. & Phillipsen, S. (1997) Global plate velocities from the Global Position System. *Journal of Geophysical Research*, 102: 9961-9981.

Lensen, G.J. (1968) Analysis of progressive fault displacement during downcutting at Branch River terraces, South Island, New Zealand. *Geological Society of America Bulletin* 79, 545-556.

Lensen, G.J. (1976) Sheets N28D, O28C & N29B. Hillersen (1st Edition): sheets O28D, P28A & P28C. Renwick (1st Edition). "Late Quaternary Tectonic Map of New Zealand 1:50 000," 2 maps and text (20p). Department of Scientific and Industrial Research, Wellington, New Zealand.

Little, T.A., Grapes, R. & Berger, G.W. (1998) Late Quaternary strike slip on the eastern part of the Awatere fault, South Island, New Zealand. *Geological Society of America Bulletin* 110, 127-148.

Little, T.A. & Jones, A. (1998) Seven million years of strike-slip and related off-fault deformation, northeastern Malbourough fault system, South Island, New Zealand. *Tectonics* 17, No. 2, 285-302.

McCalpin, J.P. Paleoseismology (ed J.P. McCalpin) Academic Press, Inc. A Division of Harcourt Brace & Company. San Diego, California.

McLean, G.W. (1986) Structure and metamorphism near the Alpine and Awatere Faults, Lewis Pass. Unpublished M.Sc. Thesis. University of Canterbury, Christchurch, New Zealand.

McMorran, T.J. (1992) The Hope Fault at Hossack Station east of Hamner Basin, North Canterbury. Unpublished MSc thesis, University of Canterbury, Christchurch, New Zealand.

McSaveney, M.J. (1992) A manual for weathering-rind dating of grey sanstones of the Torlesse Supergroup, New Zealand. Institute of Geological and Nuclear Sciences Report 92/4. 52 p. Institute of Geological and Nuclear Sciences Limited.

Norris, R.J. & Cooper, A.F. (1995) Origin of small - scale segmentation and transpressional thrusting along the Alpine Fault, New Zealand. *Geological Society of America Bulletin* 107, 231-240.

Norris, R.J. & Cooper, A.F. (1997) Erosional control on the structural evolution of a transpressional thrust complex on the Alpine fault, New Zealand. *Journal of Structural Geology* 19, 1323-1342.

Norris, R.J. & Cooper, A.F. (2000) Late Quaternary slip rates and slip partitioning on the Alpine Fault, New Zealand. *Journal of Structural Geology* 12, 715-725.

Norris, R.J., Cooper, A.F., Wright, C., Wrigth, T., Berryman, K., Sutherland, R. & Villamor, P. (2001) Late Quaternary slip rates and prehistoric earthquakes on the Alpine Fault. In Litchfield, N.J. (Comp.) 2001. Ten years of paleoseismology in the ILP: progress and prospects. 17-21 December 2001, Kaikoura, New Zealand.

Programme and abstracts. Institute of Geological and Nuclear Sciences information series 50.

Norris, R.J., Koons, P.O. & Cooper, A.F. (1990) The obliquely –convergent plate boundary in the South Island of New Zealand: implications for ancient collision zones. *Journal of Structural Geology* 12, 715-725.

Pantosti, D., Schwartz, D.P. & Valensise, G. (1993) Paleoseismology Along the 1980 Surface Rupture of the Irpinia Fault: Implications for Earthquake Recurrence in the Southern Apennines, Italy. *Journal of Geophysical Research* 98/B4, 6561-6577.

Pettinga, J.R., Yetton, M.D., Van Dissen, R.J. & Downes, G. (2001) Earthquake Source Identification and Characterisation for the Canterbury Region, South Island, New Zealand. *Bulletin of the New Zealand Society for Earthquake Engineering,* 34/4: 282-314.

Pettinga, J.R. & Wise, D.U. (1994) Paleostress adjacent to the Alpine fault: Broader implications from fault analysis near Nelson, South Island, New Zealand. *Journal of Geophysical Research,* 99/B2: 2727-2736.

Reyners, M.E. (1989) New Zeland seismicity 1964-87; an interpretation. New Zealand *Journal of Geology and Geophysics*, 32/3, 307-315.

Rose, R.V. (1986) Structure and metamorphism of the Haast Schist and Torlesse Zones between the Alpine Fault and the D'Urville Valley, South Nelson. Unpublished MSc thesis, University of Canterbury, Christchurch, New Zealand.

Schwartz, D.P & Coppersmith, K.J. (1984) Fault Behaviour and Characteristic Earthquakes: Examples from the Wasatch and San Andreas Fault Zones Journal of Geophysical Research, 89/B7, 5681-5698.

Schwartz, D.P & Coppersmith, K.J. (1986) Seismic Hazards: New Trends in Analysis Using Geologic Data. Active Tectonics (Studies in Geophysics), National Academy Press, Washington D C, United States of America.

Sibson, R.H. Stopping of earthquake ruptures at dilational fault jogs. *Nature.* Vol 316, No. 6025, 248-251.

Sibson, R.H., White, S.H., Atkinson, B.K. (1979) Fault rock distribution and structure within the Alpine Fault Zone: a preliminary account. In: Walcott, R.I., Creswell, M.M. (Eds.), The Origin of the Southern Alps. *Bulletin of the Royal Society of New Zealand* 18, 55-65.

Sieh, K.E. (1978) Slip along the San Andreas fault associated with the Great 1857 Earthquake. *Bulletin of the Seismological Society,* 68/5, 1421-1448.

Stirling, M.W., Wesnousky, S.G. & Berryman, K.R. (1998) Probabilistic seismic hazard analysis of New Zealand. *New Zealand Journal of Geology and Geophysics* 41: 355-375.

Suggate, R.P. (1965) Late Pleistocene geology of the northern part of the South Island, New Zeland. *New Zealand Geological Survey Bulletin 77.*

Suggate, R.P. (1988a) The high terraces of the Upper Buller Gorge: sequence, nomenclature and deformation. In: Suggate, R.P. (ed.) Quaternary deposition and deformation in the Buller and tributary valleys. New Zealand Geological Survey Record, 25, 5-11.

Suggate, R.P. (1988b) Late Otiran Glaciation in the upper Buller valley, Nelson, New Zealand. In: Suggate, R.P. (ed.) Quaternary deposition and deformation in the Buller and tributary valleys. New Zealand Geological Survey Record, 25, 13-25.

Suggate, R.P. (1988c) The Speargrass Surface (c. 18,000 year BP) and its deformation in the Buller and tributary valleys. In: Suggate, R.P. (ed.) Quaternary deposition and deformation in the Buller and tributary valleys. New Zealand Geological Survey Record, 25, 27-43.

Suggate, R.P. (1990) Late Pliocene and Quaternary glaciations of New Zealand. *Quaternary Science Reviews* 9, 175-197.

Sutherland, R. & Norris R.J. (1995) Late Quaternary displacement rate, paleoseismicity, and geomorphic evolution of the Alpine Fault: evidence from Hokuri Creek, South Westland, New Zealand. *New Zealand Journal of Geology and Geophysics,* 38, 419-430.

Sylvester, A.G. (1988) Strike-slip faults. *Geological Society of America Bulletin*, 100, 1666-1703.

Van Dissen, R.J. & Nicol, A (1998) Paleoseismicity of the middle Clarence Valley section of the Clarence Fault, Marlborough, New Zealand. Geological Society of New Zealand Miscellaneous Publication 101A: 233.

Van Dissen, R.J. & Yeats, R.S. (1991) Hope Fault, Jordan Thrust, and uplift of the Seaward Kaikoura Range, New Zealand. *Geology*, 19/4, 393-396.

Walcott, R.I. (1998) Modes of Oblique Compression: Late Cenozoic Tectonics of the South Island of New Zealand. *Reviews of Geophysics*, 36, 1:1-26.

Wellman, H.W (1955) New Zealand Quaternary tectonics. *Geologische Rundschau* 43, 248-257.

Wells, A., Duncan, R.P. & Stewart, G.H. (2001) Forest dynamics in Westland, New Zealand: the importance of large, infrequent earthquake induced disturbance. *Journal of Ecology* 89, 1006-1018.

Wells, A., Yetton, M.D., Stewart, G.H. & Duncan, R.P. (1999) Prehistoric dates of the most recent Alpine Fault earthquakes, New Zealand. *Geology,* 27 No 11: 995-998.

Wells, D.L., Coppersmith, K.J. (1994) New empirical relationships among magnitude, rupture length, rupture width, rupture area, and surface displacement. *Bulletin of the Seismological Society of America,* 84: 974-1002.

Wesnousky, S.G. (1988) Seismological and structural evolution of strike-slip faults. *Nature* 335, 340-343.

Wesnousky, S.G. (1990) Seismicity as a function of cumulative offset: some observations from Southern California. *Bulletin of the Seismological Society of America,* 80: 1374-1381.

Wright, C.A. (1998) Geology and Paleoseismology of the central Alpine Fault, Westland, New Zealand. Unpublished MSc Thesis, lodged in the Library. University of Otago, Dunedin, New Zealand.

Wright, C.A., Norris, R.J. & Cooper, A.F. (1998) Paleoseismological history of the Central Alpine Fault. Geological Society of New Zealand and New Zealand Geopysical Society, Joint Annual Conference, Christchurch, New Zealand. Abstract only: 249.

Yetton, M.D. (2000) The probability and consequences of the next Alpine Fault earthquake, South Island, New Zealand. Unpublished Ph.D thesis, University of Canterbury, Christchurch, New Zealand.

Yetton, M.D. (1998) Progress in understanding the paleoseismicity of the central and northern Alpine Fault, Westland, New Zealand. *New Zealand Journal of Geology and Geophysics,* 41:475-483.

Yetton, M.D (2002) Paleoseismic investigation for the North and West Wairau Sections of the Alpine Fault, South Island, New Zealand. Earthquake Commission Research Report No. 99/353. Earthquake Commision Research Foundation, Wellington, New Zealand.

Yetton, M.D., Wells, A. & Traylen, N.J. (1998) The probability and consequences of the next Alpine Fault earthquake. EQC research report 95/193, New Zealand Earthquake Commission, Wellington, New Zealand.

Zachariasen, J., Berryman, K., Prentice, C., Langridge, R., Stirling, M., Villamor, P. & Rymer, M. (2001) Size and timing of large prehistoric earthquakes on the Wairau Fault, South Island. EQC research report 99/389. Institute of Geological Sciences client report 2001/13. 41p.

APPENDIX ONE

PROCESSING OF RINDS AND DETERMINATION OF AGE

The methodology of collection and processing of weathering rind rock chips was performed in accordance with McSaveney (1992). Chip samples were taken from the upper side of Torlesse Group cobbles of sand-sized grains on exposed surfaces. It is necessary to collect more than fifty chips and ideally more than one hundred, to allow for statistical analysis and identification of inherited rinds not removed by abrasion, therefore predating the latest depositional feature (McSaveney, 1992). To ensure maximum rind thickness, rock chips were removed with a sledgehammer from boulders that were not covered with vegetation.

LABORATORY PROCEDURE

Laboratory preparation was similar to McSaveney (1992):

- Samples soaked in dilute HCl (1×HCl concentrate: 5 water) for 24 hrs;
- Full water rinse;
- Soaked in dilute household bleach for 24 hrs;
- Full water rinse;
- Stubborn lichens still attached, so soaked in Hydrogen Peroxide (50% conc.) and water for 24 hrs;

- Rinse and light scrub;
- Sun, then oven dried at 100° C for 24 hrs.

RIND MEASUREMENT

Rock chips were assigned an identification number and the thickest part of the rind was permanently marked and measured using a pair of digital callipers held to avoid parallax error.

DATA PROCESSING

Data was entered onto an Excel spreadsheet. In accordance with McSaveney, (1992), rind thickness was binned into lots of 0.2 mm increments. The number of measurements in each bin were normalised, however as the sample size of the sets is low, the data is better presented by cumulative frequency graphs. A moving average trendline is shown on the WRD cumulative frequency graphs. This trendline is peaky when a running mean of two is calculated. A smoother trend for the five sample running mean is shown on the cumulative frequency graphs, although the small sample size is not conducive to running means or statistical analyses.

WRD #1		WRD #2		WRD #3		WRD #4		WRD #5		WRD #6		WRD #7		WRD #8		WRD #9	
Chip Numb	Rind Thickn	Chip Number	Rind Thickness (mm)	Chip Numb	Rind Thickn	Chip Numb	Rind Thickn	Chip Numb	Rind Thickn	Chip Numb	Rind Thickn	Chip Numb	Rind Thickn	Chip Numb	Rind Thickn	Chip Numb	Rind Thickness (mm)
1	5.04	1	0.92	1	6.89	1	3.41	1	3.31	1	4.87	1	4.37	1	3.41	1	4.77
2	4.84	2	1.09	2	6.51	2	3	2	3.33	2	6.81	2	2.11	2	3.09	2	3.09
3	4.68	3	5.48	3	5.4	3	3.98	3	3.22	3	6.29	3	4.18	3	1.69	3	4.74
4	4.36	4	3.17	4	4.82	4	3.02	4	3.27	4	6.28	4	4.02	4	1.9	4	5.72
5	3.71	5	3.34	5	2.19	5	4.26	5	4.78	5	5.69	5	2.47	5	3.21	5	6.03
6	4.96	6	2.53	6	5.59	6	3.23	6	2.28	6	2.44	6	4.01	6	3.29	6	5.56
7	4.66	7	3.87	7	4.38	7	4.19	7	3.79	7	5.06	7	1.53	7	2.97	7	4.75
8	5.8	8	0.93	8	4.08	8	4.47	8	1.66	8	5.76	8	4.68	8	1.88	8	5.82
9	6.5	9	5.93	9	5.04	9	4.1	9	4.6	9	5.69	9	1.54	9	2.71	9	5.7
10	5.38	10	4.99	10	2.37	10	3.88	10	3.87			10	1.94	10	2.37	10	5.3
11	5.18	11	5.71	11	4.87	11	3.93	11	3.69			11	3.78	11	1.86	11	5.39
12	4.33	12	3.18	12	5.45	12	3.58	12	1.87			12	3.75	12	1.92	12	5.84
13	6.61	13	4.21	13	6.81	13	5.65	13	1.99			13	2.16	13	2.65	13	5.6
14	6.37	14	3.36	14	5.44	14	3.67	14	2.09			14	2.9	14	3.37	14	5.76
15	3.4			15	6.81	15	4.08	15	3.49			15	1.5	15	1.1	15	5.85
16	7.18	WRD #2A		16	5.44	16	3.19	16	2.83			16	3.32	16	2.62	16	5.84
17	4.56			17	3.03	17	2.81	17	3.29			17	4	17	2.46	17	5.15
18	3.94	Chip Number	Rind Thickness (mm)	18	7.4	18	3.25	18	3.1			18	1.37	18	2.45	18	5.52
19	3.85			19	5.91	19	3.48	19	3.71			19	2.17	19	2.52	19	5.25
20	6.82	1	4.64	20	6.93	20	4.07	20	3.92			20	1.81	20	1.94	20	5.69
21	5.38	2	5.32	21	4.49	21	3.54	21	1.88			21	4.5			21	5.1
22	2.81	3	7.39	22	5.47	22	3.4	22	2.71			22	3.43			22	4.67
23	4.73	4	0.94	23	5.55	23	3.14	23	2.85			23	3.64			23	5.09
24	4.22	5	0.78	24	5.68	24	4.18	24	3.73								
25	5.6	6	1.55	25	5.34	25	8.06	25	3.96								
26	4.72	7	4.53	26	5.62	26	3.4	26	3.83								
27	5.39	8	1.26	27	4.49	27	3.56	27	3.68								
28	2.79	9	2.46	28	5.54	28	4.7										
29	4.05	10	5.37	29	5.07												
30	5.26	11	5.11														
31	4.1	12	4.6														
32	5.66	13	1.52														
33	4.01	14	5.15														
34	3.26	15	5.36														
35	7.65	16	3.59														
36	5.65	17	2.45														
37	5.48																
38	3.96																
39	3.68																
40	4.15																
41	7.18																
42	4.24																
43	4.66																
44	3.67																
45	5.13																
46	5.8																
47	5.52																
48	6.08																
49	6.19																

Figure A1: Weathering rind calibration curve for sandstone members of the Torlesse Supergroup (McSaveney, 1992). Rinds between 0 and 4 mm (0-4 kyr)

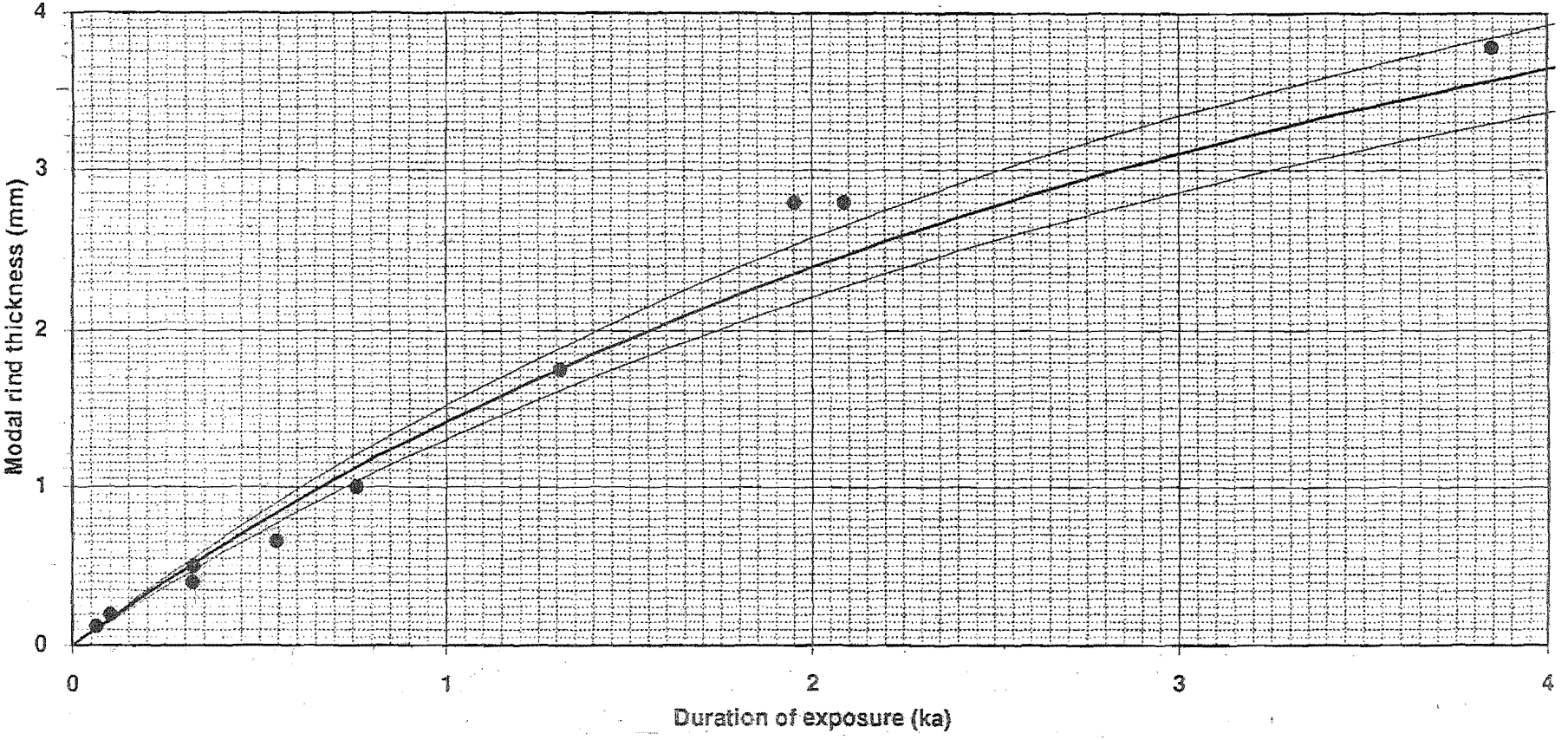

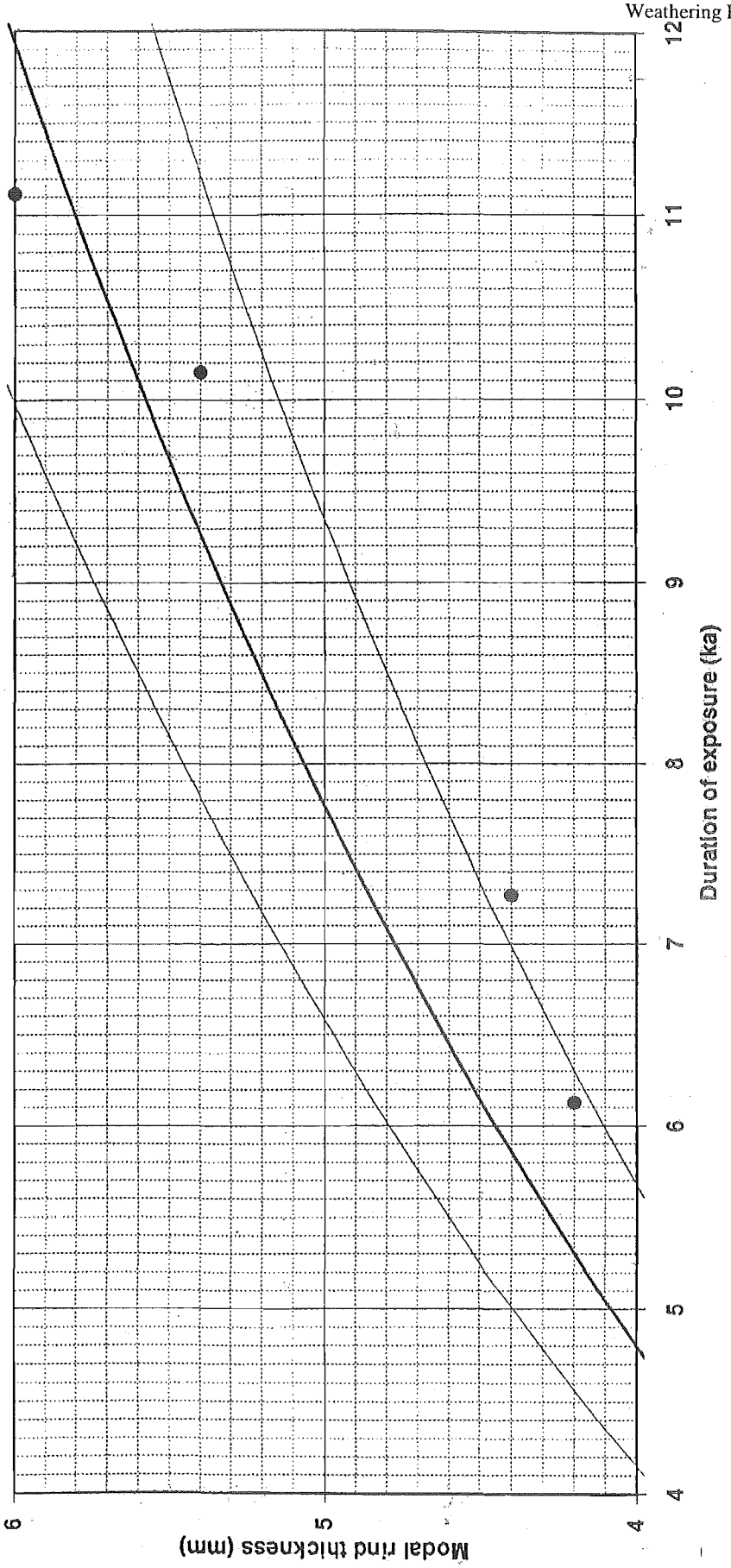

Figure A2: Weathering rind calibration curve for sandstone members of the Torlesse Supergroup (McSaveney, 1992). Rinds between 4 and 6 mm (4-12 kyr)

Figure A3: Weathering rind calibration curve for sandstone members of the Torlesse Supergroup (McSaveney, 1992). Rinds between 5 and 9 mm (10-30 kyr)

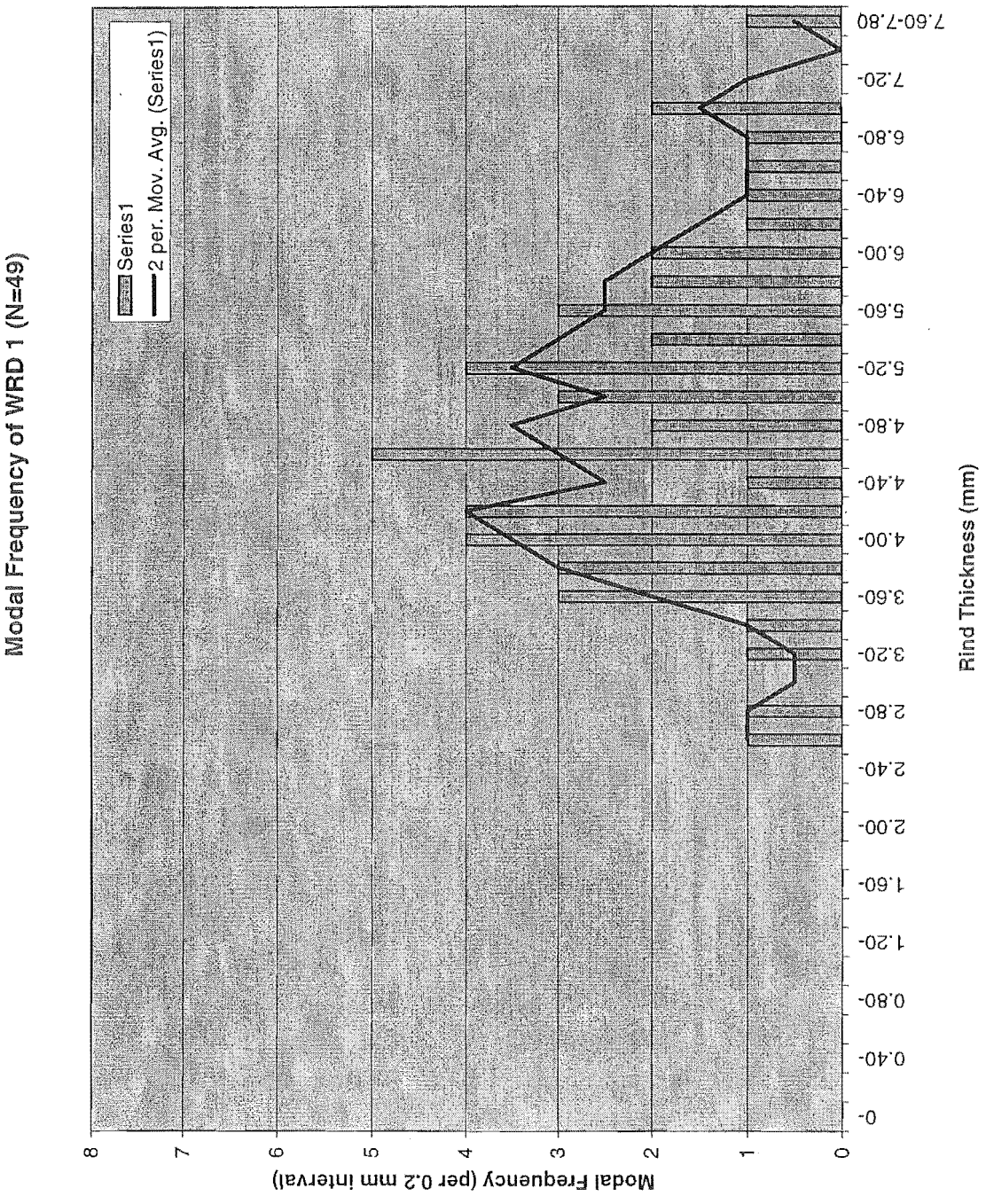
Modal Frequency of WRD 1 (N=49)
Series1
2 per. Mov. Avg. (Series1)
Modal Frequency (per 0.2 mm interval)
0
1
2
3
4
5
6
7
8
Rind Thickness (mm)
0-
0.40-
0.80-
1.20-
1.60-
2.00-
2.40-
2.80-
3.20-
3.60-
4.00-
4.40-
4.80-
5.20-
5.60-
6.00-
6.40-
6.80-
7.20-
7.60-7.80

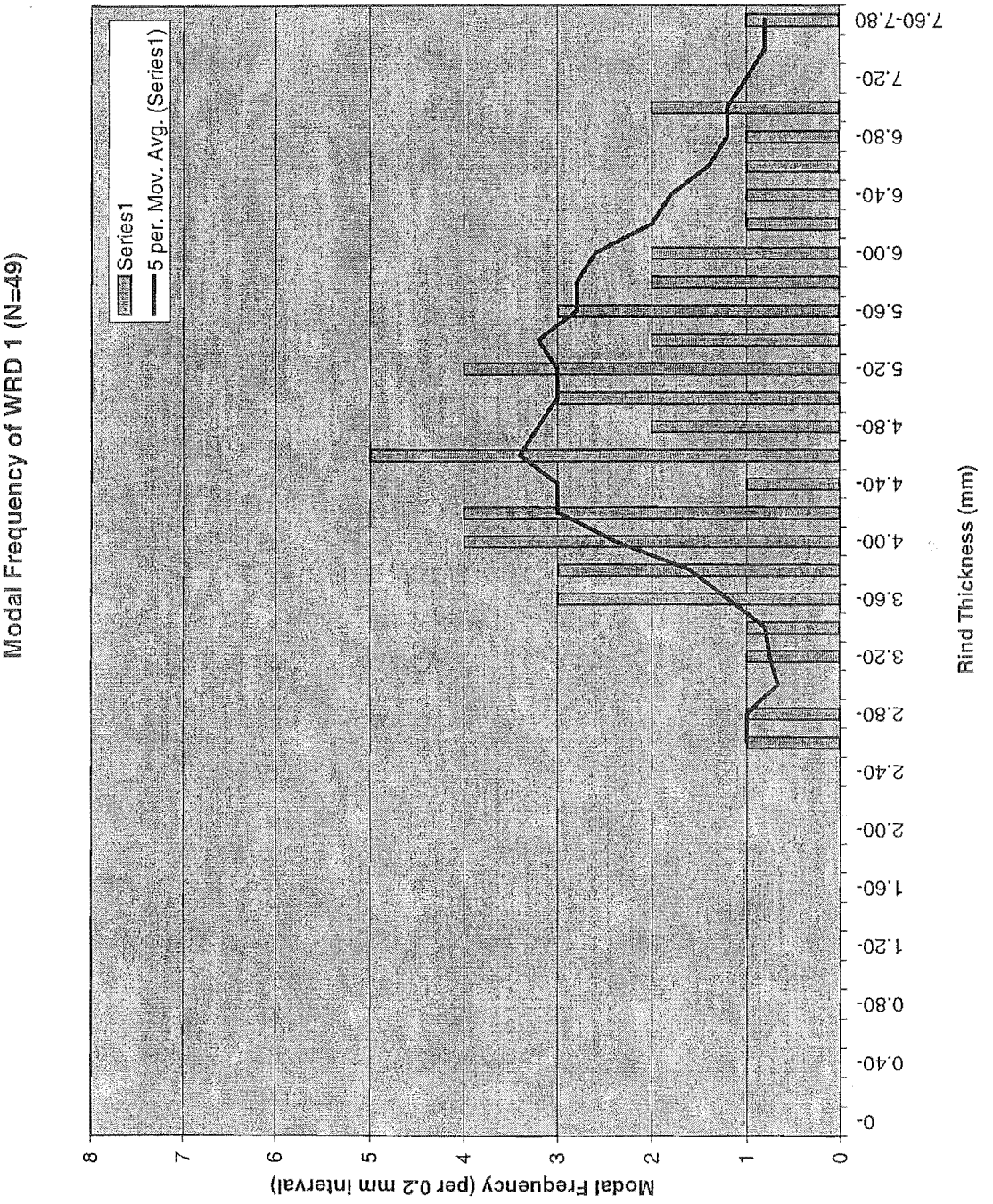
Modal Frequency of WRD 1 (N=49)
Series1
5 per. Mov. Avg. (Series1)
Modal Frequency (per 0.2 mm interval)
0
1
2
3
4
5
6
7
8
Rind Thickness (mm)
0-
0.40-
0.80-
1.20-
1.60-
2.00-
2.40-
2.80-
3.20-
3.60-
4.00-
4.40-
4.80-
5.20-
5.60-
6.00-
6.40-
6.80-
7.20-
7.60-7.80

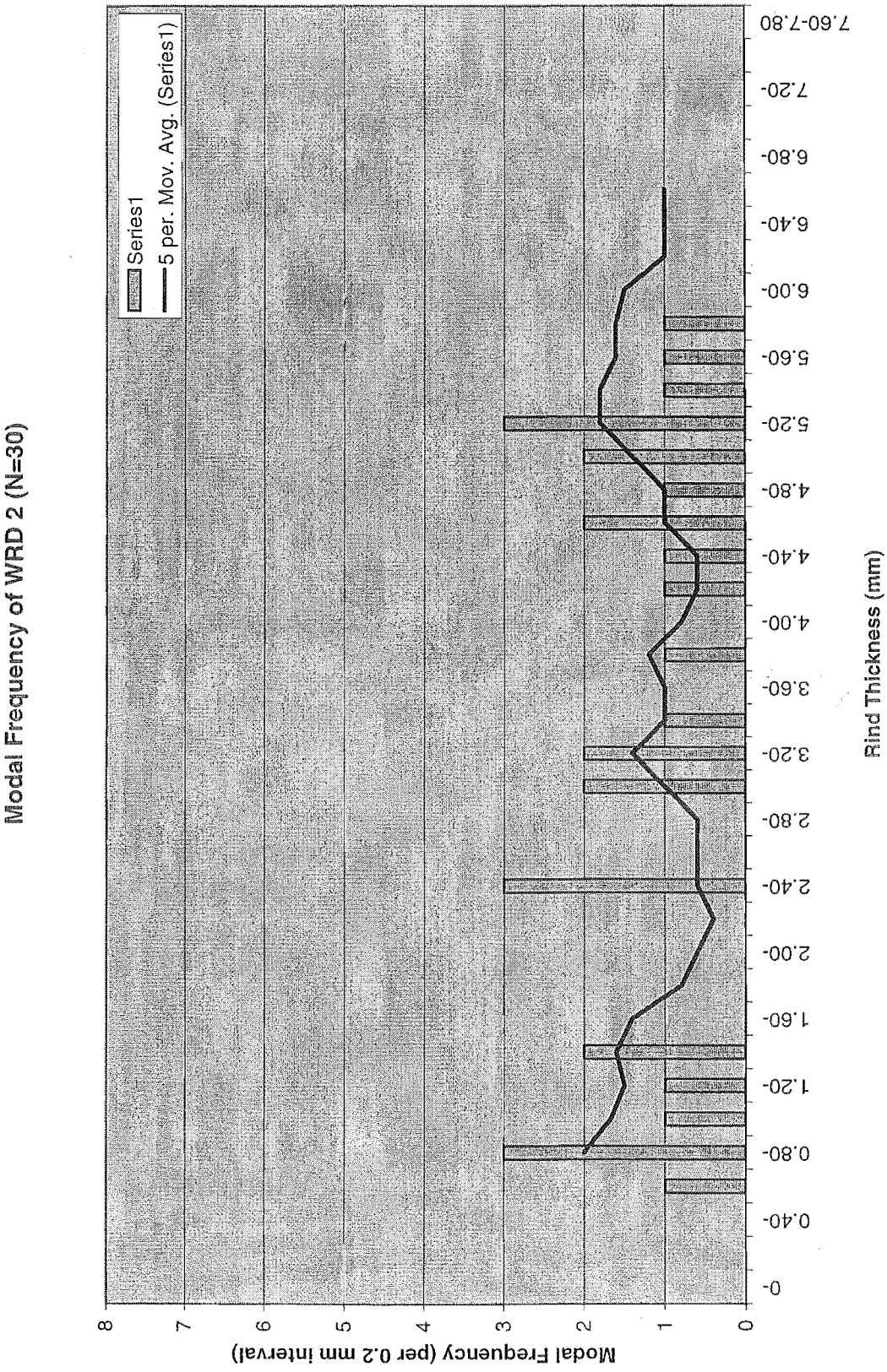
Modal Frequency of WRD 2 (N=30)
Series1
5 per. Mov. Avg. (Series1)
Modal Frequency (per 0.2 mm interval)
0
1
2
3
4
5
6
7
8
Rind Thickness (mm)
0-
0.40-
0.80-
1.20-
1.60-
2.00-
2.40-
2.80-
3.20-
3.60-
4.00-
4.40-
4.80-
5.20-
5.60-
6.00-
6.40-
6.80-
7.20-
7.60-7.80

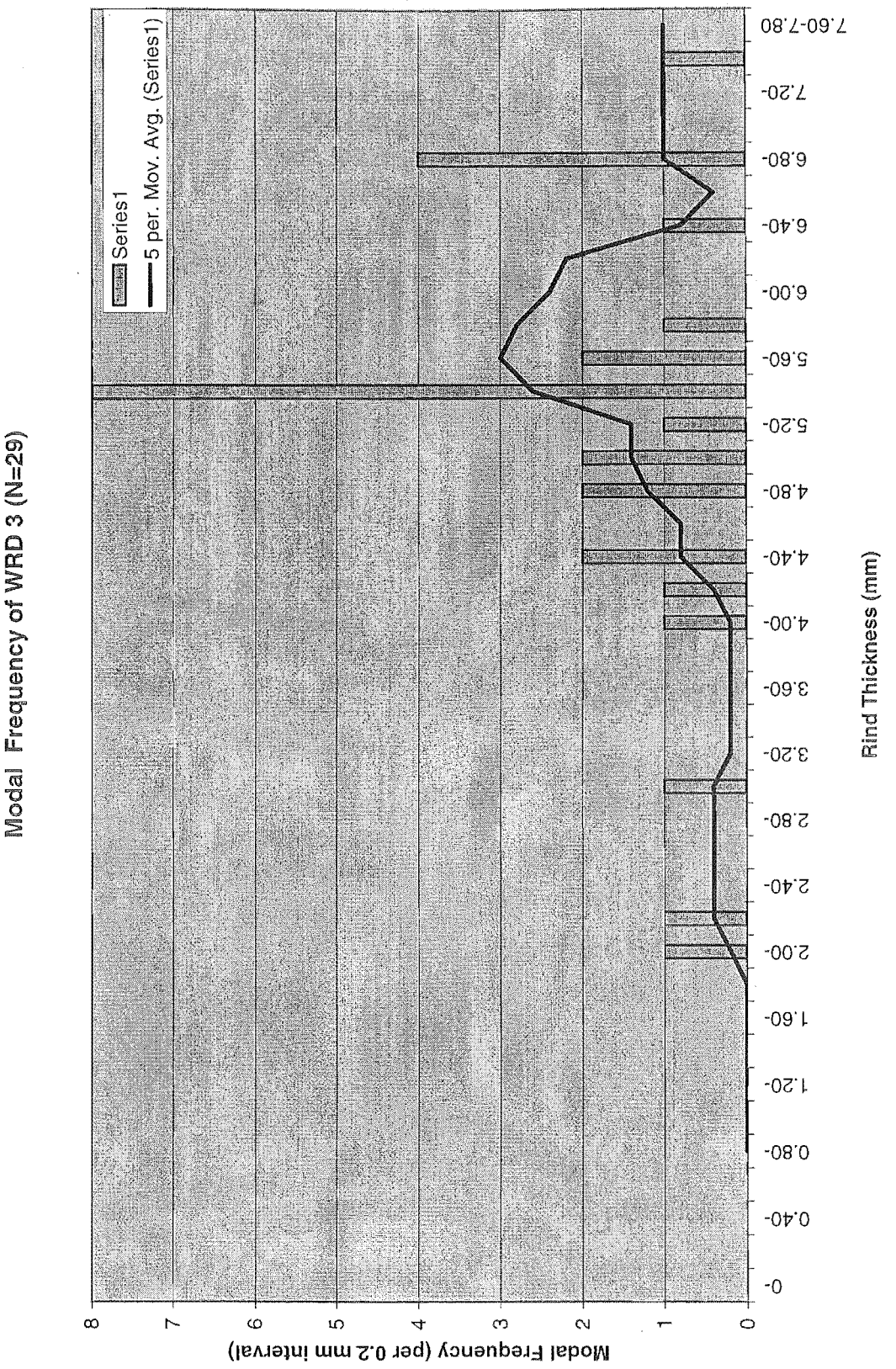
Modal Frequency of WRD 3 (N=29)
Series1
5 per. Mov. Avg. (Series1)
Modal Frequency (per 0.2 mm interval)
Rind Thickness (mm)
0
1
2
3
4
5
6
7
8
0-
0.40-
0.80-
1.20-
1.60-
2.00-
2.40-
2.80-
3.20-
3.60-
4.00-
4.40-
4.80-
5.20-
5.60-
6.00-
6.40-
6.80-
7.20-
7.60-7.80

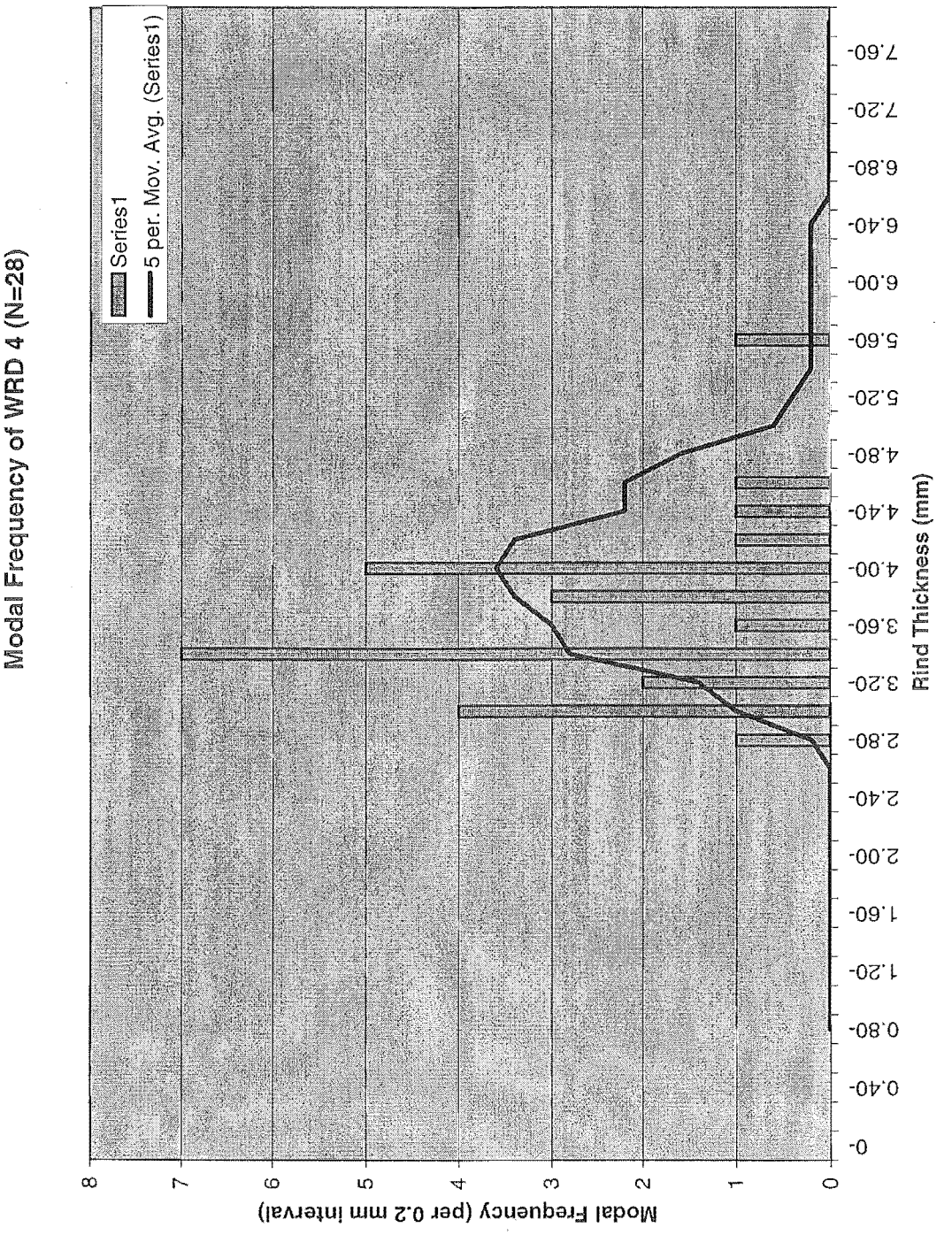
Modal Frequency of WRD 4 (N=28)
Series1
5 per. Mov. Avg. (Series1)
Modal Frequency (per 0.2 mm interval)
0
1
2
3
4
5
6
7
8
Rind Thickness (mm)
0-
0.40-
0.80-
1.20-
1.60-
2.00-
2.40-
2.80-
3.20-
3.60-
4.00-
4.40-
4.80-
5.20-
5.60-
6.00-
6.40-
6.80-
7.20-
7.60-

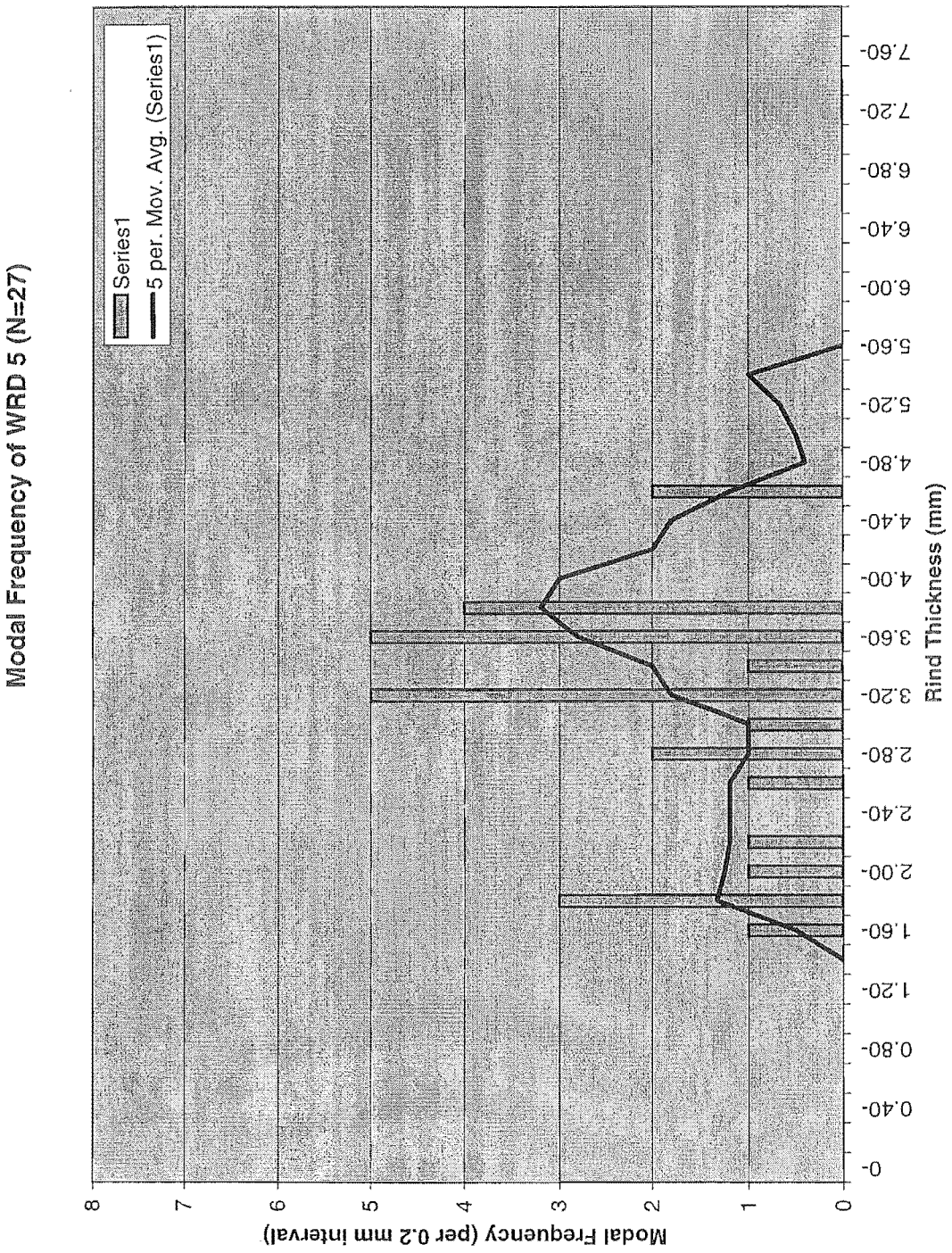
Modal Frequency of WRD 5 (N=27)
Series1
5 per. Mov. Avg. (Series1)
Modal Frequency (per 0.2 mm interval)
0
1
2
3
4
5
6
7
8
Rind Thickness (mm)
0
0.40
0.80
1.20
1.60
2.00
2.40
2.80
3.20
3.60
4.00
4.40
4.80
5.20
5.60
6.00
6.40
6.80
7.20
7.60

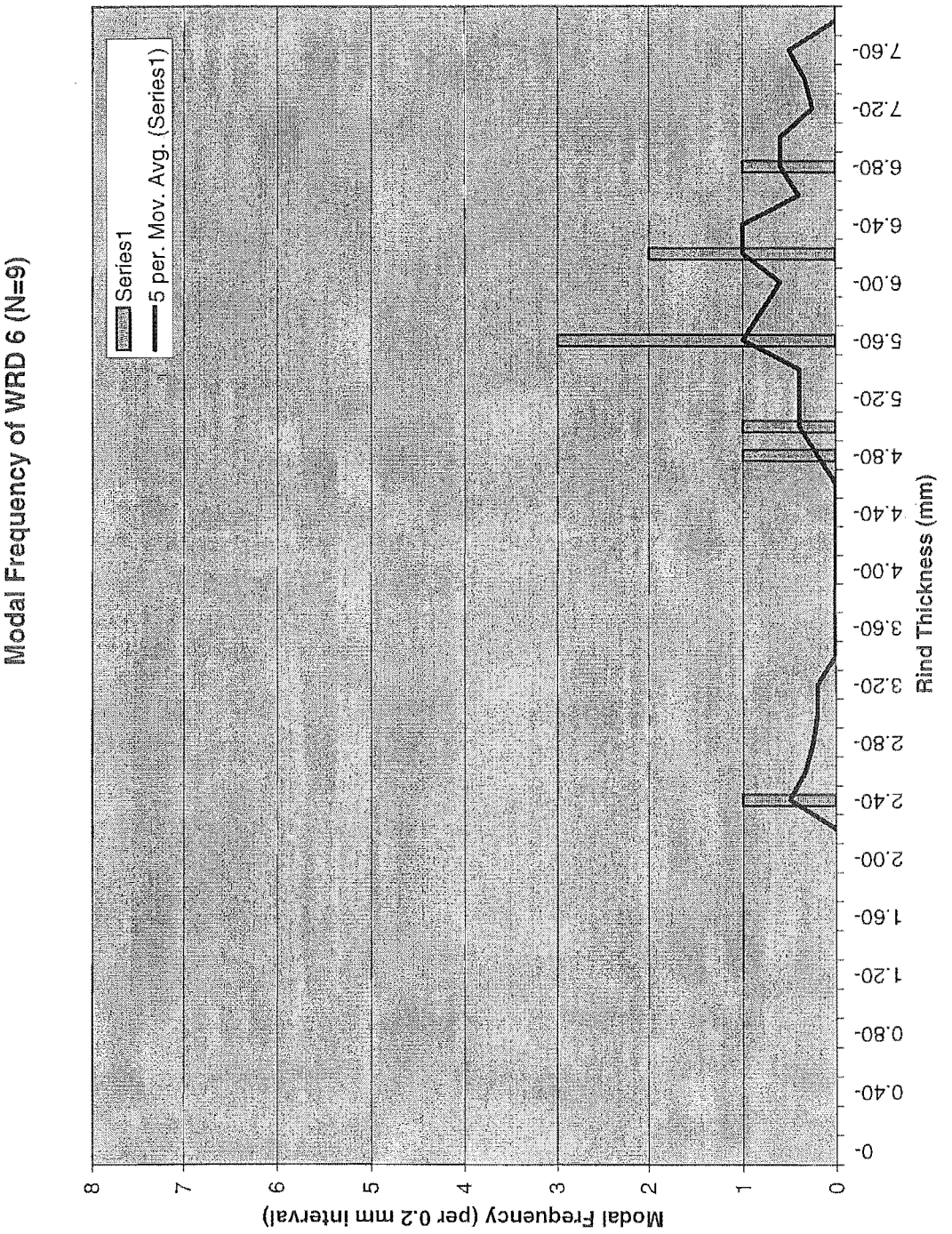
Modal Frequency of WRD 6 (N=9)
Series1
5 per. Mov. Avg. (Series1)
Modal Frequency (per 0.2 mm interval)
Rind Thickness (mm)
0
1
2
3
4
5
6
7
8
0-
0.40-
0.80-
1.20-
1.60-
2.00-
2.40-
2.80-
3.20-
3.60-
4.00-
4.40-
4.80-
5.20-
5.60-
6.00-
6.40-
6.80-
7.20-
7.60-

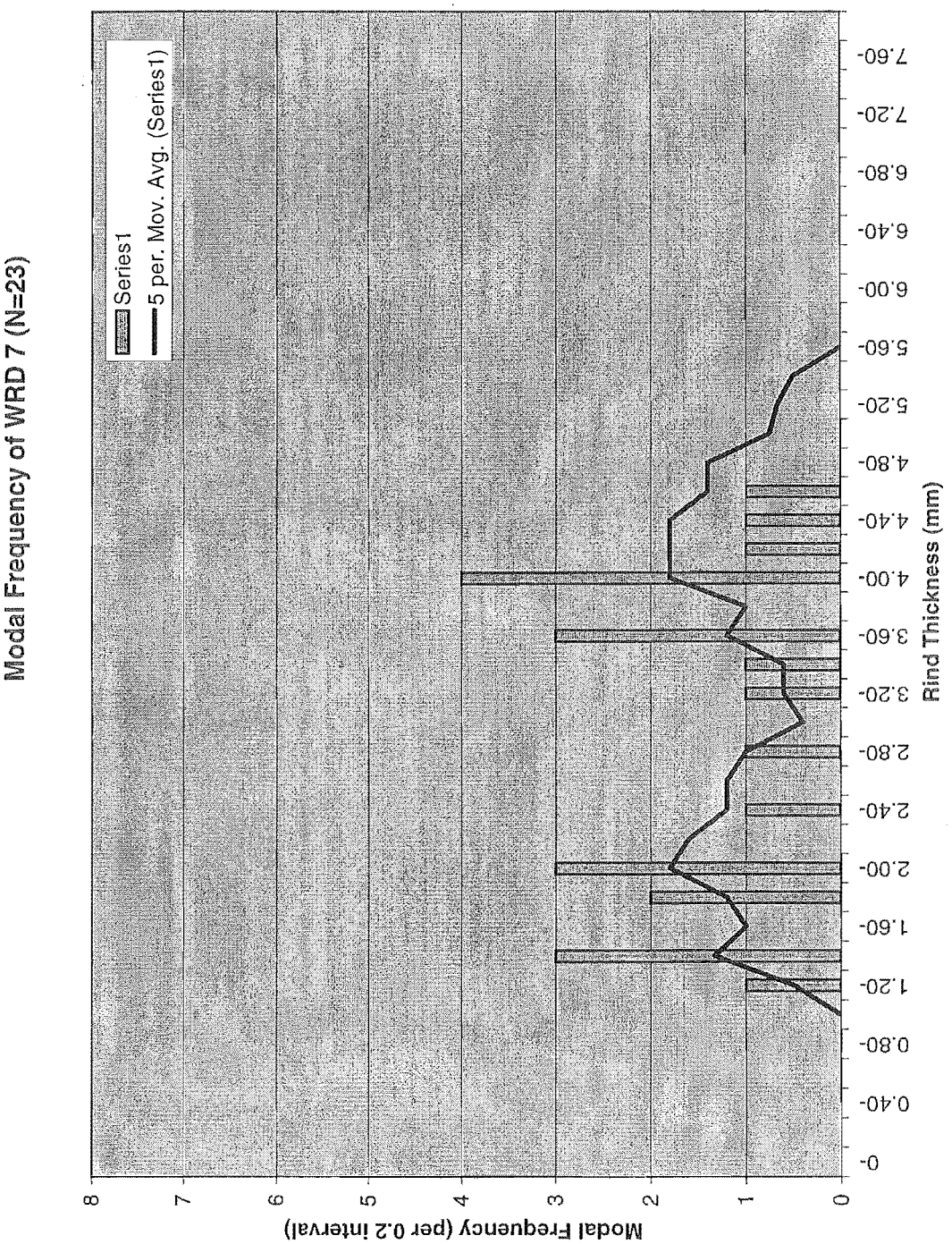
Modal Frequency of WRD 7 (N=23)
Series1
5 per. Mov. Avg. (Series1)
Modal Frequency (per 0.2 interval)
Rind Thickness (mm)
0
1
2
3
4
5
6
7
8
0-
0.40-
0.80-
1.20-
1.60-
2.00-
2.40-
2.80-
3.20-
3.60-
4.00-
4.40-
4.80-
5.20-
5.60-
6.00-
6.40-
6.80-
7.20-
7.60-

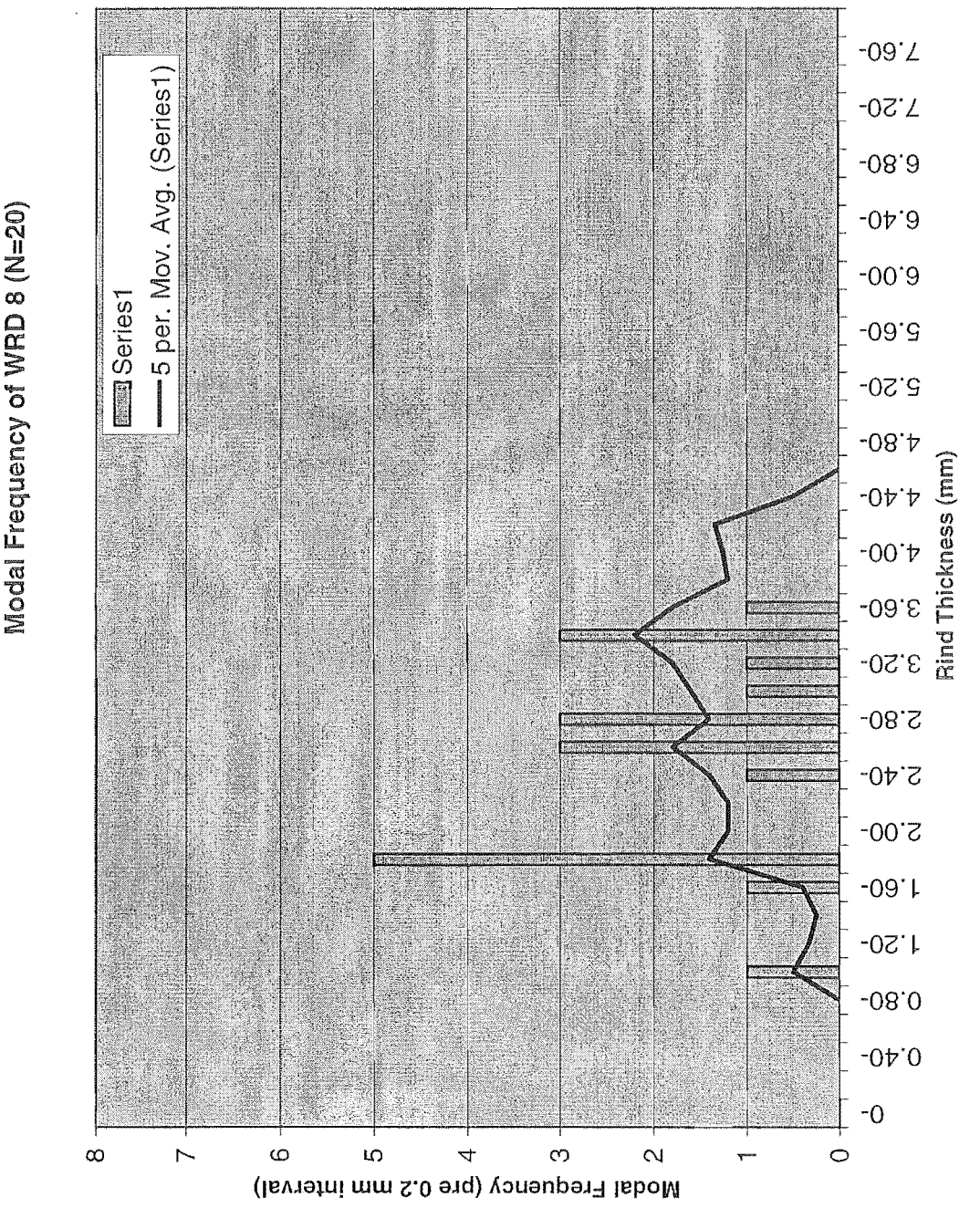
Modal Frequency of WRD 8 (N=20)
Series1
5 per. Mov. Avg. (Series1)
Modal Frequency (pre 0.2 mm interval)
0
1
2
3
4
5
6
7
8
Rind Thickness (mm)
0-
0.40-
0.80-
1.20-
1.60-
2.00-
2.40-
2.80-
3.20-
3.60-
4.00-
4.40-
4.80-
5.20-
5.60-
6.00-
6.40-
6.80-
7.20-
7.60-

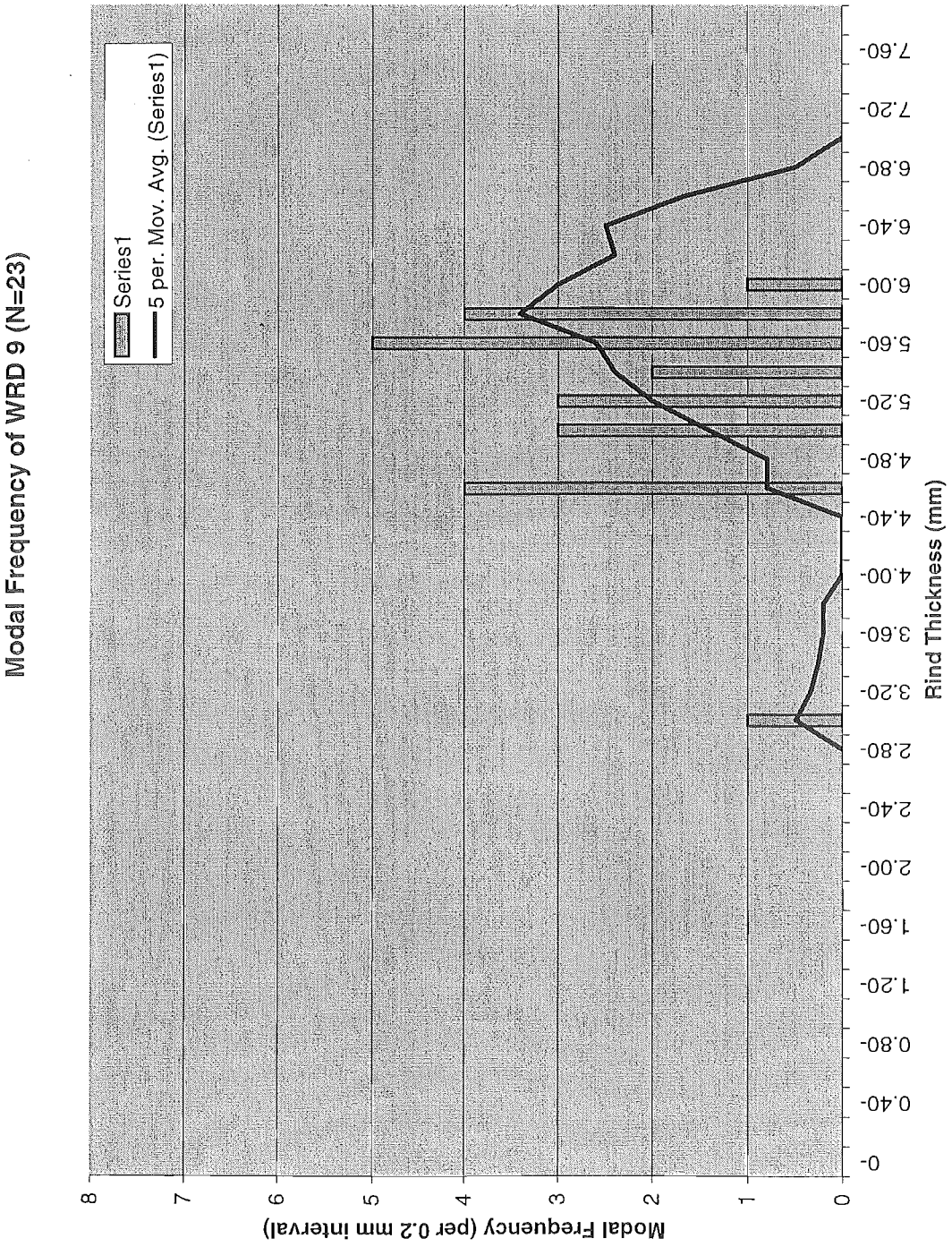
Modal Frequency of WRD 9 (N=23)
Series1
5 per. Mov. Avg. (Series1)
Modal Frequency (per 0.2 mm interval)
Rind Thickness (mm)
0
1
2
3
4
5
6
7
8
0.40
0.80
1.20
1.60
2.00
2.40
2.80
3.20
3.60
4.00
4.40
4.80
5.20
5.60
6.00
6.40
6.80
7.20
7.60

FIGURE 3.4

FACE LOG OF TOPHOUSE TRENCH ONE

Tophouse Alpine Fault Trench One (TP1)

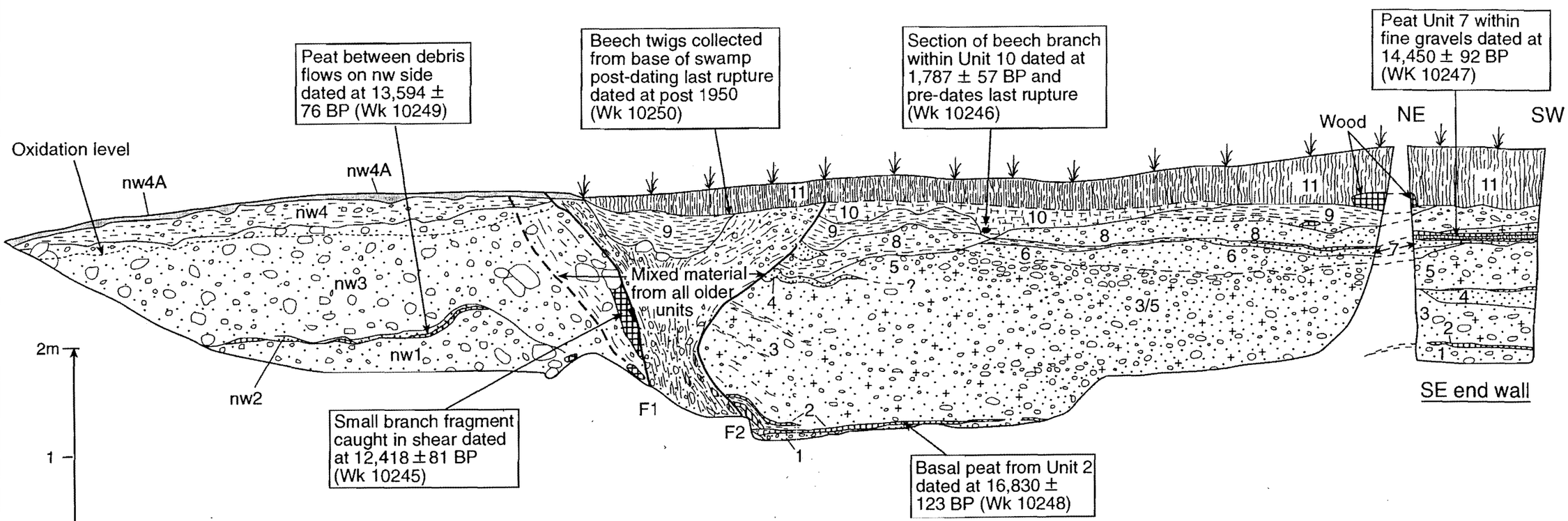

Unit	Description	Interpretation
nw 4A	Grey brown organic silty sand	"A" horizon developed on Unit 4
nw 4	Grey moderately weathered silty clay with fine angular gravel	Debris flow sediments
nw 3	Grey blue fine to medium sandy gravel with a silty clay matrix	
nw 2	Black brown dense peaty sand and sandy peat	Swamp hiatus
nw 1	Blue grey fine to medium sandy gravel with a silty clay matrix	

Probable time correlation

Unit Symbol	Description	Interpretation	Event Horizon(s)
11	Black brown fibrous peat with twigs	Recent swamp deposits with twigs from trees growing in swamp	← Event horizon
10	Grey clayey peat with some wood	Slopewash sediment and local peat and tree litter	
9	White grey silty clay locally with fine gravel and wood near base	Slopewash sediments following fan stabilisation	
8	Grey blue sandy fine angular gravel with some silt and local sand beds	Fan gravels from upslope stream systems	Numerous earlier rupture events displacing these units but no confirmed event horizons
7	Thin peat beds with grey blue silty clay and sand interbeds	Swamp deposits during hiatus in fan activity	
6	Grey blue sandy fine angular gravel with some silt and clay	Fan gravels from upslope stream systems	
5	Blue grey unsorted sandy fine subangular to subrounded gravel with a silty clay matrix	Debris flow sediments and associated minor fan gravels	
4	Grey medium sand with minor peat beds at the SE end of the trench	Fan sediments and minor swamp deposits	
3	Blue grey unsorted sandy fine subangular to subrounded gravel with a silty clay matrix	Debris flow sediments and associated fan gravels	
2	Dense brown uniform fine peat	Swamp deposits during hiatus in fan and debris flow activity	
1	Blue grey unsorted sandy fine gravel with a silty clay matrix	Debris flow sediments	

Summary

- Strike slip dominated fault zone with rupture confined to a narrow zone of repeated displacement.
- The most recent rupture post - dates 1,787±57 BP, the date obtained from the faulted Unit 10.
- The date of post 1950 from the base of the swamp near the scarp indicates the swamp in this area is a very young feature.

Figure 3.4: Face log of Tophouse Trench One

FIGURE 3.5

FACE LOG OF TOPHOUSE TRENCH TWO

Tophouse Alpine Fault Trench Two (TP2)

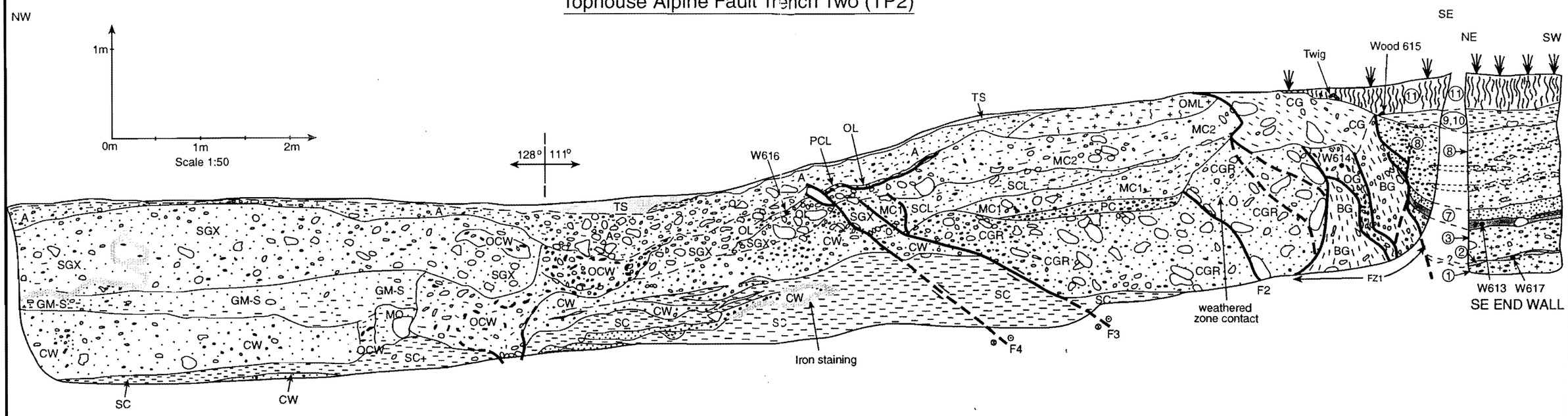

NW End

Unit Symbol	Description	Interpretation
TS	Grey brown organic silty sand, dry to moist	"A" Horizon
A	White beige clay clasts and sandstone pebbles/clasts in clayey matrix, minor organics	Colluvial wedge
OCW	Dark brown, unsorted, organic sandy gravel with some clay	Organic liquefaction intrusion
SGX	Iron stained sandy gravel with some clay matrix, gravels up to 150mm (sub rounded to sub angular)	Colluvial wedge
GM-S	Grey silty clay at base grading up to silty medium sand with some fine gravel	Pond sedimentation, followed by increased fluvial sediments
MO	Mottled orange white clayey silty sand with occasional pebbles - fine gravel sub rounded, - rounded clasts of greywacke	
CW	Greyish clayey silt with some angular to sub rounded gravel	Colluvial wedge, with occasional fuvial deposits
SC	Blue grey silty clay with minor fine gravel, no organics	Rapid sedimentation in fault related ponded area, occasional minor stream sedimentation
SC+	Sheared and mixed SC	Shear mixing of SC with intrusion of OCW

Between FZ1 and FZ4

Unit Symbol	Description	Interpretation
TS	Grey brown organic silty sand, dry to moist	"A" Horizon
A	White beige clay clasts and mudstone pebbles/clasts in clayey matrix, minor organics	Colluvial wedge
PCL	Yellow white pebbly clay	Minor slopewash sediments
OML	Slightly organic clayey silt, oxidised	Colluvial wedge deposits
MC2	Yellow to orange brown sandy gravel with some silty clay matrix, some gravel clasts up to 200mm	
SCL	Yellow grey fine to medium sand with some clay and fine gravel	
MC1	Yellow brown to orange brown sub angular to sub rounded gravel with some silty clay matrix, and coarse gravel clasts	
PC	Grey to yellow brown sub rounded fine pebble gravel with silty clay matrix	
CGR	Blue grey to light brown poorly sorted coarse sandy gravel, between F2.1 and F2 clay rich, gravel becoming finer toward F3	Debris flow sediment
SC	Blue grey silty clay with minor fine gravel	Rapid sedimentation in fault related ponded area, occasional minor stream sedimentation

Fault Zone

Unit Symbol	Description	Interpretation
CG	White cream clay matrix with poorly sorted - angular to rounded white clay and gravel clasts	Fault Gouges
OG	Dark brown organic clay matrix and sub angular to angular gravel clasts	
BG	Grey blue clay matrix with sub angular to sub rounded gravel clasts	

SE End

Unit Symbol	Description	Interpretation	Event Horizon(s)
11	Black brown fibrous peat with twigs and some wood, wet and non compressed	Recent swamp deposits, accumulation of twigs and wood from trees in a near swamp	Event Horizon
9,10	White grey clay with small rootlets and occasional sub angular gravel clasts	Slope wash sediments following fan stabilisation, rootlets marking onset of swampy peat accumulating environment	
8	Grey blue sub angular sandy fine gravel, occasional sandy lenses and blue grey fine gravel interfingering	Fan gravels from upslope stream systems, sand lenses and gravel inter-fingering from minor stream migrations	
7	Blue grey fine sand with minor silt with brown compressed peat interbeds and basal bed, peat moist to wet	Intermittent periods of swamp deposition and fan sediment accumulation	
3	Blue grey fine sand with some unsorted silty fine to medium gravel and occasional coarse gravel clasts	Fan sediments and minor debris flow sediments	
2	Thin discontinuous compressed dark brown peat, moist to wet, 40mm max thickness	Minor swamp deposits during hiatus in fan and debris flow deposition	
1	Blue grey fine to medium sand with some silty clay and fine to medium gravel	Fan deposits and periods of debris flow sedimentation	

Figure 3.5: Face log of Tophouse Trench Two